地質調査研究報告
Bulletin of the Geological Survey of Japan
Vol. 68, No. 2, P. 23–86
2017

Online ISSN：2186-490X
Print ISSN：1346-4272

地質調査研究報告

BULLETIN OF THE GEOLOGICAL SURVEY OF JAPAN

Vol. 68　No. 2　2017

特集：志摩半島，中生界堆積年代に関する新知見―5万分の1地質図幅「鳥羽」―

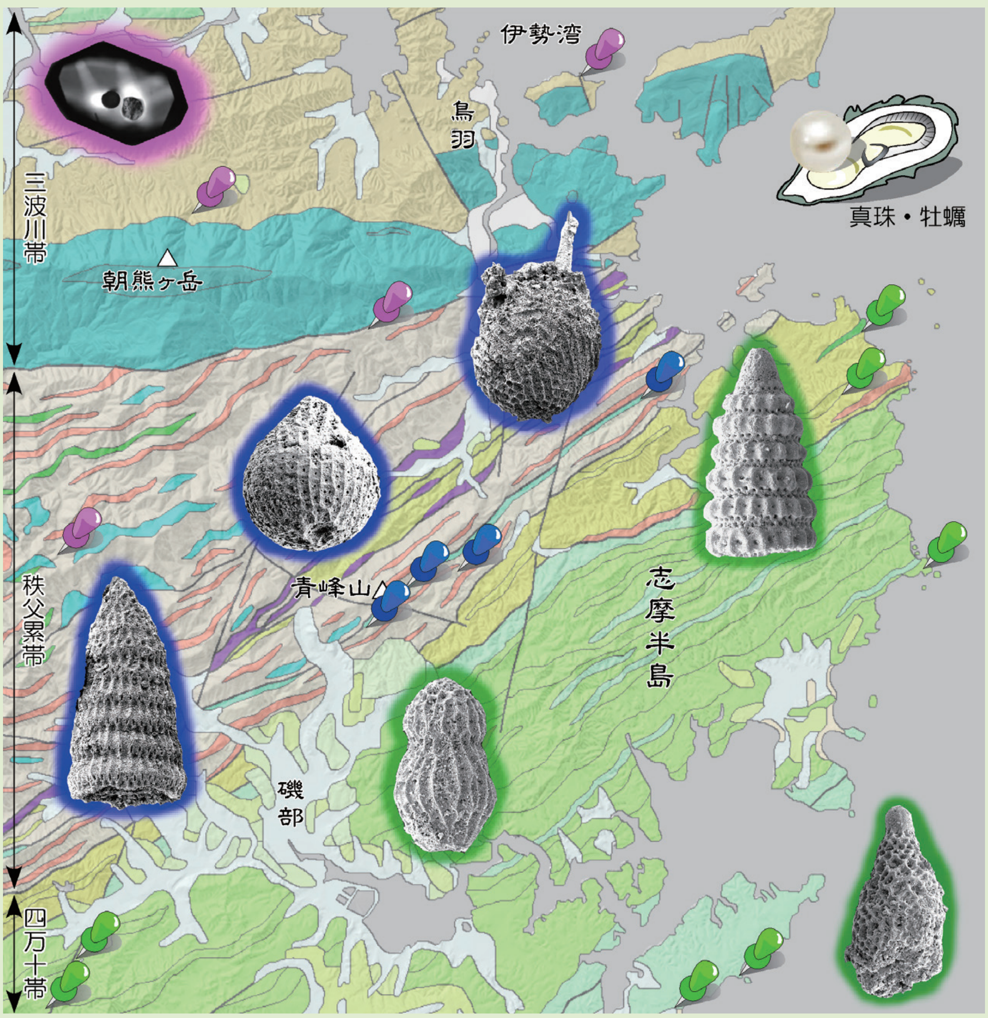

National Institute of Advanced Industrial Science and Technology
AIST
国立研究開発法人
産業技術総合研究所　地質調査総合センター

平成29年

地質調査研究報告

BULLETIN OF THE GEOLOGICAL SURVEY OF JAPAN

Vol. 68 No. 2 2017

特集：志摩半島，中生界堆積年代に関する新知見―5 万分の 1 地質図幅「鳥羽」―

巻頭言

概報

表紙の図

志摩半島中生界の堆積年代を決定する放散虫化石と砕屑性ジルコン

三重県に位置する志摩半島は，リアス式海岸の発達する景勝地のほか，真珠や牡蠣の養殖地として有名である．志摩半島の地体は，北から三波川帯，秩父累帯，四万十帯に区分され，秩父累帯は更に北帯，中帯（あるいは黒瀬川帯），南帯に細分される．本特集号では，秩父累帯南帯及び四万十帯から放散虫化石が，秩父累帯北帯及び三波川帯から砕屑性ジルコンの U–Pb 年代が報告された．表紙には，20 万分の 1 日本シームレス地質図を基図として，秩父累帯南帯と四万十帯の化石産出地点をそれぞれ青色，緑色の鋲で，秩父累帯北帯及び三波川帯のジルコン採取地点を桃色の鋲で指し示してある．また，これらの研究で抽出された代表的な放散虫化石種及びジルコンの写真をコラージュした．秩父累帯南帯の化石種（背景色：青）は右上から *Kilinora spilalis*，*Striatojaponocapsa conexa* sensu Hatakeda *et al.* (2007)，*Loopus primitivus*，四万十帯の化石種（背景色：緑）は右上から *Pseudodictyomitra tiara*，*Theocampe salillum*，*Amphipyndax tylotus* である．

（図・文：内野隆之・中江　訓）

Cover figure

Radiolarian fossils and detrital zircon constraining the depositional age of the Mesozoic in the Shima Peninsula, Mie Prefecture

The Shima Peninsula, Mie Prefecture, is famous for pearl- and oyster-farming places in Japan, in addition to scenic spots formed by the ria shoreline. The peninsula is geotectonically divided into the Sambagawa, the Chichibu Composite (further subdivided into the Northern Chichibu, Middle Chichibu (or Kurosegawa), and Southern Chichibu belts) and the Shimanto belts from the north. Radiolarian fossils from the Southern Chichibu and Shimanto belts, and U–Pb ages of detrital zircon from the Sambagawa and Northern Chichibu belts were reported in this special issue. On a base map of the Seamless Digital Geological Map of Japan (1:200,000), the fossil and the zircon dating locations are indicated with blue, green and pink tacks. In addition, pictures of the typical radiolarian fossil species and zircon were collaged to the map. The radiolarian fossil species (background color: blue) from the Southern Chichibu Belt are *Kilinora spilalis*, *Striatojaponocapsa conexa* sensu Hatakeda *et al*. (2007) and *Loopus primitivus*, and those (background color: green) from the Shimanto Belt are *Pseudodictyomitra tiara*, *Theocampe salillum* and *Amphipyndax tylotus* in descending order.

(Figure and Caption by Takayuki Uchino and Satoshi Nakae)

地質調査研究報告，第 68 巻，第 2 号，p. 23-24，2017

巻　頭　言：5 万分の 1 地質図幅「鳥羽」で得られた年代データの特集号化

内野隆之[1]

Takayuki Uchino (2017) Special issue on the depositional ages from the Toba District (Quadrangle series 1:50,000). *Bull. Geol. Surv. Japan*, vol. 68 (2), p. 23–24, 1 fig.

Keywords: Quadrangle series 1:50,000, Toba District, Shima Peninsula, Mie Prefecture, Sambagawa Belt, Chichibu Composite Belt, Shimanto Belt, radiolarian fossil, zircon, U-Pb age, depositional age

地質調査総合センターでは，志摩半島の東部域を区画とした5万分の1地質図幅「鳥羽」(以降, 鳥羽図幅と呼ぶ)を作成中であり，現在，印刷に向けての作業を進めているところである．鳥羽図幅は三波川帯，秩父累帯(秩父帯北帯，秩父帯中帯(あるいは黒瀬川帯)，秩父帯南帯)，四万十帯の3帯にまたがっており(第1図)，中古生界(基盤岩)を対象とした学術的観点からは，中古生代島弧–海溝系テクトニクスの解明に資するデータを提供できることや西南日本外帯における地質基準の確立に貢献できることが期待されている．また，本地域周辺では，5万分の1地質図幅を含め，詳細な地質図の整備が進んでおらず，防災的観点からも，東南海地震に備えた国・地方自治体による防災計画や都市計画などの基礎資料として，利活用されることが期待されている．

この鳥羽図幅の調査・研究の過程で，中古生界から堆積年代を決定する微化石や砕屑性ジルコンが見出された．本特集号では，その成果の一部について報告する．掲載された論文(概報)は，秩父累帯南帯の付加体及び整然層から得られた放散虫化石の年代(内野・石田，2017)，秩父累帯北帯の砂岩及び三波川帯の砂質片岩から得られた砕屑性ジルコンのU-Pb年代(内野，2017)，四万十帯の付加体から得られた放散虫化石の年代(Nakae and Kurihara, 2017)を内容とした3本である．以下にその概要について紹介する．

内野・石田論文は，秩父累帯南帯の築地層群(付加体)と今浦層群(浅海層)から放散虫化石を見出し，前者は中

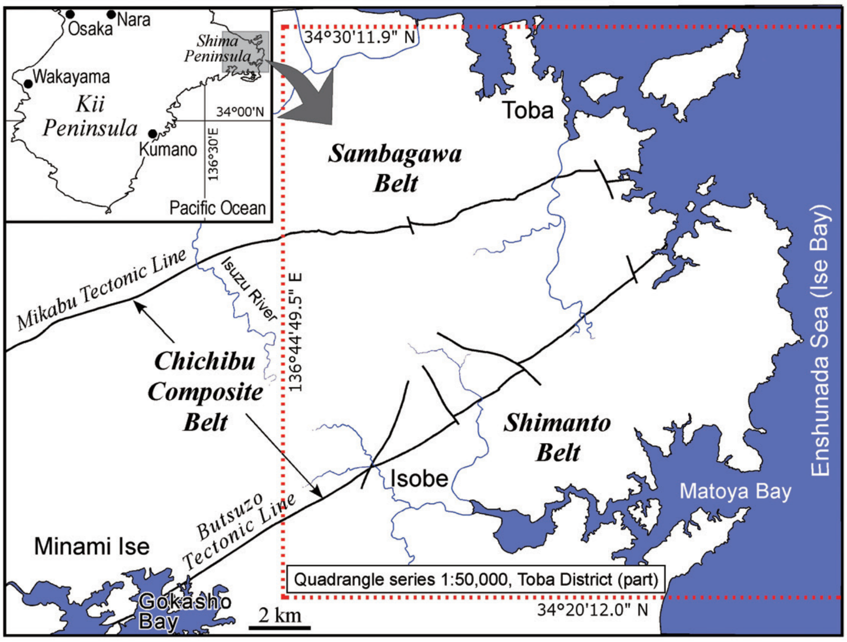

第1図　志摩半島の地体区分図と鳥羽図幅の区画(赤の点線)

Fig. 1　Geotectonic division of the Shima Peninsula and area of the Toba District (red dotted line)

[1] 産業技術総合研究所 地質調査総合センター 地質情報研究部門 (AIST, Geological Survey of Japan, Research Institute for Geology and Geoinformation)
Central 7, Higashi 1-1-1, Tsukuba, Ibaraki 305-8567, Japan

期ジュラ紀後半の年代を，後者は中期ジュラ紀後半，後期ジュラ紀前半，後期ジュラ紀後半の3つの年代を示すことを明らかにした．既存研究では泥岩から得られた微化石の標本がほとんど図示されていなかったこともあり，本論文では既存研究の結果を検証できただけでなく，堆積年代に対し制約を与えることができた点で意義がある．また，今浦層群について，浅海層にも関わらずかなり遅い堆積速度を示し得ることに対し，今後その妥当性を評価する必要があるとしている．

内野論文は，秩父累帯北帯の逢坂峠コンプレックスと河内コンプレックス，及び三波川帯の宮川層に産する砂岩または砂質片岩の砕屑性ジルコンのU–Pb年代（最若粒子集団の加重平均値）を報告した．逢坂峠コンプレックスと河内コンプレックスから得られたジルコンはそれぞれ，204 Ma（三畳紀末～ジュラ紀初頭），183 Ma（前期ジュラ紀中頃～後半）を示す．一方，宮川層には177 Ma（前期ジュラ紀後半）と95 Ma（後期白亜紀前半）といった異なる最若年代を示す試料が認められた．逢坂峠・河内コンプレックスは，標本化石写真のない学会講演要旨（都築・八尾，2006）を基に，それぞれ前期ジュラ紀，中期ジュラ紀に形成されたと考えられていたが，今回のジルコン年代値によってそれらの化石年代が妥当であることが明らかにされた．宮川層から得られた95 Maの年代については，近隣地域で得られたフェンジャイトK–Ar年代の既存研究結果（99–83 Ma：Tomiyoshi and Takasu，2010）と調和的であることが判明した．しかし，177 Maを示す試料におけるデータの妥当性に関しては，更なる検討が望まれている．

Nakae and Kurihara 論文は，四万十帯の的矢層群から放散虫化石を見出し，的矢層群が後期白亜紀の前期コニアシアン期，前期カンパニアン期ないし中期サントニアン期～中期カンパニアン期，中期～後期カンパニアン期の3つの年代を示すことを明らかにした．これまで本地域から年代決定に至る標本写真を示した放散虫化石は報告されていなかったが，本論文で初めて詳細な化石データを図示したことは意義がある．また，本論文は的矢層群が化石年代からも細分できる可能性を示し，鳥羽図幅における的矢層群の層序区分に貢献している．

なお，これまで黒瀬川帯の下部白亜系とされていた浅海層の一部から後期ペルム紀放散虫化石が見出され，志摩半島に後期ペルム紀の整然層が分布することが，内野・鈴木（2016）によって明らかにされている．また，秩父累帯北帯の南部ユニットである白木層群からも放散虫化石が初めて見出されており（内野・鈴木，未公表），本地域における年代データが蓄積しつつある．

このように，地質図幅の作成過程で得られた年代などの基礎データを，「地質調査研究報告」であらかじめ報告・議論することは，地質図幅では記述しきれない詳細かつ大量の生データやそのデータがもたらす意義などを示せる点で極めて有効である．

文　献

Nakae, S. and Kurihara, T. (2017)　Preliminary report on the radiolarian age of the Upper Cretaceous Matoya Group (Shimanto belt) in the Toba District, Mie Prefecture, Southwest Japan. *Bull. Geol. Surv. Japan*, **68**, 57–86.

Tomiyoshi, S. and Takasu, A. (2010)　K–Ar ages of lawsonite-bearing pelitic schists from the Sambagawa metamorphic belt in the Ise district, eastern Kii Peninsula, southwest Japan. *Earth Science (Chikyu Kagaku)*, **64**, 193–200.

都築　宏・八尾　昭（2006）　志摩半島東部地域の秩父北帯のジュラ紀付加コンプレックス．日本地質学会第113年学術大会講演要旨，45.

内野隆之（2017）　5 万分の1 地質図幅「鳥羽」地域における秩父累帯北帯の砂岩及び三波川帯の砂質片岩から得られた砕屑性ジルコンU–Pb年代．地調研報，**68**，41–56.

内野隆之・石田直人（2017）　5万分の1地質図幅「鳥羽」地域における秩父累帯南帯の泥岩から見出された中期及び後期ジュラ紀放散虫化石．地調研報，**68**，25–39.

内野隆之・鈴木紀毅（2016）　三重県志摩半島の黒瀬川帯から見出された後期ペルム紀整然層と広域対比．地質雑，**122**，207–222.

（受 付：2017年1月26日； 受 理：2017年1月30日）

地質調査研究報告, 第 68 巻, 第 2 号, p. 25-39, 2017

概報 - Report

5 万分の 1 地質図幅「鳥羽」地域における秩父累帯南帯の泥岩から見出された中期及び後期ジュラ紀放散虫化石

内野隆之[1,*]・石田直人[2]

Takayuki Uchino and Naoto Ishida (2017) Middle and Late Jurassic radiolarian fossils from mudstone in the Southern Chichibu Belt in the Toba District (Quadrangle series 1:50,000), Shima Peninsula, Mie Prefecture, Southwest Japan. *Bull. Geol. Surv. Japan*, vol. 68 (2), p. 25–39, 8 figs, 1 table.

Abstract: The Tsuiji Group (Middle to Late Jurassic accretionary complex) and the Imaura Group (Middle Jurassic to Early Cretaceous shallow-marine deposit) are distributed in the Southern Chichibu Belt, Shima Peninsula, Mie Prefecture. During a geological survey on the Toba District (Quadrangle series 1:50,000), we discovered Middle and Late Jurassic radiolarian fossils from mudstone of both groups and decided depositional ages in detail based on many radiolarian fossil species. A mudstone sample from the Tsuiji Group indicates early to middle Callovian, and mudstone samples from the Imaura Group are concentrated in three age groups: middle Bathonian to late Callovian, late Callovian to middle Oxfordian, and early Tithonian. The ages fall within the ranges of those that previous works reported.

Keywords: Middle Jurassic, Late Jurassic, radiolarian fossil, Tsuiji Group, accretionary complex, Imaura Group, shallow-marine deposit, Southern Chichibu Belt, Shima Peninsula, Mie Prefecture

要　旨

三重県志摩半島の秩父累帯南帯には，中期～後期ジュラ紀付加体からなる築地(ついじ)層群と中期ジュラ紀～前期白亜紀浅海層からなる今浦(いまうら)層群が分布する．5万分の1地質図幅「鳥羽」を作成する過程で，両層群の泥岩から中期及び後期ジュラ紀の放散虫化石を見出し，多くの化石種を基に，より精度の高い堆積年代を示すことができた．築地層群の泥岩はカロビアン期前半～中頃を，そして今浦層群の泥岩はバトニアン期中頃～カロビアン期後半，カロビアン期後半～オックスフォーディアン期中頃，チトニアン期前半という3つの時代を示すことが明らかになった．これらの時代はこれまで報告されていた年代データの範囲に収まる．

1．はじめに

三重県志摩半島における地体は北から三波川帯，秩父累帯，四万十帯に区分され，秩父累帯は更に北から「北帯」，「中帯」あるいは「黒瀬川帯」，「南帯」の3帯に区分される（例えば，山際・坂，1967；坂ほか，1988；坂ほか，1999；坂，2009）．北帯にはジュラ紀の付加体が分布し，中帯（坂ほか，1999以降，黒瀬川帯と呼ばれることが多い）にはジュラ紀の付加体と中期ジュラ紀～前期白亜紀の砕屑岩（浅海層）のほか，蛇紋岩，深成岩，角閃岩，デボン紀珪長質凝灰岩，ペルム紀砕屑岩（浅海層），200 Ma前後の結晶片岩などが分布する．南帯にはジュラ紀の付加体と中期ジュラ紀～前期白亜紀の砕屑岩類（浅海層）が分布している．そして，秩父累帯南側の四万十帯には白亜紀の付加体が，北側の三波川帯には苦鉄質～超苦鉄質岩類（御荷鉾緑色岩類）と泥質片岩類が分布している（第1図）．特に秩父累帯は，造構過程の議論が未だ決着していない黒瀬川帯を含むことや，同累帯全域で微化石（紡錘虫や放散虫）及び大型化石（恐竜や軟体動物）を産することから，過去より幾つもの研究がなされてきた（日下部・宮村，1958；山際・坂，1967；山際，1969，山際ほか，1979；菅野ほか，1980；吉倉・寺嶋，1984；坂・手塚，1988；坂ほか，1988；磯﨑ほか，1992；杉山ほか，1993；梅田・山際，1997；坂ほか，1999；冨田ほか，2001；太田ほか，2012；内野・鈴木，2016）．

産業技術総合研究所地質調査総合センターでは，三波川帯，秩父累帯，四万十帯にまたがる志摩半島の東部

[1] 産業技術総合研究所 地質調査総合センター 地質情報研究部門 (AIST, Geological Survey of Japan, Research Institute of Geology and Geoinformation)
[2] 鳥取大学大学院工学研究科社会基盤工学専攻 (Department of Social Systems and Civil Engineering, Graduate school of Engineering, Tottori University)
[*] Corresponding author: T.Uchino, Central 7, Higashi 1-1-1, Tsukuba, Ibaraki 305-8567, Japan, Email: t-uchino@aist.go.jp

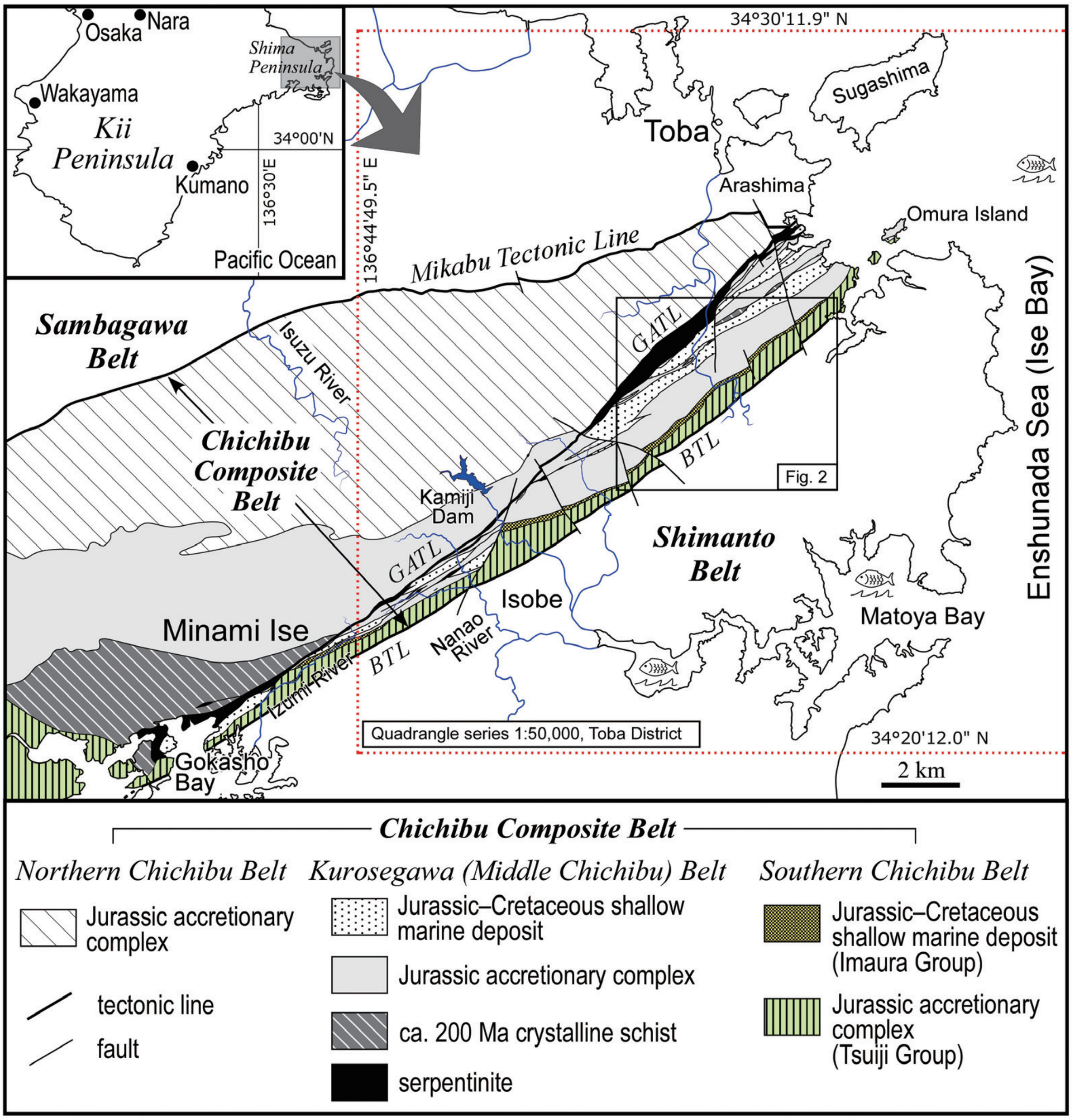

第1図　志摩半島における秩父累帯の地質概略図．南伊勢町の秩父累帯の分布については坂(2009)による．緯度・経度は世界測地系を使用．
BTL：仏像構造線，GATL：五ヶ所–安楽島構造線．

Fig. 1　Geological map of the Chichibu Composite Belt in the Shima Peninsula. Distribution of the Chichibu Composite Belt around Minami Ise Town is from Saka (2009). Latitude and longitude are represented by the world geodetic system. BTL: Butsuzo Tectonic Line, GATL: Gokasho–Arashima Tectonic Line.

域を区画とした5万分の1地質図幅「鳥羽」の作成を現在行っている(第1図)．その調査・研究過程において，秩父累帯南帯の泥岩から中期及び後期ジュラ紀の放散虫化石を見出した．この放散虫化石が示す地質時代のデータは，中～後期ジュラ紀付加体とその被覆層との関係や，ジュラ紀～白亜紀にかけての付加体の発達過程を検討する上で重要である．

なお，本地域の地質体にはこれまで基本層序単元である「層」が無いまま「層群」が使用されていることが多い．これは，地層命名規約上不適切ではあるが，本論では従来から使用されてきた地層名(例えば，今浦(いまうら)層群)を踏襲する．

２．秩父累帯南帯の地質

本地域の秩父累帯南帯(以下，南帯と表記する)は，鳥羽市大村島から度会郡南伊勢町(わたらいぐんみなみいせちょう)まで最大1 km程度の幅を持ち北東–南西方向に帯状に分布する(第1図)．南帯の中央～南部にかけては中期～後期ジュラ紀付加体からなる築地(ついじ)層群が最大900 mの幅で分布し，また同帯の北部には中期ジュラ紀～前期白亜紀浅海層からなる今浦層群が最大200 mの幅で狭長に分布している．南帯と南側の四万十帯との境界は中角北傾斜の仏像構造線であり，これまでに2箇所で断層露頭が確認されている(山際ほか，1976；坂・山口，1985)．一方，南帯と北側の黒瀬川帯(中帯)との境界も岩石の分布状況から高角の断層と推定されており，この断層の北東部については恵利原–櫛ヶ峰(えりはら–くしがみね)断層と呼ばれている(坂ほか，1988)．南伊勢町における南帯と黒瀬川帯との境界断層には小規模な蛇紋岩が伴われることがある(坂ほか，1979)．築地層群と今浦層群の境界は主に高角断層と考えられているが，2箇所で不整合とみなされる露頭が報告されている(坂，1983；坂ほか，1999)．

2．1　築地層群

築地層群は，山際・坂(1967)により命名され，厚い塊状砂岩と側方に連続性の良い層状チャートが構造的に繰り返し分布する「チャート–砕屑岩コンプレックス」(Kimura and Hori，1993)をなし，玄武岩，海山型石灰岩及び混在岩を僅かに含む．また，本層群は志摩半島に分布する付加体の中では変形が比較的弱く，整然相を示す部分も多い．

化石については，石灰岩から*Yabeina*属などの中期ペルム紀(原典では後期ペルム紀)の有孔虫化石が報告されている(山際，1969)ほか，チャートから中期三畳紀と中期ジュラ紀(一部，前期ジュラ紀？)の放散虫化石が，そして珪質泥岩から中期ジュラ紀～後期ジュラ紀前半の放散虫化石が報告されている(菅野ほか，1980；坂・手塚，1988；Ohba and Adachi，1995)．また，泥岩からも中期ジュラ紀～後期ジュラ紀前半の放散虫化石が報告されている(坂・手塚，1988)．

本層群は，岩相及び放散虫化石年代から，四国の斗賀野(とがの)層群(松岡，1984)に対比されている(坂・手塚，1988)．

2．2　今浦層群

今浦層群は提唱された当初，山際(1957)により今浦層と命名された．その後，山際・坂(1967)によって今浦層群として層序単元の階層が格上げされた．本層群は泥岩，砂岩，砂岩泥岩互層を主体とし，陸棚型石灰岩を僅かに伴う．泥岩は植物片化石を多く含み，風化部分は数mm～数cm角で細かく割れる特徴を示す．砂岩泥岩互層は断層沿い以外では整然相を示す．石灰岩は暗灰色を呈し，短径が最大数～10数m，長径が最大数10 mの岩塊として泥岩中に産する．これらの石灰岩は，ハンマーで叩くと石油臭がすること，陸源性砕屑物を含むこと，含有化石の種類などの特徴により，古くから礁性の鳥巣(とりのす)式石灰岩として認識されている(例えば，飯塚，1929)．

産出化石については，石灰岩から後期ジュラ紀を示すとされる珊瑚や層孔虫の化石が報告されている(例えば，藤本，1942；坂ほか，1979；山際ほか，1979)．また，泥岩から中期ジュラ紀，後期ジュラ紀，前期白亜紀の3つの異なる時代を示す放散虫化石が報告されている(坂・手塚，1988)ほか，後期ジュラ紀を示すアンモナイト(佐藤ほか，2005)，ウニ，二枚貝などの大型化石も報告されている(山際・坂，1967)．

今浦層群は付加体(築地層群)を被覆した前弧海盆堆積物であると考えられており(坂・手塚，1988)，四国の鳥巣層群に対比されている(山際・坂，1967；坂ほか，1979)．

３．放散虫化石年代

3．1　試料採取地点

付加体からなる築地層群の1地点(T1)，浅海層からなる今浦層群の3地点(I1 ～ 3)の泥岩から放散虫化石が得られた．それらの試料採取地点及び周辺ルートマップをそれぞれ第2図と第3図に示す．

3．1．1　築地層群

T1試料は，青峰山(あおのみねさん)東北東，鳥羽市松尾町の岳河内川(たけこうちがわ)(鈴串川(すずくしがわ)支流)枝沢に露出する砂岩泥岩互層中の泥岩である．この砂岩泥岩互層は露頭幅約4 mで，層厚30 cm以下の砂岩と泥岩が等量で互層し，整然相を示す．露頭は連続しないが，南隣(下位)にはチャート岩塊を含む混在岩が，北隣(上位)には砂岩優勢砂岩泥岩互層が産する(第3図a)．

3．1．2　今浦層群

I1試料は，青峰山東北東の岳河内川に注ぐ小沢(T1から西南西に約750 m離れた地点)に露出する泥岩である(第3図a)．この泥岩は露頭幅約3 mで，層厚2 mの砂岩層を挟有し，全体として整然相を示す．露頭は連続しないが，西隣(上位)には塊状砂岩が，東隣には数mm ～数cm角で細かく割れる特徴を示す泥岩を優勢に含む砂岩泥岩互層が産する．なお，この谷では長径4 m以下の鳥巣式石灰岩の転石が幾つかみられた．

I2試料は，青峰山南南西，磯部町沓掛(くつかけ)から青峰山へ向かう青峰登山道(磯部道)の6合目付近の西斜面，標高約115 m地点に産する泥岩である(第3図b)．この泥岩は露頭幅約3 mで，層厚数cm単位で成層しており，数mm～数cm角で細かく割れる特徴を示す．露頭は連続しな

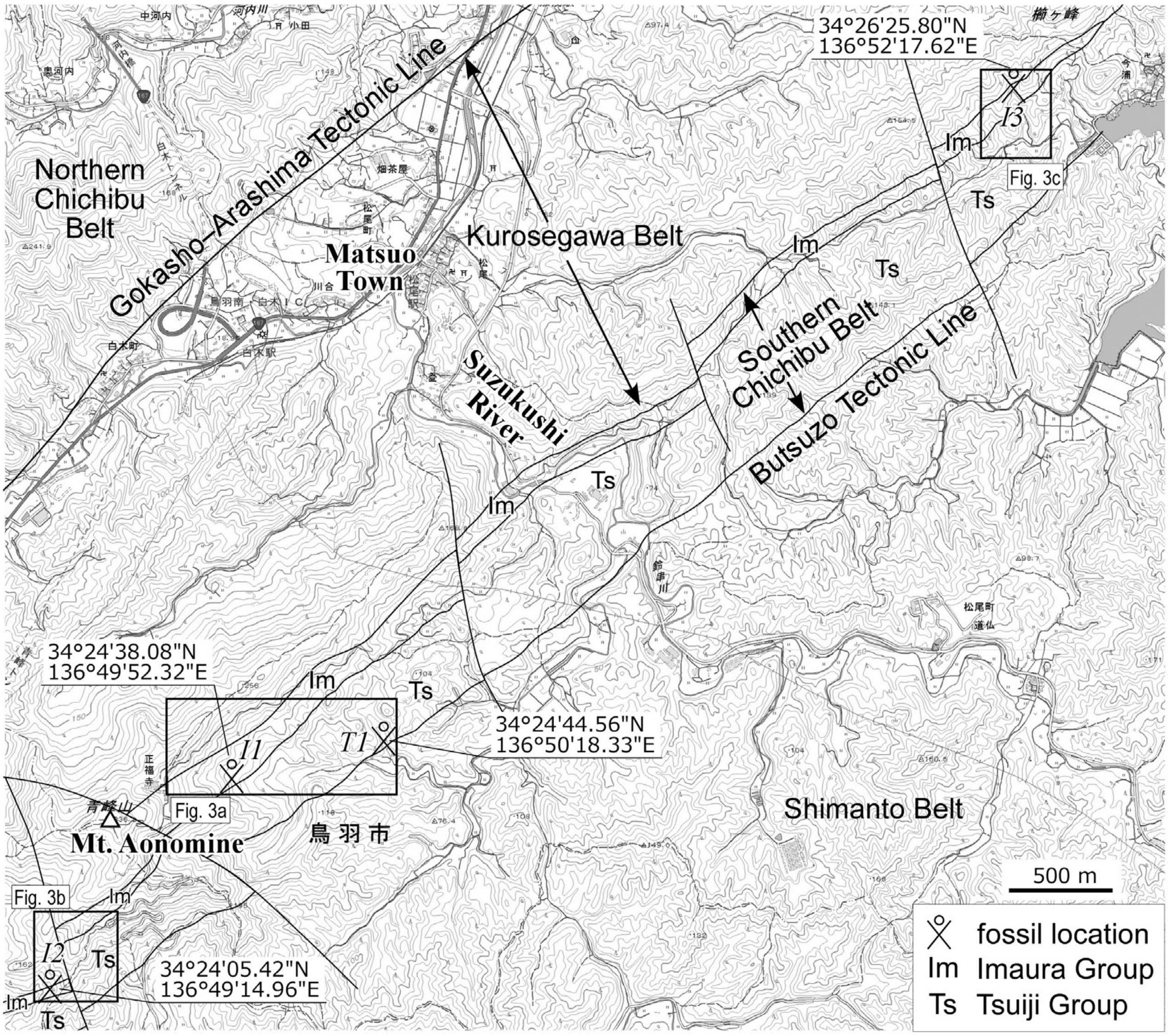

第2図　ジュラ紀放散虫化石産出地点．T1：築地層群の化石地点．I1–3：今浦層群の化石地点．地形図は地理院地図（http://maps.gsi.go.jp/#15/34.421105/136.851201/）を使用．

Fig. 2　Locations of Jurassic radiolarian fossils. T1: fossil location in the Tsuiji Group, I1–3: fossil location in the Imaura Group. Topographic map is from the GIS map (http://maps.gsi.go.jp/#15/34.421105/136.851201/) of the Geospatial Information Authority of Japan.

いが，北隣（上位）には整然相を示す砂岩泥岩互層が産する．なお，本地点から約300 m北方の標高約190 m地点には，藤本（1942）や山際ほか（1979）で報告された珊瑚化石を含む鳥巣式石灰岩が産している．この石灰岩露頭と含放散虫泥岩露頭との間には，黒瀬川帯のジュラ紀付加体青峰層群（山際・坂，1967）や南帯の築地層群が分布するため，I2を含む今浦層群は左横ずれを示す北北西–南南東走向の胴切断層により相対的に南にずれていると判断される（第3図b）．

I3試料は，鳥羽市の浦村町今浦付近の板敷川（いたじきがわ）に注ぐ小沢に露出する泥岩である（第3図c）．この泥岩は露頭幅約2 mで，数mm～数cm角で細かく割れる特徴を示す．露頭は連続しないが，南隣（下位）には塊状の砂岩が，北隣（上位）には整然相を示す砂岩泥岩互層が産する．

3. 2　微化石抽出処理方法

岩石試料は5%のフッ化水素酸溶液に約18時間浸した後にふるいで選別し，目合い65 μmと250 μmのふるいの間の残渣を得る操作を3回行った．残渣を乾燥した後，実体顕微鏡下で1試料につき約200個体の放散虫殻を拾い上げ，電子顕微鏡で観察・撮影し，そこから分類形質が残るものを検討対象とした．

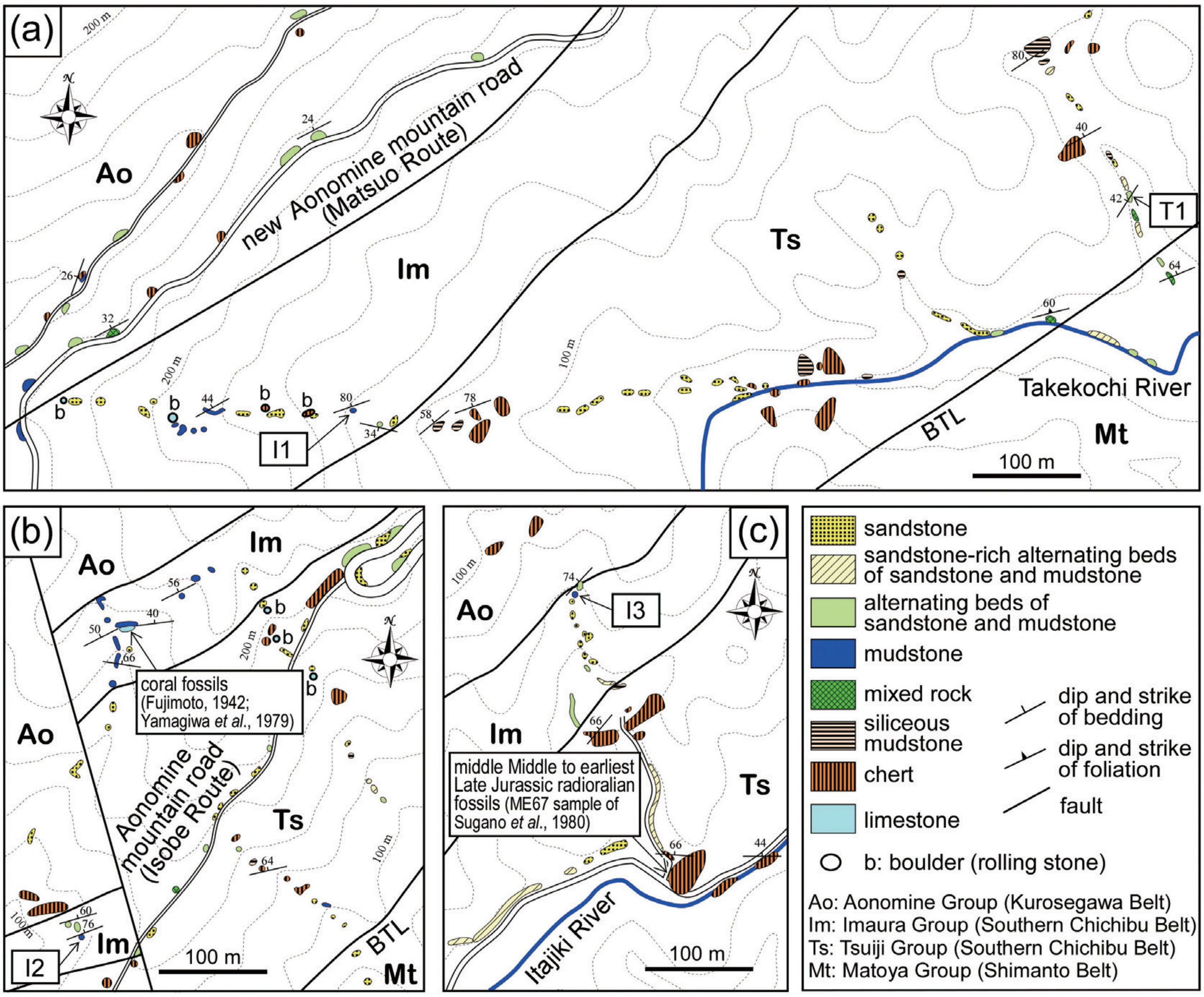

第3図　放散虫化石を産した露頭周辺のルートマップ．(a) 岳河内川北西のT1及びI1地点．(b) 青峰登山道（磯部道）西方のI2地点．(c) 板敷川北方のI3地点．

Fig. 3　Route maps around the Jurassic radiolarian fossil locations. (a) T1 and I1, northwest of Takekochi River. (b) I2, west of Aonomine mountain road (Isobe Route). (c) I3, north of Itajiki River.

3. 3　産出化石と時代

放散虫化石の化石帯は，特に断りが無い限り，Matsuoka (1995a) を改訂した松岡(2007) に従った．また，INTERRAD Jurassic-Cretaceous Working Group (1995) で使用されるUnitary Associations Zones (UAZ) との化石帯・時代対比はBaumgartner *et al.* (1995)のFigure 13及びMatsuoka (1995a) のFigure 3に基づいた．

3. 3. 1　T1地点（築地層群）

T1地点の泥岩からは，種レベルで同定された放散虫化石として，*Archaeodictyomitra* aff. *apiarium*，*Archaeospongoprunum imlayi*，*Cinguloturris carpatica*，*Crucella* cf. *theokaftensis*，*Emiluvia salensis*，*Eucyrtidiellum* cf. *ptyctum*，*Gongylothorax favosus oviformis*，*Homoeoparonaella* aff. *elegans* sensu Baumgartner *et al*. (1995)，*Hsuum brevicostatum*，*Orbiculiforma*? *heliotropica*，*Paronaella* aff. *pygmaea*，*Podobursa* cf. *spinosa*，*Pseudodictyomitra*? sp. D sensu Matsuoka and Yao (1985)，*Stichocapsa robusta*，*Stichomitra annibill* sensu Suzuki and Gawlick (2003)，*Striatojaponocapsa conexa* sensu Hatakeda *et al*. (2007)，*Striatojaponocapsa synconexa* sensu Hatakeda *et al*. (2007)，*Tricolocapsa tetragona*，*Tritrabs rhododactylus*，*Triversus* cf. *hexagonatus*，*Williriedellum carpathicum*，*Williriedellum* cf. *marcucciae*，*Zhamoidellum ovum*が見出された（第4図；第1表）．その他，属レベルで同定されたものとして*Eoxitus* sp.，*Napora* sp.や*Xitus* sp.などがある．

この群集は*Striatojaponocapsa conexa*を含んでおり，本種の産出期間を示したMatsuoka (1995b) を参考にすると，本群集の示す期間は*Striatojaponocapsa conexa*帯から*Kilinora spiralis*帯に至ると判断できる．また，*Striatojaponocapsa synconexa*は上記期間にも産するとされ(Hatakeda *et al*., 2007)，*Striatojaponocapsa synconexa*が共存することも，本群集が*Striatojaponocapsa conexa*帯～*Kilinora spiralis*帯に相当することと矛盾しない．Aita (1987) や西園 (1996) によると，本群集に含まれる*Cinguloturris carpatica*は，Aita (1987) の*Pseudoristola tsunoensis* (原典では*Amphipyndax tsunoensis*) 間隔帯 (*Striatojaponocapsa conexa*帯上部に相当) あるいは西園 (1996) の*Stichomitra*? *tairai*亜帯 (J6B) から産出し始める．*Stichomitra*? *tairai* Aita のシノニムである*Stichomitra annibill* (Suzuki and Gawlick, 2003) は，Aita (1987) の*Pseudoristola tsunoensis* 間隔帯 (*Striatojaponocapsa conexa*帯上部に相当) から*Zhamoidellum mikamense*帯最下部 (*Hsuum maxwelli*帯最下部に相当) にかけて産出する (Aita, 1987)．一方，本群集には，*Kilinora spiralis*帯に産する*Kilinora spiralis*をはじめとする*Kilinora*属や，同帯に初出現がみられる*Loopus primitivus*，*Solenotryma*? *ichikawai*，*Guexella nudata*，*Stichocapsa naradaniensis*などが含まれていない．すなわち，本群集は*Kilinora spiralis*帯を示す化石を含まない．

以上より，本試料の時代は*Striatojaponocapsa conexa*帯の上部に相当するカロビアン期前半～中頃の可能性を示す．

ところで，*Tricolocapsa tetragona*と*Williriedellum carpathicum*については，従来知られている生存期間との相違が認められるため，一考を要する．*Tricolocapsa tetragona*は，日本において*Striatojaponocapsa plicarum*帯最上部から*Striatojaponocapsa conexa*帯中部付近に産出が知られている (例えば，Matsuoka，1983；Aita，1987；西園，1996)．また，Matsuoka (1986) によると，*Williriedellum carpathicum* (原典では*Tricolocapsa yaoi*) は*Kilinora spiralis*帯の上部を初産出層準としている．しかし一方で，Suzuki and Gawlick (2003) によると，*Tricolocapsa tetragona*は*Kilinora spiralis*帯から産することが，また，Baumgartner *et al*. (1995) やBeccaro (2006) によると，*Williriedellum carpathicum*は*Kilinora spiralis*帯よりも下位の層準から産出することが報告されている．このことは，これら２種が*Striatojaponocapsa conexa*帯上部でも産出し得ることを示唆するものであるが，これらの種の生存期間と本群集との共存関係については今後更なる検討が必要である．

3. 3. 2　I1 地点 (今浦層群)

I1 地点の泥岩からは，種レベルで同定された放散虫化石として，*Archaeodictyomitra* aff. *rigida*，*Bistarkum* cf. *irazuense*，*Cinguloturris carpatica*，*Gongylothorax favosus oviformis*，*Loopus doliolum*，*Loopus primitivus*，*Paronaella* cf. *bronnimanni*，*Paronaella* cf. *mulleri*，*Pseudodictyomitra*? sp. D sensu Matsuoka and Yao (1985)，*Pseudoristola* cf. *tsunoensis*，*Tritrabs zealis*，*Triversus* aff. *japonicus*，*Xitus* aff. *pulcher* sensu Baumgartner *et al*. (1995)，*Zhamoidellum ovum*が，属レベルで同定されたものとして*Hsuum* sp.，*Napora* sp.，*Pantanellium* sp.，*Podobursa* sp.，*Praeparvicingula* sp.，*Xitus* sp.などがある (第 5 図；第 1 表)．

この群集には，*Loopus primitivus*帯の指標種である*Loopus primitivus*が含まれる．この種の初産出層準は*Kilinora spiralis*帯であり (Hori *et al*., 2002；Ishida，2008)，最終産出層準は*Pseudodictyomitra carpatica*帯の下部である (Matsuoka，1992)．この群集に含まれる*Cinguloturris carpatica*の初産出及び最終産出層準は，それぞれ*Striatojaponocapsa conexa*帯 (西園，1996)，ジュラ系／白亜系境界付近 (Baumgartner *et al*., 1995) とされており，Hori (1999) によると，*Pseudodictyomitra carpatica*帯にも産出が知られている．これら 2 種の共存関係から，この群集は*Kilinora spiralis*帯から*Pseudodictyomitra carpatica*帯の下部に産出が限定される．また，*Striatojaponocapsa plicarum* 帯上部から*Hsuum maxwelli* 帯に生存期間を持つ*Hsuum maxwelli* gr. (Matsuoka, 1995b) 及び*Pseudodictyomitra carpatica*帯から産出し始める*Pseudodictyomitra carpatica*が含まれないことから判断すると，この群集は*Loopus primitivus*帯から産するものに限定でき，チトニアン期前半の可能性を示す．

一方，Aita (1987)によると，*Pseudoristola tsunoensis*は，*Pseudoristola tsunoensis* 間隔帯 (*Striatojaponocapsa conexa*

(p. 31 →)

第 4 図　築地層群の地点T1 の泥岩から得られたカロビアン期前半～中頃の放散虫化石の電子顕微鏡画像.

Fig. 4　Scanning electron microscope images of early–middle Callovian radiolarians extracted from mudstone at the location T1, the Tsuiji Group.

1: *Archaeodictyomitra* aff. *apiarium* (Rüst), 2–9: *Archaeodictyomitra* spp., 10: *Pseudodictyomitra*? sp. D sensu Matsuoka and Yao (1985), 11–12: *Cinguloturris carpatica* Dumitrică, 13: *Cinguloturris* sp., 14: *Stichomitra annibill* Kocher sensu Suzuki and Gawlick (2003), 15–16: *Xitus* spp., 17: *Eoxitus* sp., 18: *Triversus* cf. *hexagonatus* (Heitzer), 19: *Hsuum brevicostatum* (Ozvoldová), 20: *Wrangellium*? sp., 21–25: *Tetracapsa* spp., 26: *Tetracapsa*? sp., 27: *Stichocapsa robusta* Matsuoka, 28: *Zhamoidellum* sp., 29: *Zhamoidellum ovum* Dumitrică, 30: *Williriedellum* cf. *marcucciae* Cortese, 31: *Williriedellum* sp., 32: *Williriedellum carpathicum* Dumitrică, 33: *Gongylothorax favosus oviformis* Suzuki and Gawlick, 34–35: *Striatojaponocapsa synconexa* O'Dogherty *et al*. sensu Hatakeda *et al*. (2007), 36–37: *Striatojaponocapsa conexa* (Matsuoka) sensu Hatakeda *et al*. (2007), 38: *Tricolocapsa tetragona* Matsuoka, 39: *Helvetocapsa*? sp., 40: *Eucyrtidiellum* cf. *ptyctum* (Riedel and Sanfilippo), 41: *Spongurus* sp., 42: *Napora* sp., 43: *Podobursa* cf. *spinosa* (Ozvoldová), 44: *Podobursa* sp., 45–46: *Spongotripus* sp., 47: *Archaeospongoprunum imlayi* Pessagno, 48: *Archaeospongoprunum* sp., 49: *Homoeoparonaella* aff. *elegans* (Pessagno) sensu Baumgartner *et al*. (1995), 50: *Paronaella* aff. *pygmaea* Baumgartner, 51: *Emiluvia salensis* Pessagno, 52: *Orbiculiforma*? *heliotropica* Baumgartner, 53: *Crucella* cf. *theokaftensis* Baumgartner, 54–56: *Tritrabs rhododactylus* Baumgartner.

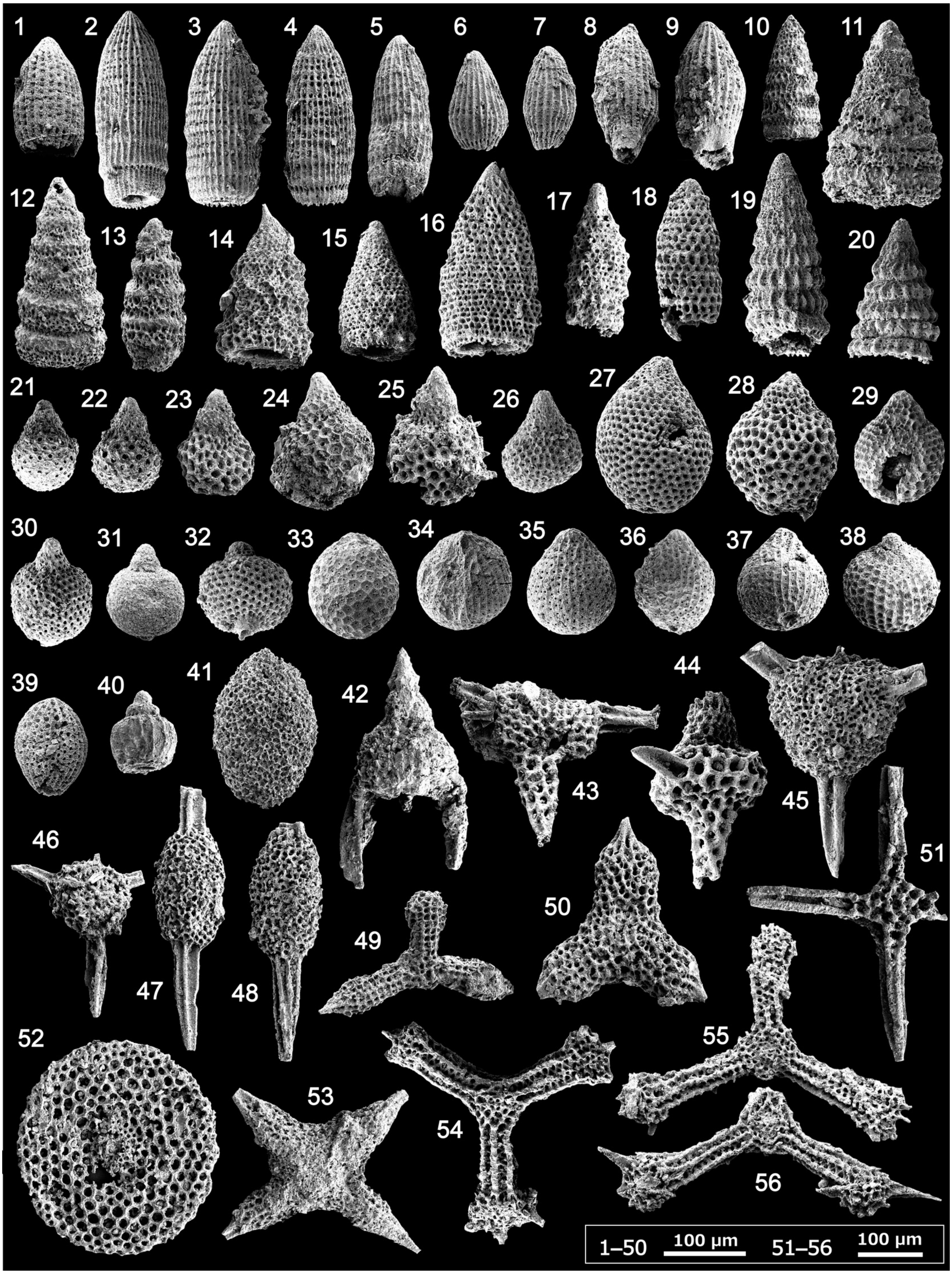
1
2
3
4
5
6
7
8
9
10
11
12
13
14
15
16
17
18
19
20
21
22
23
24
25
26
27
28
29
30
31
32
33
34
35
36
37
38
39
40
41
42
43
44
45
46
47
48
49
50
51
52
53
54
55
56
1–50 100 µm
51–56 100 µm

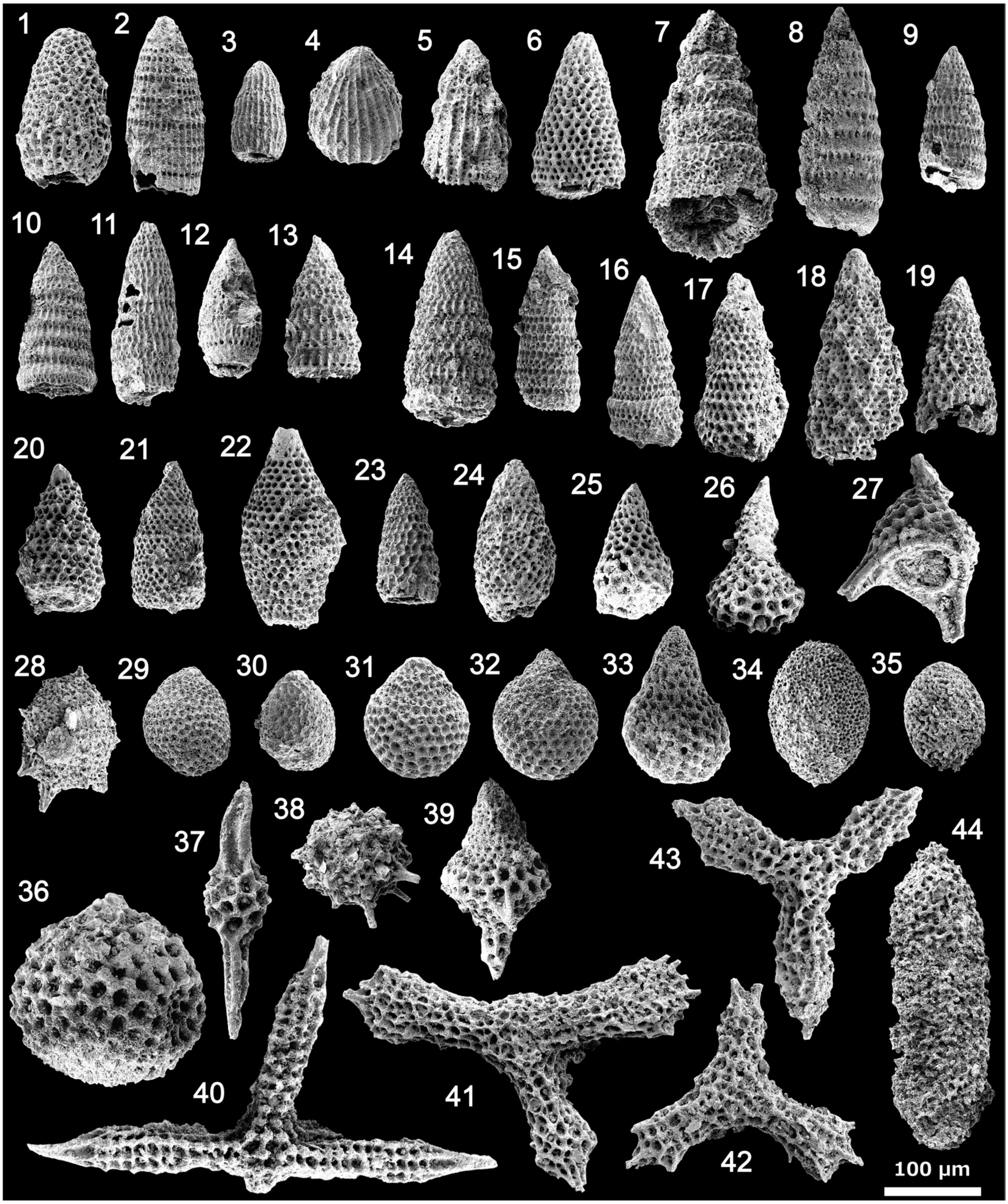

第 5 図　今浦層群の I1 地点の泥岩から得られたチトニアン期前半の放散虫化石の電子顕微鏡画像.

Fig. 5　Scanning electron microscope images of early Tithonian radiolarians extracted from mudstone at the I1 location, the Imaura Group.

1: *Droltus* sp., 2: *Archaeodictyomitra* aff. *rigida* Pessagno, 3–4: *Archaeodictyomitra* spp., 5: *Hsuum* sp., 6: *Triversus* aff. *japonicus* Takemura, 7: *Cinguloturris carpatica* Dumitrică, 8: *Loopus doliolum* Dumitrică, 9–11: *Loopus primitivus* (Matsuoka and Yao), 12: *Loopus*? sp., 13: *Wrangellium*? sp., 14: *Dictyomitrella*? sp., 15–16: *Pseudodictyomitra*? sp. D sensu Matsuoka and Yao (1985), 17: *Pseudoristola* cf. *tsunoensis* (Aita), 18: *Xitus* aff. *pulcher* Pessagno sensu Baumgartner *et al*. (1995), 19: *Xitus* sp., 20: *Xitus*? sp., 21–26: Nassellaria gen. et sp. indet., 27: *Napora* sp., 28: *Orbiculiforma*? sp., 29: *Zhamoidellum* sp., 30: *Gongylothorax* cf. *favosus oviformis* Suzuki and Gawlick, 31–32: *Zhamoidellum ovum* Dumitrică, 33: *Tetracapsa* sp., 34: *Spongurus* sp., 35: *Archicapsa*? sp., 36: Spumellaria gen. et sp. indet., 37: *Pantanellium* sp., 38: *Actinomma* sp., 39: *Podobursa* sp., 40: *Tritrabs zealis* (Ozvoldová), 41–42: *Paronaella* cf. *bronnimanni* Pessagno, 43: *Paronaella* cf. *mulleri* Pessagno, 44: *Bistarkum* cf. *irazuense* (Aita).

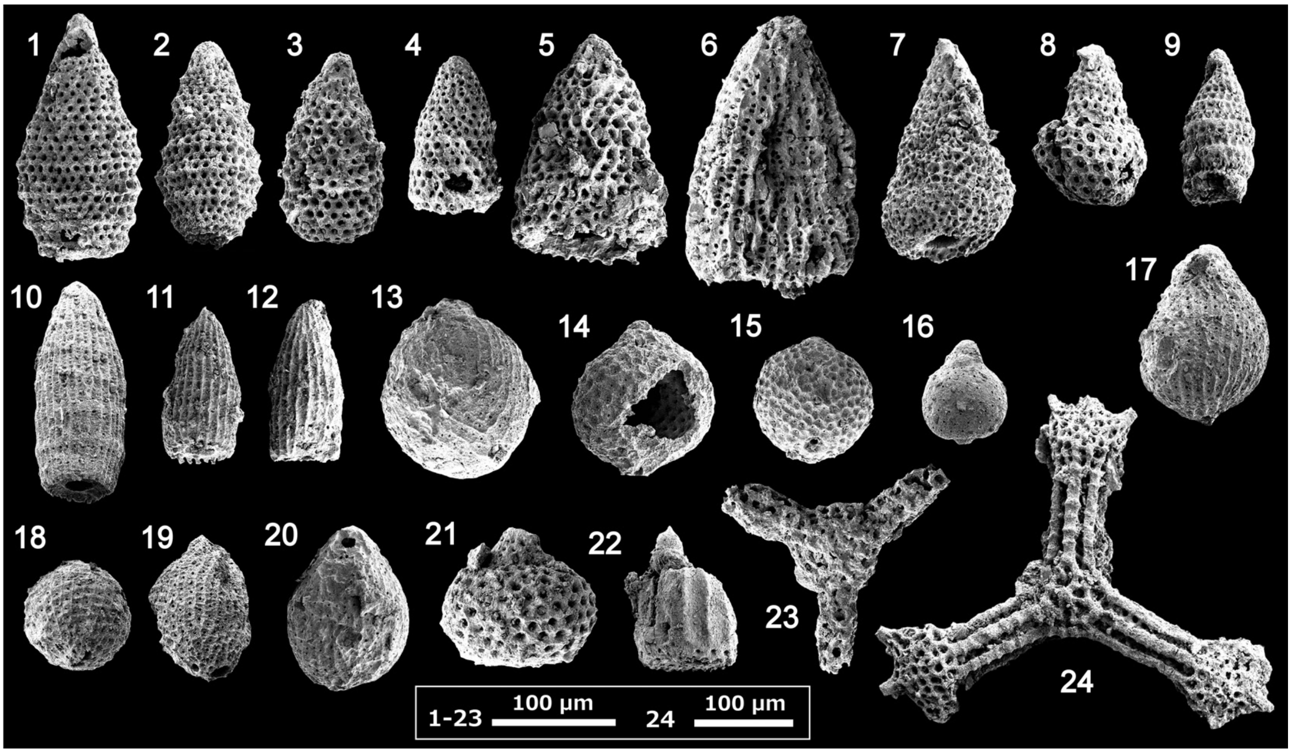

第6図　今浦層群のI2地点の泥岩から得られたバトニアン期中頃～カロビアン期後半の放散虫化石の電子顕微鏡画像.

Fig. 6　Scanning electron microscope images of middle Bathonian to late Callovian radiolarians extracted from mudstone at the I2 location, the Imaura Group.

1–2: *Tethysetta* spp., 3: *Triversus hungaricus* (Kozur), 4. *Triversus* aff. *schardti* O'Dogherty *et al*., 5: *Triversus* sp., 6: *Hsuum* sp., 7: *Spongocapsula* sp., 8: *Hiscocapsa*? sp., 9: *Pseudodictyomitra* sp., 10–12: *Archaeodictyomitra* spp., 13: *Kilinora*? sp., 14–15: *Williriedellum dierschei* Suzuki and Gawlick, 16: *Williriedellum* sp., 17: *Striatojaponocapsa synconexa* O'Dogherty *et al*. sensu Hatakeda *et al*. (2007), 18–19: *Striatojaponocapsa conexa* (Matsuoka) sensu Hatakeda *et al*. (2007), 20–21: Nassellaria gen. et sp. indet., 22: *Eucyrtidiellum* cf. *ptyctum* (Riedel and Sanfilippo), 23: Spumellaria gen. et sp. indet., 24: *Tritrabs exotica* (Pessagno).

帯上部に相当）から*Gongylothorax sakawaensis* 帯（*Kilinora spiralis*帯に相当）に産するとされる．すなわち本種は，現在の知見では本試料の群集帯（*Loopus primitivus*帯）よりも古い時代を示すため，本種の生存期間と本群集との共存関係については今後更なる検討が必要である．また，Aita (1987) では，*Bistarkum irazuense*（原典では*Amphibrachium irazuense*）も*Pseudoristola tsunoensis*と同じ産出期間を示すとしているが，INTERRAD Jurassic-Cretaceous Working Group (1995) ではUAZ 14～21（前期白亜紀の*Pseudodictyomitra carpatica*帯上部～ *Acanthocircus carinatus*帯に相当）に産するとしており，本種の産出は長期間にわたる可能性がある．

3. 3. 3　I2地点（今浦層群）

I2地点の泥岩からは，種レベルまで同定された放散虫化石として，*Eucyrtidiellum* cf. *ptyctum*，*Striatojaponocapsa conexa* sensu Hatakeda *et al*. (2007)，*Striatojaponocapsa synconexa* sensu Hatakeda *et al*. (2007)，*Tritrabs exotica*，*Triversus hungaricus*，*Triversus* aff. *schardti*，*Williriedellum dierschei*が，属レベルで同定されたものとして*Archaeodictyomitra* sp.，*Hsuum* sp.，*Kilinora*? sp.，*Pseudodictyomitra* sp.，*Tethysetta* sp.などがある（第6図；第1表）．

この群集には*Striatojaponocapsa conexa*と*Striatojaponocapsa synconexa*が含まれるが，この2種の共存関係はHatakeda *et al*. (2007) によれば*Striatojaponocapsa conexa*帯最下部から*Kilinora spiralis*帯にかけて知られている．*Kilinora spiralis*は*Kilinora spiralis*帯下半部に生存期間があるが（例えば，Matsuoka，1986），この群集には含まれていない．また，*Kilinora spiralis*帯上部での産出が知られる*Loopus primitivus*や*Solenotryma*? *ichikawai*，*Stichocapsa naradaniensis*（例えば，Matsuoka，1986；INTERRAD Jurassic-Cretaceous Working Group，1995）などが含まれないことから判断して，この群集は*Striatojaponocapsa conexa*帯から産するものに相当すると考えられる．すなわち，本試料の時代はバトニアン期中頃～カロビアン期後半の可能性がある．

3. 3. 4　I3地点（今浦層群）

I3地点の今浦層群の泥岩からは，種レベルまで同定された放散虫化石として，*Archaeodictyomitra cellulata*, *Cinguloturris* cf. *carpatica*, *Dictyomitrella*? *kamoensis*, *Eucyrtidiellum nodosum*, *Helvetocapsa*? cf. *prealpina*, *Hsuum* aff. *baloghi*, *Hsuum brevicostatum*, *Hsuum maxwelli*, *Kilinora spiralis*, *Obesacapsula magniglobosa*, *Parahsuum carpathicum*, *Paronaella kotura*, *Paronaella pygmaea*, *Plicaforacapsa catenarum*, *Praewilliriedellum cephalospinosum*, *Praewilliriedellum spinosum*, *Protunuma*? *ochiensis*, *Pseudoeucyrtis* cf. *firmus*, *Pseudoristola nova*, *Pseudoristola tsunoensis* sensu O'Dogherty *et al*. (2006), *Sethocapsa aitai*, *Stichocapsa* aff. *magnipora*, *Striatojaponocapsa synconexa* sensu Hatakeda *et al*. (2007), *Triversus japonicus*が見出された．また，属レベルで同定されたものとして*Tethysetta* sp.などがある(第7図；第1表)．

本群集は*Kilinora spiralis*帯の指標種である*Kilinora spiralis*を含む．この種の初産出層準は*Kilinora spiralis*帯の基底を定義し，生存期間は同帯下半部にある(例えば，Matsuoka，1986)．また，*Plicaforacapsa catenarum*は，*Kilinora spiralis*とほぼ同じ生存期間を示す(Matsuoka, 1986)．*Sethocapsa aitai* は，Chiari *et al*. (2002)によりアルバニア北部のミルディタ(Mirdita)オフィオライトの被覆層から新種記載され，その産出期間はUAZ 6 〜 7 (*Kilinora spiralis* 帯に相当)とされている．*Archaeodictyomitra cellulata*, *Helvetocapsa*? *prealpina*, *Pseudoristola tsunoensis* sensu O'Dogherty *et al*. (2006) は，O'Dogherty *et al*. (2006)によってアルプスのゲッツナップと呼ばれる地層から見出された種で，その時代はUAZ 6付近(*Kilinora spiralis*帯下部に相当)を示すとされている．

したがって，この群集の示す時代は*Kilinora spiralis*帯下半部に相当するカロビアン期後半〜オックスフォーディアン期中頃である．

4．考　察

築地層群及び今浦層群の泥岩からこれまで得られた放散虫化石の時代を整理し，今回のデータと合わせて年代層序図を作成した(第8図)．なお，陸源性砕屑岩の時代を議論するため，付加体である築地層群に関してはジュラ紀以降のデータを示してある．本章では，今回得られた放散虫化石が，それぞれの地層群において持つ意義について触れる．

4．1　築地層群

築地層群では，菅野ほか(1980)が鳥羽市浦村町今浦の板敷川沿い林道脇のチャート(例えば，ME67試料；第3図のc参照)から，中〜後期ジュラ紀の放散虫化石を報告した．この論文は志摩半島から初めて放散虫化石を報告した画期的なものであるが，当時はまだジュラ紀の放散虫化石の分類及び化石帯区分が十分に確立されていなかったため，生存期間に基づく時代決定には限界があった．菅野ほか(1980)の図版に掲載されたME67試料の放散虫化石写真を再検討したところ，*Diacanthocapsa*? sp. (菅野ほか，1980のPlate 3のFig. 2)は*Striatojaponocapsa synconexa*に，*Hsuum*? sp. (同Plate 4のFig. 5)は*Hsuum brevicostatum*に，*Parvicingula hsui* (同Plate 4のFig. 7)は*Tethysetta elongatus*に，*Tricolocapsa* sp. A (同Plate 3のFig. 3)は*Praezhamoidellum* aff. *yaoi*に同定でき，それらに加え*Striatojaponocapsa*(原典では*Tricolocapsa*属) *plicarum*, *Hsuum maxwelli*, *Tricolocapsa* cf. *rüsti*などが含まれていることから，それらの種で構成される群集が示す時代は，現在の知見では*Striatojaponocapsa plicarum*帯上部〜 *Striatojaponocapsa conexa*帯(バトニアン期〜オックスフォーディアン期初頭)に限定することができる．

坂・手塚(1988)は，鳥羽市浦村町生浦(おうのうら)湾の海岸や青峰山南斜面の登山道沿いにおいて複数地点の泥岩から放散虫化石を見出し，それらの化石群集から本層群の泥岩が中期ジュラ紀後半〜後期ジュラ紀初頭(*Stratiojaponocapsa conexa*帯)と後期ジュラ紀前半(*Kilinora spiralis*帯〜 *Hsuum maxwelli*帯下部)の2つの時代を示すとした．ちなみに，Ohba and Adachi (1995)は鳥羽市今浦から*Kilinora spiralis*で代表される後期ジュラ紀前半(*Kilinora spiralis*帯)を示す珪質泥岩を見出している．なお，彼らは鳥羽市大村島(第1図)より*Kilinora spiralis*を含む後期ジュラ紀前半(*Kilinora spiralis*帯)を示す泥岩を見出し，これを築地層群のものと考えた．しかし，この泥岩は中期ジュラ紀〜前期白亜紀の浅海層からなる松尾層群(山際，1957)より北側に産し，岩相的にも黒瀬川帯のジュラ紀付加体(青峰層群)に含められるべきであるため，本議論からは除外する．

築地層群の泥岩から放散虫化石を報告した坂・手塚(1988)では，放散虫化石の標本写真は掲載されていない．本研究では，豊富な化石種の写真を提示し，築地層群の泥岩についてカロビアン期前半〜中頃といったより精度の高い堆積年代を明らかにすることができた(第8図)．そして，この時代は，中期ジュラ紀中頃〜後期ジュラ紀前半という坂・手塚(1988)が示した年代データの範囲に収まる．

4．2　今浦層群

今浦層群の堆積年代に関しては，鳥巣式石灰岩及び泥岩中の化石に基づき，これまで後期ジュラ紀と考えられていた(例えば，山際ほか，1979;坂ほか，1979)．例えば，泥岩中から得られたアンモナイト化石は後期ジュラ紀のキンメリッジアン期後半〜チトニアン期前半を示している(佐藤ほか，2005)．

しかし，坂・手塚(1988)は，南伊勢町泉川(鳥羽地域西隣の区画)や磯部町恵利原の泥岩から放散虫化石を抽出し，*Striatojaponocapsa plicarum*と*Japonocapsa*

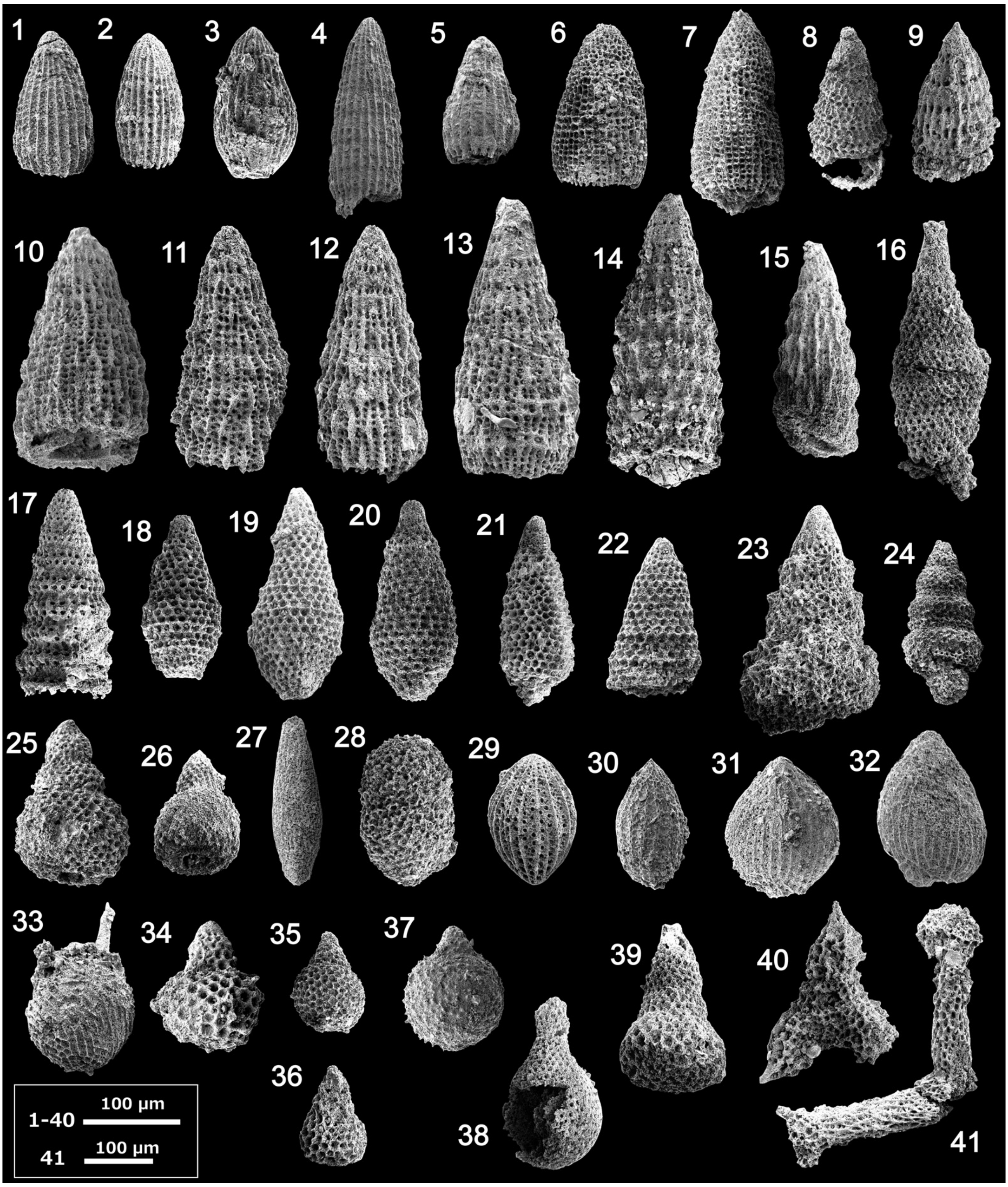

第7図　今浦層群（南帯）のI3地点の泥岩から得られたカロビアン期後半〜オックスフォーディアン期中頃の放散虫化石の電子顕微鏡画像.

Fig. 7　Scanning electron microscope images of late Callovian to middle Oxfordian radiolarians extracted from mudstone at the I3 location, the Imaura Group.

1: *Archaeodictyomitra cellulata* O'Dogherty *et al*., 2–5: *Archaeodictyomitra* spp., 6: *Parahsuum* aff. *carpathicum* Widz and De Wever, 7: *Parahsuum carpathicum*, 8: *Dictyomitrella*? *kamoensis* Mizutani and Kido, 9: *Loopus*? sp., 10–12: *Hsuum maxwelli* Pessagno, 13: *Hsuum* aff. *baloghi* Grill and Kozur, 14: *Hsuum brevicostatum* (Ozvoldová), 15: *Hsuum* sp., 16: *Pseudoeucyrtis* cf. *firmus* Hull, 17: *Dictyomitrella*? sp., 18: *Tethysetta* sp., 19: *Tethysetta*? sp., 20: *Pseudoristola tsunoensis* (Aita) sensu O'Dogherty *et al*. (2006), 21: *Triversus* sp., 22: *Triversus japonicus* Takemura, 23: *Obesacapsula magniglobosa* Aita, 24: *Cinguloturris* cf. *carpatica* Dumitrică, 25: *Sethocapsa aitai* Chiari *et al*., 26: *Eucyrtidiellum nodosum* Wakita, 27: *Helvetocapsa*? cf. *prealpina* O'Dogherty *et al*., 28: *Spongurus* sp., 29: *Protunuma*? *ochiensis* Matsuoka, 30: *Plicaforacapsa catenarum* (Matsuoka), 31–32: *Striatojaponocapsa synconexa* O'Dogherty *et al*. sensu Hatakeda *et al*. (2007), 33: *Kilinora spiralis* (Matsuoka), 34: *Tetracapsa* sp., 35: *Tetracapsa*? sp., 36: *Stichocapsa* aff. *magnipora* Chiari *et al*., 37: *Praewilliriedellum spinosum* Kozur, 38: *Praewilliriedellum cephalospinosum* Kozur, 39: *Pseudoristola nova* Yang and Wang, 40: *Paronaella pygmaea* Baumgartner, 41: *Paronaella kotura* Baumgartner.

第 1 表　築地層群及び今浦層群から得られた放散虫化石のリスト.
Table 1　List of the radiolarian fossils extracted from the Tsuiji and Imaura groups.

Location	T1	I1	I2	I3
Group	Tsuiji	Imaura	Imaura	Imaura
Actinomma sp.		*		
Archaeodictyomitra apiarium (Rüst)	aff.			
Archaeodictyomitra cellulata O'Dogherty *et al.*				*
Archaeodictyomitra rigida Pessagno		aff.		
Archaeodictyomitra sp.	*	*	*	*
Archaeospongoprunum imlayi Pessagno	*			
Archaeospongoprunum sp.	*			
Archicapsa sp.		?		
Bistarkum irazuense (Aita)		cf.		
Cinguloturris carpatica Dumitrică	*	*		cf.
Cinguloturris sp.	*			
Crucella theokaftensis Baumgartner	cf.			
Crucella sp.	*			
Dictyomitrella? *kamoensis* Mizutani and Kido				*
Dictyomitrella sp.		?		?
Droltus sp.		*		
Emiluvia salensis Pessagno	*			
Eoxitus sp.	*			
Eucyrtidiellum nodosum Wakita				*
Eucyrtidiellum ptyctum (Riedel and Sanfilippo)	cf.		cf.	
Gongylothorax favosus oviformis Suzuki and Gawlick	*	cf.		
Helvetocapsa? *prealpina* O'Dogherty *et al.*				cf.
Helvetocapsa sp.	?			
Hiscocapsa sp.			?	
Homoeoparonaella elegans (Pessagno) sensu Baumgartner *et al*. (1995)	aff.			
Hsuum baloghi Grill and Kozur				aff.
Hsuum brevicostatum (Ozvoldová)	*			*
Hsuum maxwelli Pessagno				*
Hsuum sp.		*	*	*
Kilinora spiralis (Matsuoka)				*
Kilinora sp.			?	
Loopus doliolum Dumitrică		*		
Loopus primitivus (Matsuoka and Yao)		*		
Loopus sp.		?		?
Napora sp.	*	*		
Obesacapsula magniglobosa Aita				*
Orbiculiforma? *heliotropica* Baumgartner	*			
Orbiculiforma sp.		?		
Pantanellium sp.		*		
Parahsuum carpathicum Widz and De Wever				*, aff.
Paronaella bronnimanni Pessagno		cf.		
Paronaella kotura Baumgartner				*
Paronaella mulleri Pessagno		cf.		
Paronaella pygmaea Baumgartner	aff.			*
Plicaforacapsa catenarum (Matsuoka)				*
Podobursa spinosa (Ozvoldová)	cf.			
Podobursa sp.	*	*		
Praewilliriedellum cephalospinosum Kozur				*
Praewilliriedellum spinosum Kozur				*
Protunuma? *ochiensis* Matsuoka				*
Pseudodictyomitra? sp. D sensu Matsuoka and Yao (1985)	*	*		
Pseudodictyomitra sp.			*	
Pseudoeucyrtis firmus Hull				cf.
Pseudoristola nova Yang and Wang				*
Pseudoristola tsunoensis (Aita)		cf.		
Pseudoristola tsunoensis (Aita) sensu O'Dogherty *et al*. (2006)				*
Sethocapsa aitai Chiari *et al.*				*
Spongocapsula sp.			*	
Spongotripus sp.	*			
Spongurus sp.	*	*		*
Stichocapsa magnipora Chiari *et al.*				aff.
Stichocapsa robusta Matsuoka	*			
Stichomitra annibill sensu Suzuki and Gawlick (2003)	*			
Striatojaponocapsa conexa (Matsuoka) sensu Hatakeda *et al*. (2007)	*		*	
Striatojaponocapsa synconexa O'Dogherty *et al.* sensu Hatakeda *et al*. (2007)	*		*	*
Tethysetta sp.			*	*, ?
Tetracapsa sp.	*, ?	*		*, ?
Tricolocapsa tetragona Matsuoka	*			
Tritrabs exotica (Pessagno)			*	
Tritrabs rhododactylus Baumgartner	*			
Tritrabs zealis (Ozvoldová)		*		
Triversus hexagonatus (Heitzer)	cf.			
Triversus hungaricus (Kozur)			*	
Triversus japonicus Takemura		aff.		*
Triversus schardti			aff.	
Triversus sp.			*	*
Williriedellum carpathicum Dumitrică	*			
Williriedellum dierschei Suzuki and Gawlick			*	
Williriedellum marcucciae Cortese	cf.			
Williriedellum sp.	*		*	
Wrangellium sp.	?	?		
Xitus aff. *pulcher* Pessagno sensu Baumgartner *et al*. (1995)		*		
Xitus sp.	*	*, ?		
Zhamoidellum ovum Dumitrică	*	*		
Zhamoidellum sp.	*	*		

（原典では*Tricolocapsa*?）*fusiformis*の産出で示される中期ジュラ紀中頃（*Striatojaponocapsa plicarum*帯），*Striatojaponocapsa conexa*や*Dictyomitrella*? *kamoensis*の産出で示される中期ジュラ紀後半～後期ジュラ紀前半（*Striatojaponocapsa conexa*帯～*Kilinora spiralis*帯），*Kilinora spiralis*や *Cinguloturris carpatica*の産出で示される後期ジュラ紀前半（*Kilinora spiralis*帯）だけでなく（ジュラ紀放散虫化石の標本写真は不掲載），*Acaeniotyle umbilicata*, *Holocryptocanium astiensis*, *Pseudodictyomitra* cf. *carpatica*, *Pseudodictyomitra* cf. *depressa*, *Thanarla* cf. *conica*, *Williriedellum peterschmittae*などの産出で示される前期白亜紀バランギニアン期～バレミアン期（*Pseudodictyomitra carpatica*帯上部～*Acanthocircus carinatus*帯）の時代が識別できることを明らかにした（第8図）．今浦層群がこのように中期ジュラ紀～前期白亜紀の長期間にわたる時代を示すことに関し，坂・手塚（1988）や坂ほか（1999）は，鳥巣石灰岩が泥岩中のレンズ状岩塊として産することや，一部にチャートや砂岩を岩塊として含む産状が認められることを根拠として，ジュラ紀の化石を含む泥岩の再堆積による可能性を支持している．

本研究では前期白亜紀の放散虫化石は得られなかったものの，泥岩からの豊富な化石種に基づき，バトニアン期中頃～カロビアン期後半（*Striatojaponocapsa conexa*帯付近），カロビアン期後半～オックスフォーディアン期中頃（*Kilinora spiralis*帯付近），チトニアン期前半（*Loopus primitiva*帯付近）という異なる3つの時代を示す放散虫化石が得られた（第8図）．このことは，今浦層群の泥岩が比較的長い堆積年代幅（約2,000万年）を持つという点で坂・手塚（1988）の結果と類似している．本研究では，放散虫化石が抽出された泥岩が礫質であったり，露頭周辺で崩壊堆積物や土石流堆積物などが認められたりといった，放散虫化石あるいは含化石泥岩の再堆積に繋がる証拠は確認できていない．したがって，現時点では今浦層群の堆積年代にはある程度の幅があると考えておく．ただし，分布幅から推定される今浦層群全体の層厚は200 m程度とさほど厚くなく，遠洋性堆積物に比べ一般に堆積速度の速い陸源性砕屑物を主体とする今浦層群が中期ジュラ紀から前期白亜紀までゆっくりと堆積した（堆積速度は1,000年で1 cm）のかどうか，すなわち付加テクトニクスが進行する基盤上で長期間安定的に堆積できるかについては，今後検討されるべき課題である．

5. まとめ

志摩半島に分布する秩父累帯南帯の築地層群（付加体）と今浦層群（浅海層）の泥岩から放散虫化石を見出した．前者は中期ジュラ紀後半（カロビアン期前半～中頃）の時代を，後者は中期ジュラ紀後半（バトニアン期中頃～カロビアン期後半），後期ジュラ紀前半（カロビアン期後半～オックスフォーディアン期中頃），後期ジュラ紀後半（チトニアン期前半）という3つの時代を示す．これらの時代はこれまでの既存研究で示された年代データの範囲に収まる．

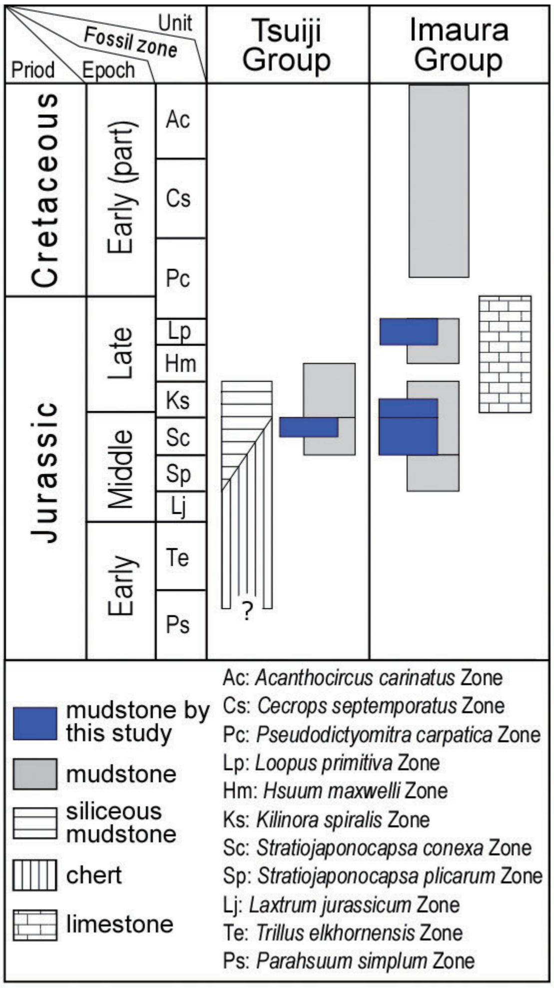

第8図　築地及び今浦層群の岩相・放散虫化石年代を示した年代層序図．築地層群に関してはジュラ紀以降のものを記した．放散虫化石帯は松岡（2007）に従った．

Fig. 8　Chronostratigraphic column illustrating the relation between lithofacies and radiolarian age of the Tsuiji and Imaura groups.
The post-Triassic ages are shown for the Tsuiji Group. Radiolarian zonation is from Matsuoka (2007).

謝辞：地質調査総合センター地質試料調製グループの技官諸氏には薄片を作成していただいた．査読者の中江訓博士（地質情報研究部門）には原稿改善に有益なご指摘をいただいた．記して感謝の意を表する．

文　献

Aita, Y.（1987）Middle Jurassic to Lower Cretaceous radiolarian biostratigraphy of Shikoku with reference to selected sections in Lombardy basin and Sicily. *Tohoku Univ. Sci. Rep*., *Second series (Geology)*, **58**, 1–91.

Baumgartner, P. O., O' Dogherty, L., Gorican, S., Dumitrică-Jud, R., Dumitrică, P., Pillevuit, A., Urquhart, E., Matsuoka, A., Danelian, T., Bartolini, A., Carter, E. S., De Wever, P., Kito, N., Marcucci, M. and Steiger, T.（1995）Radiolarian catalogue and systematics of Middle Jurassic to Early Cretaceous Tethyan genera and species. *In* Baumgartner, P. O. *et al*., eds., *Middle Jurassic to Lower Cretaceous Radiolaria of Tethys: Occurrences*, *Systematics*, *Biochronology*. Mém. Géol. (Lausanne), no. 23, 37–685.

Beccaro, P.（2006）*Radiolarian biostratigraphy of Middle-Upper Jurassic pelagic siliceous successions of western Sicily and the southern Alps (Italy)*. Mém. Géol. (Lausanne), no. 45, 120p.

Chiari, M., Marcucci, M. and Prela, M.（2002） New species of Jurassic radiolarians in the sedimentary cover of ophiolites in the Mirdita area, Albania. *Micropaleontology*, **48**, 61–88.

藤本治義（1942）　三重県鳥羽地方の地質について．地質雑，**49**，585.

Hatakeda, K., Suzuki, N. and Matsuoka, A.（2007）Quantitative morphological analyses and evolutionary history of the Middle Jurassic polycystine radiolarian genus *Striatojaponocapsa* Kozur. *Marine Micropaleontology*, **63**, 39–56.

Hori, N.（1999）Latest Jurassic radiolarians from the northeastern part of the Torinoko Block, Yamizo Mountains, central Japan. *Sci. Rep. Inst. Geosci.*, *Univ. Tsukuba*, *Section B*, **20**, 47–114.

Hori, N., Saito, M. and Toshimitsu, S.（2002）Late Jurassic radiolarian fauna from the Ikenohara Formation of the Kurosegawa Belt in the Toyo-Izumi area, Kumamoto Prefecture, Kyushu, Japan. *Bull. Geol. Surv. Japan*, **53**, 689–724.

飯塚保五郎（1929）７万５千分の１「鳥羽」図幅および同説明書．商工省地質調査所，28p.

INTERRAD Jurassic-Cretaceous Working Group（1995）*Middle Jurassic to Lower Cretaceous Radiolaria of Tethys: Occurrences, Systematics, Biochronology*. Mém. Géol. (Lausanne), no. 23, 1230p.

Ishida, N.（2008）Late Jurassic radiolarian assemblages in the Southern Chichibu Terrane, Western Kyushu, Southwest Japan. *Stratigraphy*, **5**, 22–38.

磯﨑行雄・橋口孝泰・板谷徹丸（1992）　黒瀬川クリッペの検証．地質雑，**98**，917–941.

Kimura, K. and Hori, R.（1993）Offscraping accretion of Jurassic chert–clastic complexes in the Mino-Tamba belt, central Japan. *Jour. Structural Geol*. **15**, 145–161.

日下部吉彦・宮村　学（1958）　伊勢市南方の古生層について．地質雑，**64**，269–280.

Matsuoka, A.（1983）Middle and Late Jurassic radiolarian biostratigraphy in the Sakawa and adjacent areas, Shikoku, Southwest Japan. *Jour. Geosci.*, *Osaka City Univ*., **26**, 1–48.

松岡　篤（1984）　高知県西部秩父累帯南帯の斗賀野層群．地質雑，**90**，455–477.

Matsuoka, A.（1986）*Tricolocapsa yaoi* Assemblage (Late Jurassic Radiolarians) from the Togano Group in Shikoku, Southwest Japan. *Jour. Geosci.*, *Osaka City Univ*., **29**, 101–115.

Matsuoka, A.（1992）Jurassic and Early Cretaceous radiolarians from Leg 129, Sites 800 and 801, western Pacific Ocean. *In* Larson, R. L., Lancelot, Y. *et al*., eds., *Proc. Ocean Drilling Prog.*, *Sci. Results*, **129**, 203–220.

Matsuoka, A.（1995a）Middle Jurassic-Lower Cretaceous radiolarian zonation in Japan and the Western Pacific, and age assignments based on the Unitary Associations methods. *In* Baumgartner, P. O. *et al*., eds., *Middle Jurassic to Lower Cretaceous Radiolaria of Tethys: Occurrences, Systematics, Biochronology*. Mém. Géol. (Lausanne), no. 23, 1049–1057.

Matsuoka, A.（1995b）Jurassic and Lower Cretaceous radiolarian zonation in Japan and in the western Pacific. *Island Arc*, **4**, 140–153.

松岡　篤（2007）　ジュラ系放散虫化石帯区分の改訂と主要放散虫種の垂直分布．日本古生物学会2007年年会講演予稿集，73.

Matsuoka, A. and Yao, A.（1985）Latest Jurassic Radiolarians from the Torinosu Group in Southwest Japan. *Jour. Geosci., Osaka City Univ*., **28**, 125–145.

西園幸久（1996）　放散虫化石層序に基づく秩父帯南帯の堆積史とその収束過程．熊本大理紀要（地球科学），**14**，45–226.

O'Dogherty, L., Bill, M., Goričan, S., Dumitrică, P. and Masson, H.（2006）Bathonian radiolarians from an ophiolitic mélange of the Alpine Tethys (Gets Nappe, Swiss-French Alps). *Micropaleontology*, **51**, 425–485.

Ohba, H. and Adachi, M.（1995）Permian, Triassic and Jurassic radiolarians from Omura and Ogura Island in the eastern part of the Shima Peninsula, Southwest Japan. *Jour. Earth Planet. Sci. Nagoya Univ*., **42**, 55–67.

太田　亨・今井智文・石田直人・坂　幸恭（2012）　三重

県志摩半島東部の黒瀬川帯中生界から見出されたジュラ紀・白亜紀放散虫化石．地質雑，**118**，588–593.

坂　幸恭（1983）　志摩半島西部，秩父帯のジュラ紀層について（予報）．早稲田大学教育学部学術研究[生物学・地学]，**32**，29–39.

坂　幸恭（2009）　中・古生界，紀伊半島東部地域．日本地質学会編，日本地方地質誌5：近畿地方，朝倉書店，134–140.

坂　幸恭・手塚茂雄（1988）　志摩半島の秩父帯南帯．地学雑，**97**，10–24.

坂　幸恭・山口宗司（1985）　志摩半島中央部，磯部町における仏像構造線の露頭．地質雑，**91**，235–238.

坂　幸恭・塚本員久・大矢芳彦・海野龍一（1979）　志摩半島西部，秩父帯の上部中生界．地質雑，**85**，81–96.

坂　幸恭・手塚茂雄・岡田洋一・市川昌則・高木秀雄（1988）　蛇紋岩メランジュ帯としての志摩半島，五ヶ所–安楽島構造線．地質雑，**94**，19–34.

坂　幸恭・加藤　潔・津村善博・大場穂高（1999）　志摩半島の秩父帯と黒瀬川帯．日本地質学会第106年学術大会見学旅行案内書，163–186.

佐藤　正・水野吉昭・蜂矢喜一郎・安井　謙（2005）　三重県志摩半島から採集されたジュラ紀アンモナイト．瑞浪市化石博紀要，**32**，235–243.

菅野耕三・中世古幸次郎・脇本礼子（1980）　志摩半島東部に分布する築地層群から産する放散虫化石について．大阪教育大紀要Ⅲ，**28**，111–121.

杉山和弘・小澤智生・畔柳勇生・古谷　裕（1993）　三重県志摩半島東部のジュラ系白根崎層（新称）および白亜系松尾層群の層序と放散虫化石．大阪微化石研究会誌特別号，no. 9，191–203.

Suzuki, H. and Gawlick, H. -J.（2003）Biostratigraphie und Taxonomie der Radiolarien aus den Kieselsedimenten der Blaa Alm und nördlich des Loser (Nordliche Kalkalpen, Callovium–Oxfordium). *Mitteilungen der Gesellschaft der Geologie und Bergbaustudenten in Österreich*, **46**, 137–228.

冨田幸光・桂嘉志浩・東　洋一・亀井節夫（2001）　鳥羽市恐竜化石の記載と分類．三重県大型化石発掘調査団編，鳥羽の恐竜化石，三重県鳥羽市産恐竜化石調査研究報告書，三重県立博物館，13–31.

内野隆之・鈴木紀毅（2016）　三重県志摩半島の黒瀬川帯から見出された後期ペルム紀整然層と広域対比．地質雑，**122**，207–222.

梅田真樹・山際延夫（1997）　三重県鳥羽地域の黒瀬川帯から産出したデボン紀放散虫化石．地質雑，**103**，1081–1084.

山際延夫（1957）　志摩半島東部中古生界の層序と構造．地質雑，**63**，263–272.

山際延夫（1969）　志摩半島東部に分布する築地層群．大阪教育大学紀要第Ⅲ部門，**18**，71–81.

山際延夫・坂　幸恭（1967）　志摩半島東部の中・古生界．日本地質学会第74年年会地質見学案内書，24p.

山際延夫・坂　幸恭・岩橋豊彦・杉田福松（1976）　志摩半島の仏像構造線についての新知見．地質雑，**82**，409–412.

山際延夫・鳴橋憲一・辻井安喜・藤田孝子・和田朋子（1979）　志摩半島東部に分布する上部ジュラ系今浦層群産出の珊瑚化石について（第1報）．地学雑，**88**，29–39.

吉倉紳一・寺嶋禎一（1984）　志摩半島中央部の五ヶ所–安楽島構造線から見い出された角閃岩の地質学的意義．岩鉱，**79**，311–317.

（受 付：2016年10月24日； 受 理：2017年1月17日）

地質調査研究報告，第 68 巻，第 2 号，p. 41–56，2017

概報 - Report

5 万分の 1 地質図幅「鳥羽」地域における秩父累帯北帯の砂岩及び三波川帯の砂質片岩から得られた砕屑性ジルコン U–Pb 年代

内野隆之 [1,*]

Takayuki Uchino (2017) U-Pb ages of detrital zircon grains from sandstones of the Northern Chichibu Belt and psammitic schists of the Sambagawa Belt in the Toba District (Quadrangle series 1:50,000), Shima Peninsula, Mie Prefecture, Southwest Japan. *Bull. Geol. Surv. Japan*, vol. 68 (2), p. 41–56, 4 figs, 6 tables, 3 appendixes.

Abstract: The Geological Survey of Japan is now making a geological map and its explanatory text of geology of the Toba District (Quadrangle series 1:50,000), Shima Peninsula, Mie Prefecture. During its study, detrital zircon U–Pb ages from sandstone in the Northern Chichibu Belt and from psammitic schist in the Sambagawa Belt were measured in order to reveal accretion ages of the accretionary complexes in the both belts.

The peak ages of the youngest clusters of the detrital zircon grains from the Osakatoge Complex and the Kochi Complex in the Northern Chichibu Belt are 204.4 ± 4.0 Ma and 183.4 ± 2.9 Ma, respectively. These ages are consistent to the depositional ages (Early and Middle Jurassic) of terrigenous deposits assumed from radiolarian fossils by a previous work.

The peak ages of the youngest clusters of the detrital zircon grains from two samples in the Miyakawa Formation in the Sambagawa Belt are 177.1 ± 1.6 Ma and 95.5 ± 2.5 Ma. The latter is acceptable according to 99–83 Ma phengite K–Ar ages (metamorphic or cooling age on a subduction zone) from psammitic schist shown by a previous work in the Ise District (west of the Toba District). On the other hand, the former is much older than the latter although the both samples may belong to a same unit. Therefore, more data such as phengite K–Ar ages or additional detrital zircon U–Pb ages are necessary to verify the scientific validity of the former (Early Jurassic age).

Keywords: U–Pb age, detrital zircon, Jurassic, Cretaceous, Osakatoge Complex, Kochi Complex, Miyakawa Formation, Northern Chichibu Belt, Sambagawa Belt, Shima Peninsula, Mie Prefecture

要　旨

地質調査総合センターでは現在，5万分の1地質図幅「鳥羽」の作成を行っている．その研究過程で，志摩半島に分布する秩父累帯北帯及び三波川帯の付加体の付加年代を決定することを目的に，砂岩及び砂質片岩中の砕屑性ジルコンのU–Pb年代を測定した．

秩父累帯北帯逢坂峠（おうさかとうげ）コンプレックスの砂岩中ジルコンの最若粒子集団は204.4 ± 4.0 Ma（三畳紀末〜ジュラ紀初頭）を示し，また同帯河内（こうち）コンプレックスの砂岩中のジルコンの最若粒子集団は183.4 ± 2.9 Ma（前期ジュラ紀中頃〜前期ジュラ紀後半）を示すことが明らかになった．これらは放散虫化石から想定されている陸源性砕屑岩の時代（付加年代）と矛盾しない．また，三波川帯宮川（みやかわ）層の砂質片岩中のジルコンの最若粒子集団は177.1 ± 1.6 Ma（前期ジュラ紀後半）と95.5 ± 2.5 Ma（後期白亜紀前半）を示すことが判明した．後者は，伊勢地域（図幅西隣）から得られている99–83 MaのフェンジャイトK–Ar年代（変成・冷却年代）と調和的である．しかし，前者は後者よりも有意に古い年代を示す結果となった．前者の妥当性を検証するため，今後更なる砕屑性ジルコンU–Pb年代やフェンジャイトK–Ar年代などのデータ追加が必要である．

1．はじめに

地質調査総合センターでは，志摩半島に分布する三波川帯，秩父累帯，四万十帯の3地体にまたがっている5万分の1地質図幅「鳥羽」の作成を現在行っている（第1図）．

秩父累帯は北から「北帯」，「中帯（あるいは黒瀬川帯）」，

[1] 産業技術総合研究所 地質調査総合センター 地質情報研究部門（AIST, Geological Survey of Japan, Research Institute of Geology and Geoinformation）

[*] Corresponding author: T.Uchino, Central 7, Higashi 1-1-1, Tsukuba, Ibaraki 305-8567, Japan, Email: t-uchino@aist.go.jp

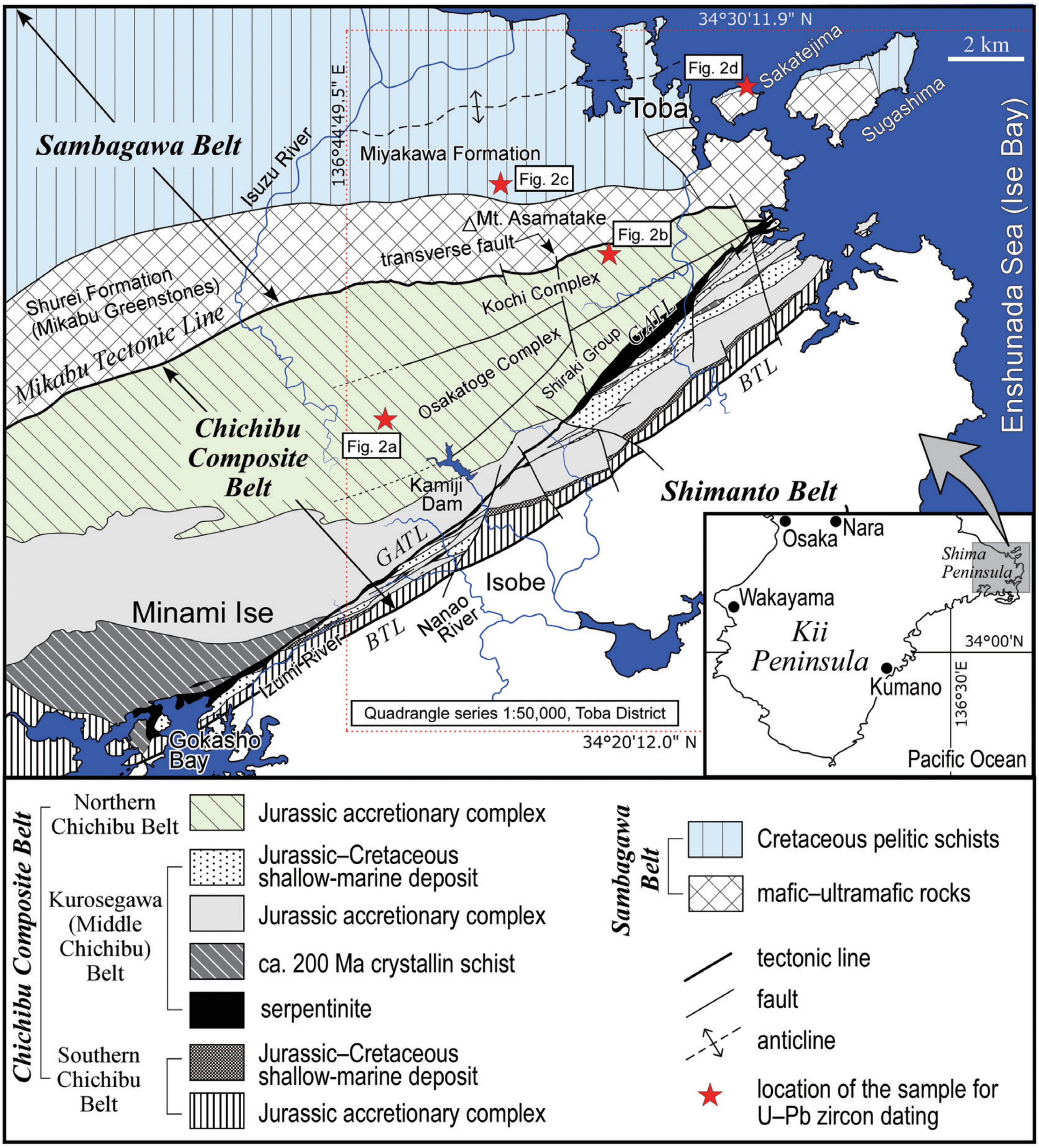

第1図　志摩半島の地質概略図．南伊勢町周辺の秩父累帯の分布は坂(2009)に，秩父累帯北帯の区分は山際・坂(1967)による．緯度・経度は世界測地系に従った．
BTL：仏像構造線，GATL：五ヶ所–安楽島構造線.

Fig. 1　Geological map of Shima Peninsula. Distribution of the Chichibu Composite Belt around Minami Ise Town is from Saka (2009), Division of the Northern Chichibu Belt is after Yamagiwa and Saka (1967). Latitude and longitude follow the world geodetic system.
BTL: Butsuzo Tectonic Line, GATL: Gokasho–Arashima Tectonic Line.

「南帯」に区分される(例えば，山際・坂，1967；坂ほか，1988；坂ほか，1999；坂，2009)．北帯にはジュラ紀付加体が分布し，中帯(坂ほか，1999以降，黒瀬川帯と呼ばれることが多い)にはジュラ紀付加体及び中期ジュラ紀～前期白亜紀浅海層のほか，蛇紋岩，深成岩，角閃岩，デボン紀堆積岩，ペルム紀浅海層，200 Ma前後の結晶片岩が分布する．南帯にはジュラ紀の付加体と後期ジュラ紀～前期白亜紀の浅海層が分布している．そして，四万十帯には白亜紀の付加体が分布し，三波川帯には超苦鉄質～苦鉄質岩類(御荷鉾緑色岩類)と泥質片岩を主体とした結晶片岩類が分布している．

本図幅地域を含め志摩半島の秩父累帯北帯の地質体は，かつて石灰岩から得られた紡錘虫化石によって石炭紀あるいはペルム紀に形成されたと考えられていた(例えば，日下部・宮村，1958)．1970年代にプレートテクトニクス論が日本に導入され，古生層と考えられていた地層の多くがジュラ紀の付加体であることが理解された．そして，志摩半島でも菅野ほか(1980)の放散虫化石報告を皮切りに，相次いでジュラ紀付加体の存在が確認されてきた．しかし，北帯に関してはジュラ紀の付加体と推測されることは多かったが，放散虫化石の報告はなかった．また，北帯の中央部ユニットについてはペルム紀付加体と考えられた例(磯﨑ほか，1992)もある．そのような中，都築･八尾(2006)によって漸く，中央部ユニットから前期ジュラ紀の放散虫化石が，北部ユニットから中期ジュラ紀の放散虫化石がそれぞれ報告され，北帯にもジュラ紀の付加体が広く分布していることが明らかになった．ただし，この報告は学会での講演であったため，講演要旨からは標本写真や採取位置など詳細な情報を得ることができず，検証が困難な状況にある．

本地域三波川帯の泥質片岩を主体とするユニットに関しては，研究報告がほとんどない．近年，日本列島の三波川帯の砕屑岩から砕屑性ジルコンU-Pb年代が相次いで報告されており，三波川帯の一部の原岩が四万十帯の“北帯”に相当する後期白亜紀の付加体であることが明らかになってきた(例えば，青木ほか，2010)．紀伊半島西部でも，三波川帯中軸部の原岩は，四万十帯“北帯”相当の付加体であるとされている(大藤ほか，2010)．このような状況から，本地域の三波川帯の原岩年代についても解明が望まれている．

以上の背景を踏まえて，秩父累帯北帯及び三波川帯に産する砕屑岩中の砕屑性ジルコンのU-Pb年代測定を行った．本論ではその結果についての報告と評価を行う．

2．地質概説

本地域の秩父累帯北帯は北部ユニットの河内コンプレックス(都築・八尾，2006)，中央部ユニットの逢坂峠コンプレックス(都築・八尾，2006)，南部ユニットの白木層群(山際・坂，1967)からなり，放散虫化石に基づいて河内コンプレックスは中期ジュラ紀に，逢坂峠コンプレックスは前期ジュラ紀にそれぞれ形成されたとされている(都築・八尾，2006)．一方，本地域の三波川帯は，北部ユニットの宮川層と南部ユニットの鷲嶺層からなる(飯塚，1929)．以下に砕屑性ジルコン年代測定の対象となった試料が所属する逢坂峠コンプレックス，河内コンプレックス及び宮川層について概要を記述する．

2. 1　逢坂峠コンプレックス(秩父累帯北帯)

本地域秩父累帯北帯の中央部を南北に走る胴切断層(第1図のtransverse fault)以西において，北側の河内コンプレックスと南側の白木層群に挟まれて分布する．層理面は北東–南西ないし東北東–西南西走向で北あるいは南の概ね低角傾斜を示す．玄武岩，石灰岩，チャート，泥岩，砂岩，混在岩を主体とし，5万分の1地質図規模で混在相を示す．石灰岩の卓越と低角な地質構造で特徴付けられる．

石灰岩からは，前期ペルム紀の紡錘虫化石や珊瑚化石が報告されている(加藤・杉，1927；日下部・宮村，1958；山際・坂，1967；山際，2015)．都築・八尾(2006)は，産地や標本写真を明示していないが，チャートから*Albaillella* sp.やoertlispongidsの放散虫化石を見出し，その時代をそれぞれペルム紀及び中期三畳紀と考えている．また，彼らは泥岩から*Bagotum* sp.，*Lupherium* sp.，*Pantanellium* sp.及び*Stichocapsa* sp.の放散虫化石を見出し，その時代を前期ジュラ紀と考えている．

2. 2　河内コンプレックス(秩父累帯北帯)

本地域秩父累帯北帯の北部に分布する(第1図)．層理面は北東–南西ないし東北東–西南西走向で概ね中角の北あるいは南傾斜を示す．玄武岩，石灰岩，チャート，泥岩，砂岩，混在岩を主体とし，5万分の1地質図規模で混在相を示す．玄武岩・チャート岩体の卓越と片岩～準片岩の産出で特徴付けられる．

石灰岩からは，前期ペルム紀の紡錘虫化石や珊瑚化石が報告されている(日下部・宮村，1958；山際・坂，1967)．都築・八尾(2006)は，産地や標本写真を明示していないが，チャートから*Albaillella* sp. と*Pseudostylosphaera* sp.及び*Triassocampe* sp. の放散虫化石を見出しており，前者を含むチャートの時代をペルム紀，後二者を含むチャートの時代を中期三畳紀と考えている．また，彼らは泥岩から*Stichocapsa fusiformis* Hinde，*Parvicingula* sp.，*Dictyomitrella* sp.の放散虫化石を見出し，その時代を中期ジュラ紀と考えている．

2. 3　宮川層(三波川帯)

泥質片岩を主体とし，苦鉄質片岩，石灰質片岩，珪質片岩，砂質片岩及び混在岩を僅かに伴う．層理面あるい

は片理面は，西北西–東南東ないし東北東–西南西走向を示し，また概ね中角の北あるいは南傾斜を示す．場所によっては20 〜 30°の低角傾斜を示す地層も認められる．Nakamura (1971) でも指摘されているように，大局的には中央部に東西性の背斜軸を持つ背斜構造をなす．

坂野 (1992) や上野 (2001) による本地域西隣 (伊勢地域) での研究で既に指摘されているように，本層の変成度は四国中央部三波川帯の緑泥石帯低温部に相当する．また伊勢地域では，Tomiyoshi and Takasu (2010) によって，御荷鉾緑色岩類分布域中に産する泥質片岩から99.1 ± 2.5, 97.1 ± 2.4 及び 93.2 ± 2.3 Ma (後期白亜紀初頭)，また御荷鉾緑色岩類の北側に産する泥質片岩から 84.2 ± 2.1 と 83.6 ± 2.1 Ma (後期白亜紀中頃) のフェンジャイトK–Ar年代が報告されている．

3．砕屑性ジルコン U–Pb 年代測定

3. 1　採取試料

逢坂峠コンプレックスからは逢坂峠北 (志摩路トンネル伊勢側出口付近) (34° 24′ 53.62″ N，136° 45′ 46.00″ E) の1試料，河内コンプレックスからは鳥羽レストパーク南 (山神川上流部) (34° 27′ 04.62″ N，136° 49′ 16.54″ E) の1試料，宮川層からは鳴ヶ谷川 (中流部) (34° 28′ 07.13″ N, 136° 47′ 17.17″ E) 及び坂手島 (北海岸) (34° 29′ 25.62″ N，136° 51′ 41.32″ E) の計2試料を採取した (第2図)．いずれも変形の弱い中粒〜粗粒な石質の砂岩あるいは砂質片岩である．

3. 2　分析手法

分析は株式会社京都フィッション・トラックに依頼した．分析に用いた装置は京都大学大学院理学研究科地球惑星科学専攻地質学鉱物学教室の二重収束型及び四重極型結合誘導プラズマ質量分析 (ICP-MS) 装置であり，レーザーアブレーションのためのArFエキシマ及びフェムト秒レーザーシステムを搭載している (Yokoyama *et al*, 2011；Sakata *et al*., 2014；Maruyama *et al*., 2016)．測定前にジルコン表面の鉛汚染を避けるためにワンショットクリーニングを施した．レーザー照射に際しては，包有物や割れ目を避けてジルコン粒子の中心部を狙った．レーザー照射後の最若年代集団を形成するジルコン粒子 (後述) の顕微鏡写真を付図1に，また，レーザー照射及び ICP-MSの条件を第1表と第2表に示した．

なお，年代測定結果の正確性を評価するために，2次標準試料の33 Ma のOD-3 (岩野ほか，2012；Iwano *et al*., 2013；Lukács *et al*., 2015) 及び337 MaのPlešovice (Sláma *et al*., 2008) も分析した (付表1，2)．二重収束型 ICP-MS 装置で測定したOD-3 及び Plešoviceのピーク年代 (加重平均値) はそれぞれ32.97 ± 0.63 Ma (誤差2σ) (mean square weight deviation：MSWD = 1.4)，329.9 ± 3.4 Ma (誤差2σ) (MSWD = 1.18) で，また，四重極型 ICP-MS装置で測定したOD-3 及び Plešoviceのピーク年代 (加重平均値) はそれぞれ32.66 ± 0.80 Ma (誤差2σ) (MSWD = 0.51)，338.3 ± 3.2 Ma (誤差2σ) (MSWD = 0.119) であり，いずれも2次標準試料の文献値から2％以内のずれに収まっている．

3. 3　年代分析結果

測定したジルコン粒子数は4地点の各試料とも60個である．各試料におけるジルコンの同位体比，$^{206}Pb/^{238}U$年代及び$^{207}Pb/^{235}U$年代を第3表〜第6表に示す．河内コンプレックスの試料中の1粒子を除いて，すべての粒子がコンコーディア年代を示している．なお，コンコーダントの考え方は$^{206}Pb/^{238}U$年代がA±B Ma (A：年代値，B：2σの誤差)，$^{207}Pb/^{235}U$年代がC±D Ma (C：年代値，D：2σの誤差) として，$^{207}Pb/^{235}U$年代が$^{206}Pb/^{238}U$年代よりも古く，式1 (下記) が成り立つ場合，そして$^{207}Pb/^{235}U$年代が$^{206}Pb/^{238}U$年代よりも若く，式2 (下記) が成り立つ場合をコンコーダントとみなした．

$$\frac{(A+B)-(C-D)}{A} \times 100 > 0 \qquad 式（1）$$

$$\frac{(A-B)-(C+D)}{A} \times 100 < 0 \qquad 式（2）$$

各試料のジルコン粒子のコンコーディア図及び$^{206}Pb/^{238}U$年代分布図について，秩父累帯北帯のものを第3図に，三波川帯のものを第4図に示した．これらの図は，京都フィッション・トラック社による測定値 (第3表〜第6表) を基に，マイクロソフト社の表計算ソフトExcel用のアドインモジュールであるIsoplot/Ex 4.15 (Ludwig, 2008) を用いて作成した．また年代の議論には，$^{207}Pb/^{235}U$年代よりも誤差の小さい$^{206}Pb/^{238}U$年代を採用した．

3. 3. 1　逢坂峠北の砂岩［試料no. 20140722L3（登録標本番号：GSJ R109160)］（秩父累帯北帯逢坂峠コンプレックス）

先カンブリア時代のジルコンは認められず，約370 Ma付近に集中する粒子集団 (計2個)，約260 Ma付近に集中する粒子集団 (計56個)，そして約200 Ma付近に集中する粒子集団 (計2個) が認められ，約260 Ma付近に集中する粒子が一番多い (第3図a，b)．一番若い集団 (no. 18と no. 50) の加重平均を最若ピーク年代とした場合，その値は204.4 ± 4.0 Ma (誤差2σ) である．なお，最若の砕屑性ジルコン (no. 18) の年代は203.1 ± 4.3 Maである (第3表)．

3. 3. 2　鳥羽レストパーク南の砂岩［試料no. 20140722 L1-1（登録標本番号：GSJ R109161)］（秩父累帯北帯河内コンプレックス）

先カンブリア時代のジルコンは認められず，約400 Ma

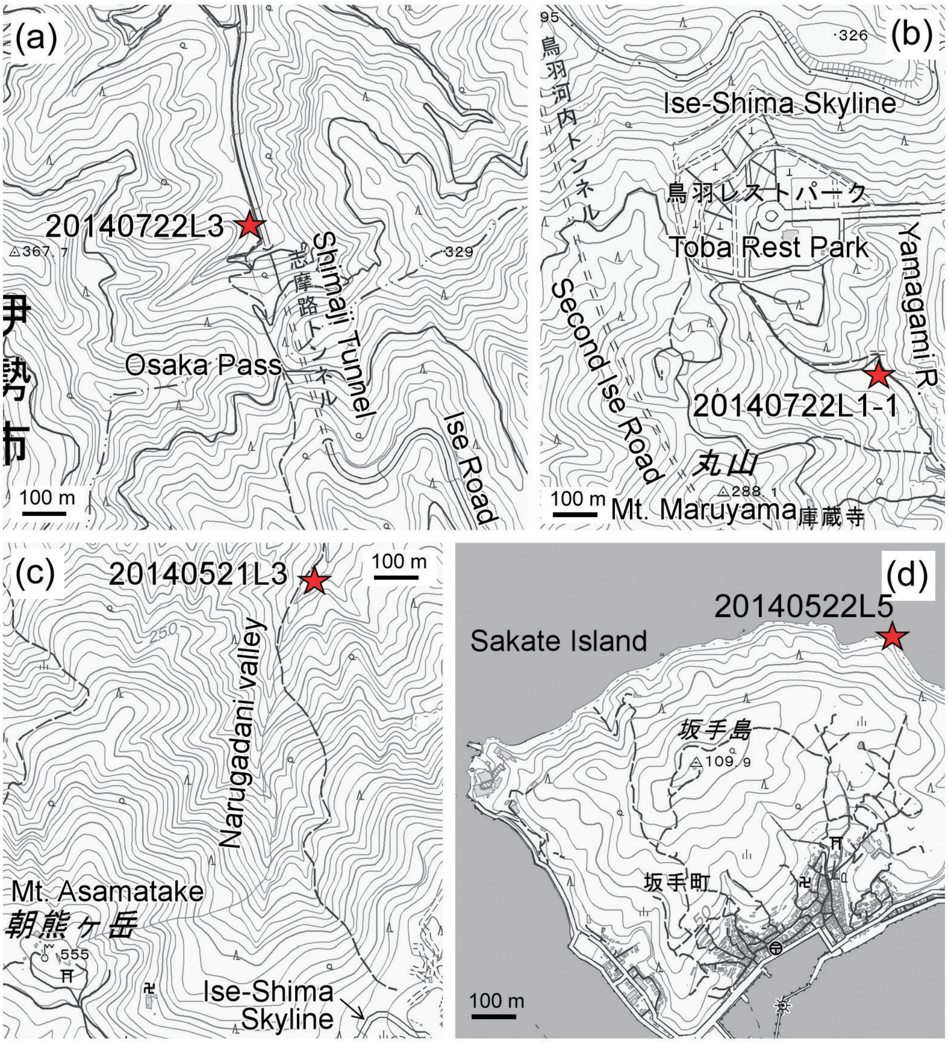

第2図　砕屑性ジルコンのU-Pb年代測定が行われた試料地点．(a) 秩父累帯北帯逢坂峠コンプレックス の砂岩採取地点（試料番号：20140722L3）．逢坂峠北．国土地理院の地理院地図（http://maps.gsi.go.jp/#18/34.415102/136.762793/）を使用．(b) 秩父累帯北帯河内コンプレックス の砂岩採取地点（試料番号：20140722L1-1）．鳥羽レストパーク南．地理院地図（http://maps.gsi.go.jp/#18/34.415102/136.821163/）を使用．(c) 三波川帯宮川層の砂質片岩採取地点（試料番号：20140521L3）．鳴ヶ谷川．地理院地図（http://maps.gsi.go.jp/#18/34.468813/136.788284/）を使用．(d) 三波川帯宮川層の砂質片岩採取地点（試料番号：20140522L5）．坂手島．地理院地図（http://maps.gsi.go.jp/#18/34.490508/136.861608/）を使用．

Fig. 2　Locations of samples for detrital zircon U–Pb dating. (a) Sandstone (sample no. 20140722L3) location from the Osakatoge Complex in the Northern Chichibu Belt, north of the Osaka Pass. Topographic map is from the GIS map (http://maps.gsi.go.jp/#18/34.415102/136.762793/) of the Geospatial Information Authority of Japan. (b) Sandstone (sample no. 20140722L1-1) location from the Kochi Complex in the Northern Chichibu Belt, south of the Toba Rest Park. Topographic map is from the GIS map (http://maps.gsi.go.jp/#18/34.451394/136.821163/). (c) Psammitic schist (sample no. 20140521L3) location from the Miyakawa Formation in the Sambagawa Belt, Narugadani River. Topographic map is from the GIS map (http://maps.gsi.go.jp/#18/34.468813/136.788284/). (d) Psammitic schist (sample no. 20140522L5) location from the Miyakawa Formation in the Sambagawa Belt, Sakate Island. Topographic map is from the GIS map (http://maps.gsi.go.jp/#18/34.490508/136.861608/).

第1表　20140521L3試料，20140522L5試料及び20140722L1-1試料を測定したレーザーアブレーション二重収束型結合誘導プラズマ質量分析装置の条件.

Table 1　LA-ICP-MS instrumentation using a double-focusing sector field mass spectrometer for the sample nos. 20140521L3, 20140522L5 and 20140722L1-1.

Laser ablation	
Model	New Wave Research NWR Femto
Laser type	Femtosecond
Energy density	2.0 J/cm^2
Spot size	15 μm
Repetition rate	5 Hz
Duration of laser ablation	20 s
Carrier gas (He)	0.5 L min^{-1}
ICP-MS	
Model	Nu Instruments AttoM
ICP-MS type	Magnetic sector field
Scanning (Operation) mode	Deflector jump
Forward power	1300 W
Carrier gas (Ar)	0.76 L min^{-1}
ThO$^+$/Th (oxide ratio)	<1%
Data acquisition protocol	Batch
Data acquisition	28 s (20 s gas blank, 8 s ablation)
Monitor isotopes	^{202}Hg, ^{204}Pb, ^{206}Pb, ^{207}Pb, ^{208}Pb, ^{232}Th, ^{238}U
Dwell time	0.1 s for each
Primary standard	Nancy 91500 *1
Secondary standard	OD-3 *2, 3, 4 , Plešovice*5

*1: Wiedenbeck *et al*. (1995); *2: Iwano *et al*. (2012); *3: Iwano *et al*. (2013); *4: Lukács *et al*. (2015); *5: Sláma *et al*. (2008).

第2表　20140722L3試料を測定したレーザーアブレーション四重極型結合誘導プラズマ質量分析装置の条件.

Table 2　LA-ICP-MS instrumentation using a quadrupole mass spectrometer for the sample no. 20140722L3.

Laser ablation	
Model	New Wave Research NWR-193
Laser type (wave length)	Excimer ArF (193 nm)
Energy density	3.3 J/cm^2
Spot size	25 μm
Repetition rate	5 Hz
Duration of laser ablation	20 s
Carrier gas (He)	0.53 L min^{-1}
ICP-MS	
Model	Thermo Fisher Scientific iCAP-Qc
ICP-MS type	Quadrupole
Scanning (Operation) mode	Standard mode (no collision gas was used)
Forward power	1400 W
Carrier gas (Ar)	0.80 L min^{-1}
ThO$^+$/Th (oxide ratio)	<1%
Data acquisition protocol	Time-resolved analysis
Data acquisition	50 s (15 s gas blank, 35 s ablation)
Monitor isotopes	^{29}Si, ^{202}Hg, ^{204}Pb, ^{206}Pb, ^{207}Pb, ^{208}Pb, ^{232}Th, ^{238}U
Dwell time	0.2 s for $^{206, 207}$Pb, 0.1 s for others
Primary standard	Nancy 91500 *1
Secondary standard	OD-3 *2, 3, 4 , Plešovice*5

*1: Wiedenbeck *et al*. (1995); *2: Iwano *et al*. (2012); *3: Iwano *et al*. (2013); *4: Lukács *et al*. (2015); *5: Sláma *et al*. (2008).

付近の粒子(1個)，約360 Ma付近の粒子(1個)，約260 Ma付近に集中する粒子集団(計45個)そして約180 Ma付近に集中する粒子集団(計12個)が認められ，逢坂峠北の試料と同様に約260 Ma付近に集中する粒子が一番多い(第3図c，d)．若い集団のうち，最若粒子を中心とした年代誤差範囲3σで年代一致の基準を設けた場合，11粒子が基準内に該当し(第4表)，それらのピーク年代(加重平均値)は183.4±2.9 Ma (誤差2σ)である．なお，最若年代を示す砕屑性ジルコン(no. 46)は174.0±10.2 Maである．

3. 3. 3　鳴ヶ谷川の砂質片岩[試料no. 20140521L3（登録標本番号：GSJ R109162)]（三波川帯宮川層）

先カンブリア時代のジルコンが多数認められ，2300 Ma付近，1800～1500 Ma，1300 Ma付近の年代を示す粒子が存在する．顕生代では，約360 Ma付近，約260 Ma付近，180 Ma付近にピークを持つ粒子集団が認められ，約260 Maと180 Ma付近に集中する粒子が多い(第4図a，b)．若い集団のうち，最若粒子を中心とした年代誤差範囲3σで年代一致の基準を設けた場合，18粒子が基準内に該当し(第5表)，それらのピーク年代(加重平均値)は177.1±1.6 Ma (誤差2σ)である．なお，最若の砕屑性ジルコン(no. 16)の年代は157.9±8.8 Maである．

3. 3. 4　坂手島の砂質片岩[試料no. 20140522L5（登録標本番号：GSJ R109163)]（三波川帯宮川層）

先カンブリア時代のジルコンが多数認められ，2300 Ma付近，1800～1400 Ma，1200 Ma付近，1000 Ma付近の年代を示す粒子が存在する．顕生代では，約260 Ma付近，約180 Ma付近，100 Ma付近にピークを持つ粒子(粒子集団)が認められ，鳴ヶ谷川の試料でもみられるように約180 Ma付近に集中する粒子が一番多い(第4図d)．若い集団のうち，最若粒子を中心とした年代誤差範囲3σで年代一致の基準を設けた場合，6粒子が基準内に該当し(第6表)，それらのピーク年代(加重平均値)は95.5±2.5 Ma (誤差2σ)である．なお，最若の砕屑性ジルコン(no. 2)の年代は90.4±6.8 Maである．

第3表　秩父累帯北帯逢坂峠コンプレックスの砂岩（20140722L3試料；逢坂峠北）の砕屑性ジルコンにおけるレーザーアブレーション四重極型結合誘導プラズマ質量分析装置によるU-Pb同位体データ．＊は最若年代集団のピーク年代（加重平均値）に採用されたジルコンを示す．

Table 3　U–Pb isotopic data determined by LA-ICP-MS using a quadrupole mass spectrometer for detrital zircon from sandstone (sample no. 20140722L3) in the Osakatoge Complex, north of the Osaka Pass, Northern Chichibu Belt.
The asterisks indicate the zircon adopted for the peak age (weighted mean) of the youngest cluster.

Grain no.	Isotopic ratios						Age (Ma)				Th/U	Remarks
	$^{207}Pb/^{206}Pb$	Error 2σ	$^{206}Pb/^{238}U$	Error 2σ	$^{207}Pb/^{235}U$	Error 2σ	$^{206}Pb/^{238}U$	Error 2σ	$^{207}Pb/^{235}U$	Error 2σ		
1	0.0512	± 0.0109	0.0437	± 0.0025	0.3087	± 0.0802	275.8	± 16.3	273.1	± 78.3	0.23	
2	0.0515	± 0.0040	0.0422	± 0.0015	0.2995	± 0.0303	266.4	± 9.7	266.0	± 30.4	0.79	
3	0.0500	± 0.0058	0.0408	± 0.0017	0.2807	± 0.0403	257.5	± 10.7	251.2	± 40.1	0.66	
4	0.0439	± 0.0096	0.0458	± 0.0026	0.2770	± 0.0728	288.7	± 16.6	248.3	± 71.4	0.31	
5	0.0537	± 0.0073	0.0408	± 0.0018	0.3020	± 0.0507	257.5	± 11.7	268.0	± 50.2	0.51	
6	0.0521	± 0.0054	0.0448	± 0.0018	0.3216	± 0.0424	282.5	± 11.3	283.1	± 42.2	0.37	
7	0.0530	± 0.0041	0.0382	± 0.0014	0.2795	± 0.0277	241.8	± 8.8	250.3	± 27.8	0.45	
8	0.0512	± 0.0090	0.0427	± 0.0022	0.3016	± 0.0643	269.4	± 13.9	267.6	± 63.3	0.58	
9	0.0547	± 0.0114	0.0389	± 0.0023	0.2936	± 0.0739	246.2	± 14.6	261.4	± 72.4	0.47	
10	0.0521	± 0.0033	0.0396	± 0.0014	0.2847	± 0.0245	250.3	± 8.8	254.4	± 24.6	0.59	
11	0.0533	± 0.0034	0.0407	± 0.0014	0.2993	± 0.0257	257.3	± 9.0	265.9	± 25.8	0.40	
12	0.0541	± 0.0050	0.0389	± 0.0015	0.2904	± 0.0337	246.2	± 9.5	258.8	± 33.7	0.66	
13	0.0501	± 0.0054	0.0409	± 0.0016	0.2826	± 0.0379	258.7	± 10.4	252.7	± 37.8	0.56	
14	0.0509	± 0.0068	0.0405	± 0.0018	0.2839	± 0.0463	255.9	± 11.3	253.8	± 45.9	0.77	
15	0.0497	± 0.0067	0.0392	± 0.0013	0.2689	± 0.0420	247.9	± 8.5	241.8	± 41.8	0.92	
16	0.0575	± 0.0069	0.0576	± 0.0019	0.4575	± 0.0691	361.3	± 12.1	382.5	± 67.8	0.50	
17	0.0463	± 0.0089	0.0408	± 0.0018	0.2608	± 0.0580	257.8	± 11.7	235.3	± 57.3	0.52	
18	0.0515	± 0.0033	0.0320	± 0.0007	0.2273	± 0.0162	203.1	± 4.3	208.0	± 16.3	0.30	*
19	0.0491	± 0.0054	0.0425	± 0.0012	0.2875	± 0.0367	268.1	± 7.9	256.6	± 36.6	0.63	
20	0.0560	± 0.0070	0.0406	± 0.0013	0.3140	± 0.0464	256.7	± 8.7	277.3	± 46.0	0.77	
21	0.0548	± 0.0061	0.0404	± 0.0012	0.3056	± 0.0400	255.4	± 7.8	270.8	± 39.8	0.51	
22	0.0603	± 0.0127	0.0402	± 0.0022	0.3346	± 0.0848	254.2	± 14.0	293.1	± 82.7	0.30	
23	0.0597	± 0.0077	0.0394	± 0.0014	0.3249	± 0.0494	249.4	± 8.8	285.7	± 48.9	0.46	
24	0.0543	± 0.0095	0.0422	± 0.0018	0.3161	± 0.0657	266.7	± 11.8	278.9	± 64.6	0.48	
25	0.0561	± 0.0071	0.0407	± 0.0014	0.3151	± 0.0468	257.5	± 8.7	278.2	± 46.4	0.78	
26	0.0493	± 0.0041	0.0423	± 0.0010	0.2877	± 0.0277	267.2	± 6.5	256.7	± 27.7	0.65	
27	0.0543	± 0.0047	0.0444	± 0.0011	0.3324	± 0.0333	279.9	± 7.1	291.4	± 33.3	0.58	
28	0.0538	± 0.0043	0.0412	± 0.0010	0.3056	± 0.0279	260.2	± 6.2	270.8	± 27.9	0.75	
29	0.0561	± 0.0040	0.0599	± 0.0013	0.4629	± 0.0392	374.8	± 8.6	386.3	± 39.1	0.62	
30	0.0533	± 0.0057	0.0412	± 0.0012	0.3032	± 0.0381	260.3	± 7.7	268.9	± 38.0	0.41	
31	0.0527	± 0.0075	0.0416	± 0.0019	0.3020	± 0.0512	262.6	± 12.3	267.9	± 50.7	0.69	
32	0.0491	± 0.0045	0.0408	± 0.0016	0.2763	± 0.0302	257.5	± 10.0	247.7	± 30.2	0.42	
33	0.0512	± 0.0039	0.0404	± 0.0015	0.2851	± 0.0259	255.1	± 9.5	254.7	± 26.0	0.51	
34	0.0481	± 0.0068	0.0438	± 0.0020	0.2906	± 0.0493	276.6	± 12.8	259.0	± 48.9	0.44	
35	0.0511	± 0.0028	0.0398	± 0.0014	0.2809	± 0.0183	251.8	± 8.8	251.4	± 18.4	0.03	
36	0.0494	± 0.0045	0.0418	± 0.0016	0.2845	± 0.0308	263.8	± 10.3	254.2	± 30.8	0.65	
37	0.0498	± 0.0046	0.0402	± 0.0015	0.2757	± 0.0301	253.9	± 9.9	247.2	± 30.2	0.56	
38	0.0523	± 0.0097	0.0416	± 0.0022	0.3001	± 0.0668	263.0	± 14.4	266.5	± 65.6	0.61	
39	0.0466	± 0.0044	0.0398	± 0.0015	0.2561	± 0.0286	251.7	± 9.8	231.5	± 28.6	0.35	
40	0.0509	± 0.0036	0.0406	± 0.0015	0.2850	± 0.0244	256.6	± 9.4	254.6	± 24.4	0.58	
41	0.0494	± 0.0039	0.0406	± 0.0015	0.2767	± 0.0257	256.7	± 9.6	248.0	± 25.8	0.64	
42	0.0525	± 0.0041	0.0409	± 0.0015	0.2963	± 0.0280	258.5	± 9.7	263.5	± 28.1	0.22	
43	0.0528	± 0.0109	0.0415	± 0.0024	0.3021	± 0.0749	262.1	± 15.5	268.1	± 73.3	0.37	
44	0.0539	± 0.0070	0.0400	± 0.0018	0.2978	± 0.0462	253.1	± 11.4	264.7	± 45.9	0.83	
45	0.0527	± 0.0075	0.0418	± 0.0019	0.3037	± 0.0518	264.1	± 12.4	269.3	± 51.3	0.49	
46	0.0509	± 0.0036	0.0398	± 0.0021	0.2796	± 0.0280	251.6	± 13.8	250.3	± 28.0	0.47	
47	0.0499	± 0.0048	0.0420	± 0.0023	0.2892	± 0.0364	265.2	± 15.1	258.0	± 36.3	0.60	
48	0.0526	± 0.0033	0.0394	± 0.0021	0.2856	± 0.0264	249.1	± 13.5	255.1	± 26.5	0.51	
49	0.0572	± 0.0077	0.0432	± 0.0026	0.3407	± 0.0585	272.7	± 16.9	297.7	± 57.7	0.58	
50	0.0498	± 0.0046	0.0339	± 0.0019	0.2326	± 0.0277	214.8	± 12.1	212.4	± 27.7	0.46	*
51	0.0519	± 0.0070	0.0444	± 0.0027	0.3177	± 0.0542	280.0	± 17.1	280.1	± 53.6	0.76	
52	0.0543	± 0.0073	0.0412	± 0.0025	0.3081	± 0.0523	260.0	± 16.0	272.7	± 51.8	0.60	
53	0.0539	± 0.0048	0.0401	± 0.0022	0.2983	± 0.0354	253.7	± 14.3	265.1	± 35.3	0.91	
54	0.0523	± 0.0079	0.0414	± 0.0026	0.2988	± 0.0562	261.5	± 16.5	265.5	± 55.5	0.51	
55	0.0508	± 0.0077	0.0400	± 0.0025	0.2799	± 0.0521	252.8	± 15.9	250.6	± 51.6	0.66	
56	0.0560	± 0.0059	0.0403	± 0.0023	0.3113	± 0.0429	254.8	± 14.8	275.2	± 42.7	0.59	
57	0.0552	± 0.0042	0.0391	± 0.0021	0.2973	± 0.0311	247.1	± 13.7	264.3	± 31.1	0.48	
58	0.0499	± 0.0057	0.0383	± 0.0022	0.2633	± 0.0381	242.2	± 14.2	237.3	± 37.9	0.62	
59	0.0512	± 0.0088	0.0405	± 0.0026	0.2858	± 0.0604	255.9	± 16.9	255.2	± 59.5	0.72	
60	0.0554	± 0.0062	0.0396	± 0.0023	0.3022	± 0.0435	250.2	± 14.7	268.1	± 43.2	0.69	

第4表　秩父累帯北帯河内コンプレックスの砂岩(20140722L1-1試料；鳥羽レストパーク南)の砕屑性ジルコンにおけるレーザーアブレーション二重収束型結合誘導プラズマ質量分析装置によるU–Pb同位体データ．＊は最若年代集団のピーク年代(加重平均値)に採用されたジルコンを示す.

Table 4　U–Pb isotopic data determined by LA-ICP-MS using a double-focusing sector field mass spectrometer for detrital zircon from sandstone (sample no. 20140722L1-1) in the Kochi Complex, south of the Toba Rest Park, Northern Chichibu Belt. The asterisks indicate the zircon adopted for the peak age (weighted mean) of the youngest cluster.

Grain no.	Isotopic ratios						Age (Ma)				Th/U	Remarks
	$^{207}Pb/^{206}Pb$	Error 2σ	$^{206}Pb/^{238}U$	Error 2σ	$^{207}Pb/^{235}U$	Error 2σ	$^{206}Pb/^{238}U$	Error 2σ	$^{207}Pb/^{235}U$	Error 2σ		
1	0.0598	± 0.0110	0.0413	± 0.0027	0.3405	± 0.0681	260.6	± 17.4	297.5	± 66.9	0.37	
2	0.0706	± 0.0157	0.0394	± 0.0030	0.3833	± 0.0929	248.9	± 19.1	329.5	± 90.2	0.45	
3	0.0501	± 0.0120	0.0449	± 0.0032	0.3106	± 0.0802	283.4	± 20.9	274.6	± 78.3	0.39	
4	0.0567	± 0.0118	0.0404	± 0.0028	0.3159	± 0.0707	255.2	± 17.9	278.7	± 69.4	0.47	
5	0.0464	± 0.0078	0.0382	± 0.0023	0.2448	± 0.0440	241.9	± 14.9	222.3	± 43.7	0.39	
6	0.0517	± 0.0069	0.0391	± 0.0022	0.2793	± 0.0407	247.5	± 14.4	250.1	± 40.5	0.51	
7	0.0538	± 0.0121	0.0396	± 0.0028	0.2944	± 0.0708	250.6	± 18.1	262.0	± 69.4	0.92	
8	0.0518	± 0.0084	0.0454	± 0.0028	0.3242	± 0.0572	286.2	± 17.7	285.1	± 56.5	0.45	
9	0.0499	± 0.0059	0.0404	± 0.0022	0.2783	± 0.0360	255.3	± 14.3	249.3	± 35.9	0.35	
10	0.0522	± 0.0051	0.0303	± 0.0016	0.2182	± 0.0233	192.5	± 10.3	200.4	± 23.4	0.37	*
11	0.0530	± 0.0105	0.0408	± 0.0027	0.2977	± 0.0636	257.6	± 17.4	264.6	± 62.6	0.76	
12	0.0474	± 0.0075	0.0410	± 0.0024	0.2683	± 0.0455	259.1	± 15.6	241.3	± 45.2	0.55	
13	0.0558	± 0.0103	0.0426	± 0.0028	0.3280	± 0.0656	268.8	± 17.8	288.0	± 64.5	0.61	
14	0.0569	± 0.0100	0.0400	± 0.0025	0.3134	± 0.0599	252.6	± 16.4	276.8	± 59.1	0.47	
15	0.0443	± 0.0161	0.0369	± 0.0034	0.2253	± 0.0864	233.4	± 21.6	206.3	± 84.2	0.44	
16	0.0475	± 0.0092	0.0421	± 0.0027	0.2756	± 0.0567	265.6	± 17.6	247.1	± 56.0	0.79	
17	0.0514	± 0.0043	0.0384	± 0.0020	0.2719	± 0.0243	242.7	± 13.0	244.2	± 24.4	0.49	
18	0.0494	± 0.0113	0.0281	± 0.0020	0.1920	± 0.0454	179.0	± 12.8	178.3	± 45.1	0.83	*
19	0.0611	± 0.0119	0.0392	± 0.0027	0.3306	± 0.0691	248.1	± 17.3	290.0	± 67.8	0.53	
20	0.0372	± 0.0139	0.0446	± 0.0039	0.2291	± 0.0903	281.4	± 25.3	209.5	± 87.7	0.51	
21	0.0541	± 0.0158	0.0362	± 0.0030	0.2706	± 0.0834	229.5	± 19.5	243.1	± 81.3	0.64	
22	0.0576	± 0.0092	0.0314	± 0.0020	0.2494	± 0.0418	199.4	± 12.6	226.0	± 41.6	0.45	*
23	0.0574	± 0.0049	0.0573	± 0.0030	0.4536	± 0.0425	358.9	± 19.6	379.8	± 42.2	0.39	
24	0.0553	± 0.0065	0.0282	± 0.0016	0.2152	± 0.0265	179.3	± 10.2	197.9	± 26.5	0.45	*
25	0.0547	± 0.0053	0.0401	± 0.0022	0.3026	± 0.0316	253.5	± 14.0	268.4	± 31.6	0.70	
26	0.0398	± 0.0071	0.0444	± 0.0027	0.2438	± 0.0461	280.2	± 17.5	221.5	± 45.8	0.45	
27	0.0485	± 0.0047	0.0423	± 0.0023	0.2831	± 0.0293	267.3	± 14.7	253.1	± 29.3	0.25	
28	0.0414	± 0.0095	0.0428	± 0.0029	0.2445	± 0.0596	270.5	± 18.9	222.1	± 58.8	0.55	
29	0.0584	± 0.0071	0.0277	± 0.0016	0.2235	± 0.0285	176.4	± 10.2	204.8	± 28.5	0.43	*
30	0.0492	± 0.0110	0.0432	± 0.0030	0.2932	± 0.0698	272.5	± 19.5	261.0	± 68.5	0.77	
31	0.0332	± 0.0114	0.0427	± 0.0029	0.1953	± 0.0694	269.6	± 18.9	181.2	± 68.2	0.66	discordant
32	0.0466	± 0.0086	0.0393	± 0.0019	0.2527	± 0.0483	248.7	± 12.2	228.7	± 47.9	0.62	
33	0.0490	± 0.0050	0.0414	± 0.0014	0.2797	± 0.0277	261.5	± 9.3	250.4	± 27.8	0.56	
34	0.0363	± 0.0095	0.0419	± 0.0024	0.2099	± 0.0572	264.8	± 15.5	193.4	± 56.5	0.35	
35	0.0559	± 0.0093	0.0390	± 0.0018	0.3010	± 0.0515	246.9	± 11.8	267.2	± 50.9	0.84	
36	0.0580	± 0.0074	0.0404	± 0.0016	0.3229	± 0.0417	255.1	± 10.4	284.1	± 41.5	0.47	
37	0.0532	± 0.0048	0.0473	± 0.0016	0.3468	± 0.0296	297.6	± 10.1	302.3	± 29.6	0.14	
38	0.0451	± 0.0138	0.0429	± 0.0030	0.2671	± 0.0861	270.7	± 19.5	240.3	± 83.9	0.61	
39	0.0505	± 0.0046	0.0385	± 0.0013	0.2683	± 0.0230	243.7	± 8.3	241.3	± 23.1	0.32	
40	0.0506	± 0.0053	0.0289	± 0.0010	0.2019	± 0.0204	183.8	± 6.6	186.7	± 20.5	0.39	*
41	0.0500	± 0.0083	0.0420	± 0.0019	0.2892	± 0.0497	265.0	± 12.3	258.0	± 49.2	0.83	
42	0.0466	± 0.0080	0.0409	± 0.0019	0.2627	± 0.0465	258.1	± 12.0	236.9	± 46.1	0.58	
43	0.0495	± 0.0060	0.0430	± 0.0016	0.2936	± 0.0358	271.4	± 10.5	261.4	± 35.7	0.48	
44	0.0474	± 0.0062	0.0429	± 0.0017	0.2802	± 0.0369	270.7	± 10.8	250.8	± 36.7	0.28	
45	0.0483	± 0.0132	0.0394	± 0.0026	0.2626	± 0.0753	249.1	± 16.7	236.7	± 73.7	0.61	
46	0.0509	± 0.0097	0.0274	± 0.0016	0.1922	± 0.0392	174.0	± 10.2	178.5	± 39.0	0.53	*
47	0.0499	± 0.0059	0.0636	± 0.0030	0.4376	± 0.0603	397.5	± 19.2	368.6	± 59.5	0.34	
48	0.0463	± 0.0064	0.0278	± 0.0014	0.1777	± 0.0266	177.0	± 8.8	166.1	± 26.7	0.45	*
49	0.0559	± 0.0071	0.0310	± 0.0015	0.2387	± 0.0336	196.7	± 9.7	217.4	± 33.6	0.77	*
50	0.0810	± 0.0222	0.0438	± 0.0038	0.4887	± 0.1498	276.2	± 24.1	404.0	± 141.8	0.40	
51	0.0468	± 0.0074	0.0401	± 0.0021	0.2587	± 0.0447	253.4	± 13.3	233.6	± 44.4	0.57	
52	0.0473	± 0.0053	0.0330	± 0.0015	0.2157	± 0.0271	209.5	± 9.7	198.3	± 27.1	0.38	
53	0.0410	± 0.0156	0.0455	± 0.0040	0.2574	± 0.1048	286.8	± 25.5	232.6	± 101.2	0.46	
54	0.0778	± 0.0245	0.0395	± 0.0037	0.4242	± 0.1472	250.0	± 24.1	359.0	± 139.4	0.51	
55	0.0545	± 0.0058	0.0392	± 0.0018	0.2943	± 0.0362	247.7	± 11.6	261.9	± 36.1	0.70	
56	0.0530	± 0.0082	0.0283	± 0.0015	0.2067	± 0.0348	179.7	± 9.6	190.8	± 34.7	0.63	*
57	0.0568	± 0.0072	0.0397	± 0.0019	0.3105	± 0.0442	250.8	± 12.5	274.6	± 43.9	0.46	
58	0.0440	± 0.0056	0.0420	± 0.0020	0.2551	± 0.0363	265.4	± 12.8	230.7	± 36.2	0.52	
59	0.0459	± 0.0062	0.0290	± 0.0014	0.1839	± 0.0271	184.6	± 9.1	171.4	± 27.2	0.49	*
60	0.0541	± 0.0067	0.0405	± 0.0019	0.3021	± 0.0423	255.7	± 12.5	268.0	± 42.1	0.77	

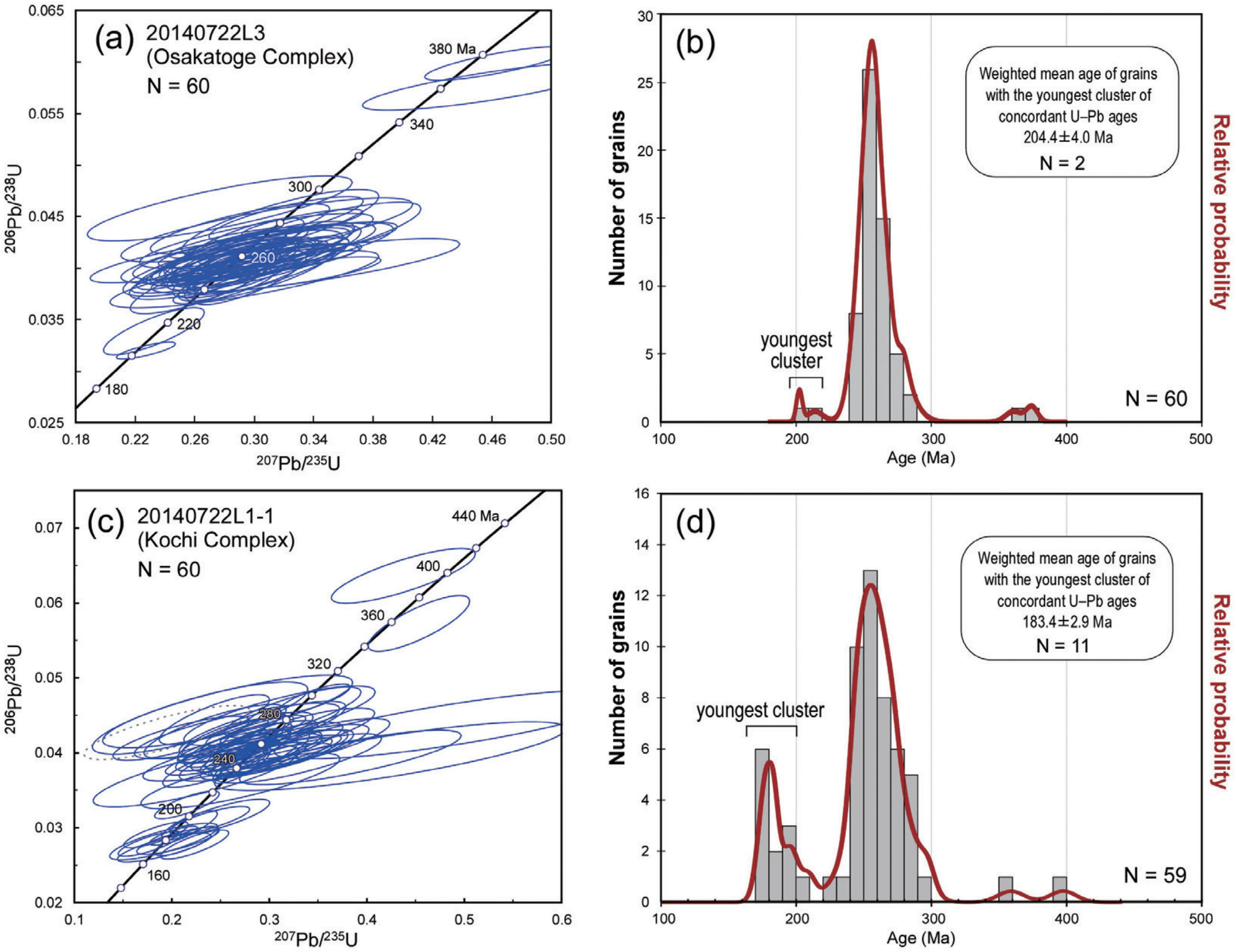

第3図　秩父累帯北帯砂岩の砕屑性ジルコンの分析データ．(a)コンコーディア図で表した20140722L3試料(逢坂峠コンプレックス)の全ジルコン粒子(60個)のデータ．(b)確率頻度曲線及びヒストグラムで表した20140722L3試料のコンコーディアを示すジルコン粒子(60個)のデータ．最若年代粒子集団(対象は2個)のピーク年代(加重平均値)は204.4 ± 4.0 Ma (誤差は2σ)を示す．(c)コンコーディア図で表した20140722L1-1試料(河内コンプレックス)の全ジルコン粒子(60個)のデータ．灰色点線楕円はディスコーダントデータを示す．(d)確率頻度曲線及びヒストグラムで表した20140722L1-1試料のコンコーディアを示すジルコン粒子(59個)のデータ．最若年代粒子集団(対象は11個)のピーク年代(加重平均値)は183.4 ± 2.9 Ma (誤差は2σ)を示す．

Fig. 3　Analytical data for detrital zircon grains from sandstones in the Northern Chichibu Belt. (a) Concordia diagram for all data (N = 60) of the sample (no. 20140722L3) from the Osakatoge Complex. (b) Probability density plot and histogram for the concordia data (N = 60) of the sample no. 20140722L3. Peak age (weighted mean) of grains with the youngest cluster (N = 2) is 204.4 ± 4.0 Ma (2σ). (c) Concordia diagram for all data (N = 60) of the sample no. 20140722L1-1, Kochi Complex. A dotted gray ellipse is the discordant data. (d) Probability density plot and histogram for the concordia data (N = 59) of the sample no. 20140722L1-1. Peak age (weighted mean) of grains with the youngest cluster (N = 11) is 183.4 ± 2.9 Ma (2σ).

4．得られた砕屑性ジルコン年代の評価

4. 1　秩父累帯北帯

都築・八尾(2006)は学会講演要旨ではあるが，逢坂峠コンプレックスの泥岩から*Bagotum* sp.，*Lupherium* sp.，*Pantanellium* sp.及び*Sichocapsa* sp.の放散虫化石を見出し，その時代を前期ジュラ紀と考えている．この報告は，現時点で逢坂峠コンプレックスの付加年代を示す唯一の根拠となっている．逢坂峠コンプレックスの砂岩から今回得られた砕屑性ジルコンのU-Pb年代のうち，最若粒子集団のピーク年代(加重平均値)は204.4 ± 4.0 Maである．204.4 ± 4.0 Maは地質年代表(Geologic Time Scale 2012) (Gradstein *et al*., 2012)では三畳紀末〜ジュラ紀初頭に相当し，本砂岩は少なくともその時代以降に堆積したといえる．したがって，都築・八尾(2006)が放散虫化石から判断した前期ジュラ紀という逢坂峠コンプレックスの付加年代は，今回の砕屑性ジルコン年代からも支持できる．

都築・八尾(2006)はまた，河内コンプレックスの

第5表　三波川帯宮川層の砂質片岩(20140521L3試料；鳴ヶ谷)の砕屑性ジルコンにおけるレーザーアブレーション二重収束型結合誘導プラズマ質量分析装置によるU–Pb同位体データ．＊は最若年代集団のピーク年代(加重平均値)に採用されたジルコンを示す．

Table 5　U–Pb isotopic data determined by LA-ICP-MS using a double-focusing sector field mass spectrometer for detrital zircon from psammitic schist (sample no. 20140521L3) in the Miyakawa Formation, Narugadani River, Sambagawa Belt. The asterisks indicate the zircon adopted for the peak age (weighted mean) of the youngest cluster.

Grain no.	Isotopic ratios						Age (Ma)				Th/U	Remarks
	^{207}Pb/^{206}Pb	Error 2σ	^{206}Pb/^{238}U	Error 2σ	^{207}Pb/^{235}U	Error 2σ	^{206}Pb/^{238}U	Error 2σ	^{207}Pb/^{235}U	Error 2σ		
1	0.0606	± 0.0112	0.0407	± 0.0025	0.3452	± 0.0684	257.2	± 16.3	301.1	± 67.2	0.46	
2	0.0563	± 0.0071	0.0588	± 0.0031	0.4629	± 0.0631	368.4	± 20.0	386.3	± 62.1	0.64	
3	0.0513	± 0.0156	0.0373	± 0.0030	0.2677	± 0.0860	236.0	± 19.5	240.9	± 83.8	0.56	
4	0.0427	± 0.0095	0.0398	± 0.0025	0.2378	± 0.0558	251.6	± 16.4	216.6	± 55.1	0.75	
5	0.0532	± 0.0084	0.0415	± 0.0024	0.3090	± 0.0523	262.4	± 15.2	273.4	± 51.8	0.61	
6	0.0565	± 0.0115	0.0406	± 0.0026	0.3211	± 0.0697	256.6	± 16.9	282.7	± 68.4	0.64	
7	0.0519	± 0.0052	0.0397	± 0.0020	0.2877	± 0.0306	250.7	± 12.6	256.7	± 30.6	0.65	
8	0.0446	± 0.0088	0.0286	± 0.0017	0.1783	± 0.0365	181.8	± 11.2	166.6	± 36.4	0.44	*
9	0.0536	± 0.0084	0.0281	± 0.0016	0.2106	± 0.0346	178.6	± 10.3	194.1	± 34.6	0.30	*
10	0.0432	± 0.0081	0.0268	± 0.0016	0.1618	± 0.0314	170.5	± 10.2	152.3	± 31.4	0.77	*
11	0.0516	± 0.0066	0.0305	± 0.0016	0.2202	± 0.0297	193.7	± 10.3	202.1	± 29.7	0.53	
12	0.0577	± 0.0101	0.0387	± 0.0023	0.3122	± 0.0583	244.5	± 15.0	275.9	± 57.5	0.51	
13	0.0451	± 0.0058	0.0346	± 0.0018	0.2183	± 0.0299	219.1	± 11.7	200.5	± 29.9	0.62	
14	0.1658	± 0.0162	0.4239	± 0.0216	9.8329	± 1.2983	2278.3	± 137.8	2419.2	± 845.0	1.08	
15	0.0534	± 0.0116	0.0386	± 0.0026	0.2883	± 0.0668	244.3	± 16.5	257.2	± 65.7	0.68	
16	0.0517	± 0.0079	0.0248	± 0.0014	0.1830	± 0.0243	157.9	± 8.8	170.6	± 24.4	0.40	*
17	0.0529	± 0.0091	0.0350	± 0.0020	0.2640	± 0.0417	221.6	± 13.1	237.9	± 41.5	0.75	
18	0.0440	± 0.0068	0.0344	± 0.0019	0.2158	± 0.0295	217.9	± 12.1	198.4	± 29.5	0.57	
19	0.0467	± 0.0088	0.0350	± 0.0021	0.2332	± 0.0412	221.9	± 13.5	212.9	± 41.0	0.56	
20	0.0470	± 0.0102	0.0333	± 0.0021	0.2231	± 0.0471	211.0	± 13.8	204.5	± 46.7	0.55	
21	0.1105	± 0.0142	0.2991	± 0.0158	4.7157	± 0.5557	1686.9	± 100.8	1770.0	± 448.7	0.20	
22	0.0504	± 0.0083	0.0387	± 0.0022	0.2781	± 0.0421	244.7	± 14.2	249.2	± 41.9	0.64	
23	0.0476	± 0.0085	0.0283	± 0.0017	0.1924	± 0.0319	179.9	± 10.7	178.7	± 31.9	0.30	*
24	0.0493	± 0.0121	0.0288	± 0.0020	0.2029	± 0.0489	183.0	± 12.9	187.5	± 48.4	0.60	*
25	0.0461	± 0.0080	0.0266	± 0.0015	0.1750	± 0.0277	169.3	± 9.9	163.8	± 27.8	0.41	*
26	0.0499	± 0.0123	0.0298	± 0.0021	0.2125	± 0.0515	189.5	± 13.5	195.7	± 51.0	0.48	*
27	0.1072	± 0.0134	0.2233	± 0.0115	3.4155	± 0.3450	1299.3	± 73.8	1508.0	± 300.9	0.07	
28	0.0663	± 0.0181	0.0281	± 0.0023	0.2659	± 0.0725	178.6	± 14.6	239.4	± 71.1	0.89	*
29	0.0467	± 0.0080	0.0398	± 0.0023	0.2651	± 0.0424	251.7	± 14.7	238.8	± 42.1	0.55	
30	0.1125	± 0.0142	0.2765	± 0.0144	4.4392	± 0.4816	1573.5	± 92.1	1719.7	± 399.2	0.18	
31	0.0511	± 0.0098	0.0379	± 0.0015	0.2674	± 0.0539	240.0	± 9.8	240.6	± 53.3	0.49	
32	0.1124	± 0.0106	0.3294	± 0.0044	5.1082	± 0.5299	1835.5	± 28.1	1837.5	± 431.8	0.42	
33	0.0492	± 0.0070	0.0253	± 0.0007	0.1721	± 0.0249	161.3	± 4.3	161.3	± 25.0	0.34	*
34	0.0482	± 0.0066	0.0396	± 0.0010	0.2633	± 0.0371	250.4	± 6.3	237.3	± 36.9	0.44	
35	0.0547	± 0.0136	0.0405	± 0.0022	0.3059	± 0.0805	256.1	± 14.5	271.0	± 78.6	0.53	
36	0.0525	± 0.0111	0.0325	± 0.0015	0.2352	± 0.0519	206.2	± 9.5	214.5	± 51.3	1.14	
37	0.0511	± 0.0127	0.0430	± 0.0023	0.3026	± 0.0801	271.2	± 15.0	268.4	± 78.2	0.54	
38	0.0498	± 0.0069	0.0375	± 0.0010	0.2574	± 0.0369	237.3	± 6.2	232.6	± 36.8	0.37	
39	0.0546	± 0.0074	0.0283	± 0.0007	0.2130	± 0.0296	179.7	± 4.7	196.1	± 29.6	0.52	*
40	0.0487	± 0.0087	0.0281	± 0.0010	0.1889	± 0.0347	178.8	± 6.5	175.7	± 34.7	0.52	*
41	0.1074	± 0.0099	0.2937	± 0.0033	4.3509	± 0.4158	1659.8	± 21.2	1703.1	± 353.1	0.12	
42	0.0460	± 0.0055	0.0298	± 0.0006	0.1893	± 0.0228	189.3	± 3.7	176.0	± 22.9	0.49	*
43	0.0455	± 0.0063	0.0417	± 0.0010	0.2617	± 0.0378	263.3	± 6.7	236.1	± 37.7	0.59	
44	0.0437	± 0.0071	0.0278	± 0.0008	0.1678	± 0.0280	176.9	± 5.4	157.5	± 28.0	0.40	*
45	0.1126	± 0.0106	0.2962	± 0.0040	4.5988	± 0.4755	1672.3	± 25.5	1749.0	± 395.0	0.08	
46	0.0516	± 0.0099	0.0292	± 0.0014	0.2077	± 0.0409	185.5	± 9.1	191.6	± 40.7	0.57	*
47	0.0531	± 0.0144	0.0402	± 0.0027	0.2948	± 0.0849	254.2	± 17.2	262.3	± 82.8	0.49	
48	0.0474	± 0.0044	0.0286	± 0.0008	0.1868	± 0.0169	181.5	± 5.5	173.9	± 17.1	0.30	*
49	0.0494	± 0.0058	0.0311	± 0.0011	0.2117	± 0.0253	197.4	± 6.8	195.0	± 25.3	0.63	
50	0.0445	± 0.0101	0.0403	± 0.0021	0.2477	± 0.0589	254.8	± 13.8	224.7	± 58.1	0.61	
51	0.0653	± 0.0137	0.0566	± 0.0033	0.5101	± 0.1187	354.9	± 21.0	418.5	± 113.9	0.39	
52	0.0450	± 0.0051	0.0339	± 0.0011	0.2105	± 0.0242	214.8	± 7.2	194.0	± 24.3	0.54	
53	0.0508	± 0.0098	0.0270	± 0.0013	0.1888	± 0.0374	171.4	± 8.5	175.6	± 37.3	0.38	*
54	0.0495	± 0.0083	0.0321	± 0.0014	0.2189	± 0.0380	203.5	± 9.0	201.0	± 37.8	0.61	
55	0.0439	± 0.0050	0.0271	± 0.0009	0.1639	± 0.0185	172.3	± 5.7	154.1	± 18.6	0.65	*
56	0.0533	± 0.0153	0.0375	± 0.0026	0.2758	± 0.0836	237.5	± 16.9	247.3	± 81.5	1.06	
57	0.0564	± 0.0063	0.0403	± 0.0014	0.3135	± 0.0358	254.6	± 8.8	276.9	± 35.7	0.87	
58	0.0575	± 0.0082	0.0280	± 0.0011	0.2223	± 0.0323	178.3	± 7.2	203.8	± 32.2	0.42	
59	0.0478	± 0.0057	0.0296	± 0.0010	0.1952	± 0.0236	188.1	± 6.5	181.1	± 23.7	0.85	
60	0.0394	± 0.0142	0.0446	± 0.0034	0.2422	± 0.0918	281.1	± 21.7	220.3	± 89.1	0.73	

第6表　三波川帯宮川層の砂質片岩(20140522L5試料；坂手島)の砕屑性ジルコンにおけるレーザーアブレーション二重収束型結合誘導プラズマ質量分析装置によるU–Pb同位体データ．＊は最若年代集団のピーク年代(加重平均値)に採用されたジルコンを示す．

Table 6　U–Pb isotopic data determined by LA-ICP-MS using a double-focusing sector field mass spectrometer for detrital zircon from sandstone (sample no. 20140522L5) in the Miyakawa Formation, Sakate Island, Sambagawa Belt. The asterisks indicate the zircon adopted for the peak age (weighted mean) of the youngest cluster.

Grain no.	Isotopic ratios						Age (Ma)				Th/U	Remarks
	^{207}Pb/^{206}Pb	Error 2σ	^{206}Pb/^{238}U	Error 2σ	^{207}Pb/^{235}U	Error 2σ	^{206}Pb/^{238}U	Error 2σ	^{207}Pb/^{235}U	Error 2σ		
1	0.0623	± 0.0132	0.0191	± 0.0011	0.1644	± 0.0345	122.1	± 6.9	154.5	± 34.5	1.00	
2	0.0517	± 0.0164	0.0141	± 0.0011	0.1007	± 0.0318	90.4	± 6.8	97.4	± 31.8	1.13	*
3	0.0475	± 0.0067	0.0277	± 0.0011	0.1815	± 0.0248	176.1	± 6.9	169.4	± 24.9	0.22	
4	0.1134	± 0.0091	0.3294	± 0.0099	5.1530	± 0.4012	1835.6	± 63.7	1844.9	± 342.5	0.38	
5	0.0381	± 0.0177	0.0272	± 0.0025	0.1431	± 0.0679	172.9	± 16.4	135.8	± 66.7	0.91	
6	0.0567	± 0.0104	0.0415	± 0.0020	0.3244	± 0.0616	261.9	± 13.1	285.3	± 60.6	0.55	
7	0.1141	± 0.0093	0.3142	± 0.0096	4.9444	± 0.4073	1761.5	± 61.7	1809.9	± 347.0	0.39	
8	0.1052	± 0.0082	0.3030	± 0.0089	4.3976	± 0.2900	1706.4	± 56.9	1711.9	± 258.6	0.03	
9	0.1046	± 0.0093	0.1752	± 0.0057	2.5295	± 0.2344	1040.8	± 36.5	1280.5	± 213.8	0.48	
10	0.1233	± 0.0099	0.1678	± 0.0050	2.8536	± 0.2053	999.8	± 32.4	1369.8	± 189.6	0.12	
11	0.1139	± 0.0093	0.3102	± 0.0095	4.8723	± 0.4094	1741.7	± 61.2	1797.5	± 348.4	0.35	
12	0.0554	± 0.0088	0.0349	± 0.0015	0.2671	± 0.0427	221.3	± 9.8	240.4	± 42.4	0.96	
13	0.0668	± 0.0107	0.0212	± 0.0010	0.1957	± 0.0307	135.5	± 6.3	181.5	± 30.7	0.95	
14	0.0525	± 0.0061	0.0249	± 0.0009	0.1804	± 0.0197	158.5	± 5.6	168.4	± 19.8	0.30	
15	0.0457	± 0.0093	0.0256	± 0.0013	0.1617	± 0.0328	163.1	± 8.1	152.2	± 32.7	0.33	
16	0.1148	± 0.0066	0.2821	± 0.0095	4.4667	± 0.3636	1602.0	± 60.7	1724.8	± 314.9	0.21	
17	0.1196	± 0.0072	0.2982	± 0.0102	4.9199	± 0.4348	1682.3	± 65.2	1805.7	± 366.6	0.15	
18	0.0477	± 0.0120	0.0223	± 0.0014	0.1466	± 0.0382	142.1	± 8.9	138.9	± 38.1	0.79	
19	0.1154	± 0.0075	0.2684	± 0.0095	4.2700	± 0.4259	1532.7	± 60.7	1687.6	± 360.3	0.28	
20	0.1443	± 0.0089	0.3267	± 0.0114	6.5012	± 0.6288	1822.3	± 72.9	2046.1	± 495.3	0.13	
21	0.0482	± 0.0047	0.0240	± 0.0009	0.1598	± 0.0177	153.1	± 5.8	150.6	± 17.8	0.34	
22	0.0451	± 0.0110	0.0154	± 0.0009	0.0954	± 0.0238	98.2	± 5.8	92.6	± 23.9	0.61	*
23	0.1128	± 0.0084	0.3291	± 0.0123	5.1192	± 0.6362	1833.8	± 78.8	1839.3	± 500.0	0.55	
24	0.0583	± 0.0084	0.0274	± 0.0012	0.2207	± 0.0347	174.5	± 8.0	202.5	± 34.6	0.43	
25	0.0510	± 0.0075	0.0285	± 0.0013	0.2006	± 0.0321	181.3	± 8.2	185.7	± 32.1	0.35	
26	0.0420	± 0.0101	0.0152	± 0.0009	0.0879	± 0.0217	97.2	± 5.6	85.5	± 21.8	1.16	*
27	0.0553	± 0.0077	0.0343	± 0.0015	0.2617	± 0.0404	217.7	± 9.8	236.1	± 40.2	0.66	
28	0.1131	± 0.0072	0.3284	± 0.0114	5.1226	± 0.5003	1830.4	± 73.3	1839.9	± 411.9	0.38	
29	0.1554	± 0.0093	0.4191	± 0.0145	8.9771	± 0.8729	2256.2	± 92.8	2335.7	± 637.1	0.88	
30	0.1370	± 0.0077	0.3310	± 0.0110	6.2550	± 0.4965	1843.2	± 70.7	2012.2	± 409.3	0.11	
31	0.0502	± 0.0099	0.0298	± 0.0016	0.2061	± 0.0427	189.0	± 10.5	190.3	± 42.5	0.63	
32	0.0459	± 0.0177	0.0152	± 0.0013	0.0961	± 0.0374	97.0	± 8.6	93.2	± 37.3	2.05	*
33	0.0492	± 0.0127	0.0284	± 0.0019	0.1926	± 0.0518	180.4	± 11.9	178.8	± 51.2	0.51	
34	0.0543	± 0.0101	0.0332	± 0.0018	0.2489	± 0.0489	210.6	± 11.5	225.7	± 48.5	0.54	
35	0.0492	± 0.0050	0.0269	± 0.0011	0.1824	± 0.0197	170.9	± 6.9	170.1	± 19.8	0.22	
36	0.0524	± 0.0055	0.0279	± 0.0011	0.2013	± 0.0225	177.3	± 7.2	186.2	± 22.6	0.11	
37	0.1227	± 0.0098	0.3192	± 0.0122	5.4007	± 0.5429	1786.1	± 78.2	1885.0	± 440.3	0.66	
38	0.1143	± 0.0086	0.2800	± 0.0104	4.4117	± 0.3767	1591.3	± 66.5	1714.5	± 324.6	0.09	
39	0.0508	± 0.0069	0.0305	± 0.0014	0.2135	± 0.0307	193.4	± 8.7	196.5	± 30.7	0.94	
40	0.1154	± 0.0086	0.2869	± 0.0106	4.5657	± 0.3785	1625.8	± 67.7	1743.0	± 326.0	0.03	
41	0.0444	± 0.0078	0.0265	± 0.0013	0.1621	± 0.0296	168.6	± 8.4	152.5	± 29.6	0.71	
42	0.1346	± 0.0103	0.3140	± 0.0118	5.8277	± 0.5344	1760.2	± 75.5	1950.5	± 434.7	0.19	
43	0.1126	± 0.0094	0.2565	± 0.0100	3.9847	± 0.4218	1471.9	± 64.0	1631.1	± 357.4	0.16	
44	0.0604	± 0.0241	0.0159	± 0.0016	0.1323	± 0.0536	101.6	± 10.3	126.2	± 53.0	1.58	*
45	0.0518	± 0.0084	0.0261	± 0.0013	0.1864	± 0.0316	166.0	± 8.2	173.6	± 31.6	0.21	
46	0.1134	± 0.0102	0.2922	± 0.0110	4.5698	± 0.5321	1652.4	± 70.2	1743.8	± 433.2	0.69	
47	0.0460	± 0.0054	0.0286	± 0.0011	0.1812	± 0.0234	181.6	± 7.3	169.1	± 23.5	0.33	
48	0.1147	± 0.0098	0.3070	± 0.0111	4.8562	± 0.5038	1726.2	± 71.2	1794.7	± 414.3	0.43	
49	0.0452	± 0.0049	0.0278	± 0.0011	0.1737	± 0.0207	177.0	± 6.9	162.6	± 20.8	0.20	
50	0.1141	± 0.0099	0.3062	± 0.0112	4.8191	± 0.5190	1722.2	± 71.8	1788.2	± 424.5	0.37	
51	0.1099	± 0.0094	0.3144	± 0.0113	4.7662	± 0.4890	1762.2	± 72.7	1779.0	± 404.2	0.52	
52	0.0482	± 0.0082	0.0172	± 0.0008	0.1144	± 0.0205	109.9	± 5.3	110.0	± 20.6	0.62	
53	0.1079	± 0.0098	0.2090	± 0.0079	3.1115	± 0.3562	1223.7	± 50.5	1435.5	± 309.3	0.08	
54	0.0572	± 0.0079	0.0305	± 0.0013	0.2407	± 0.0362	193.6	± 8.7	219.0	± 36.1	1.02	
55	0.1632	± 0.0144	0.4481	± 0.0168	10.0851	± 1.2213	2386.7	± 107.5	2442.6	± 810.4	1.14	
56	0.1163	± 0.0101	0.2819	± 0.0103	4.5202	± 0.4847	1600.9	± 66.1	1734.7	± 401.3	0.29	
57	0.0527	± 0.0124	0.0320	± 0.0020	0.2329	± 0.0583	203.3	± 12.7	212.6	± 57.5	0.70	
58	0.0494	± 0.0054	0.0284	± 0.0011	0.1937	± 0.0233	180.7	± 7.1	179.8	± 23.4	0.13	
59	0.0480	± 0.0105	0.0300	± 0.0017	0.1990	± 0.0460	190.8	± 11.0	184.2	± 45.7	0.89	
60	0.0428	± 0.0077	0.0146	± 0.0007	0.0861	± 0.0161	93.4	± 4.5	83.9	± 16.2	0.31	*

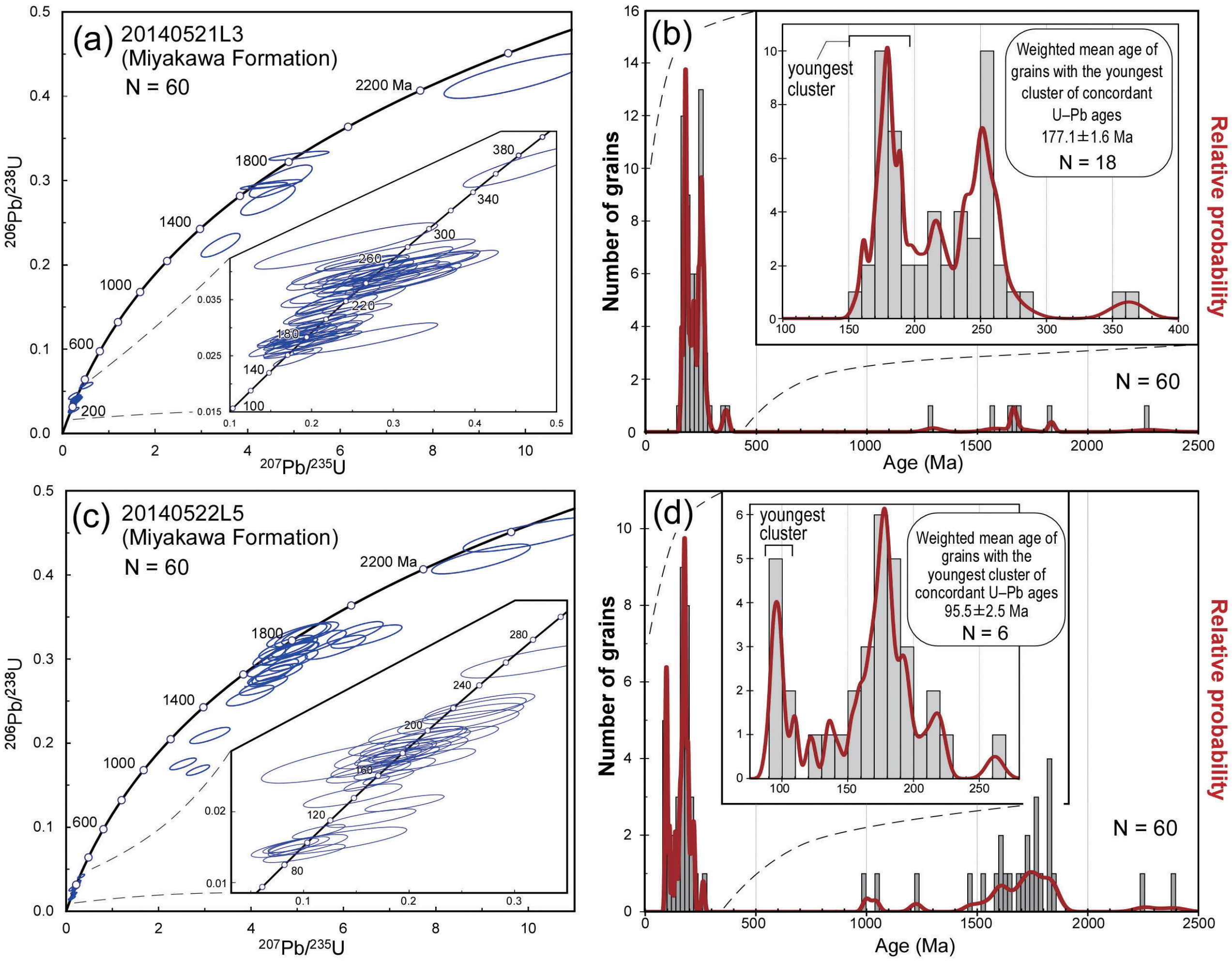

第4図　三波川帯宮川層砂質片岩の砕屑性ジルコンの分析データ．(a) コンコーディア図で表した20140521L3試料の全ジルコン粒子(60個)のデータ．(b) 確率頻度曲線及びヒストグラムで表した20140521L3試料のコンコーディアを示すジルコン粒子(60個)のデータ．最若年代粒子集団(対象は18個)のピーク年代(加重平均値)は177.1 ± 1.6 Ma (誤差は2σ)を示す．(c) コンコーディア図で表した20140522L5試料の全ジルコン粒子(60個)のデータ．(d) 確率頻度曲線及びヒストグラムで表した20140522L5試料のコンコーディアを示すジルコン粒子(60個)のデータ．最若年代粒子集団(対象は6個)のピーク年代(加重平均値)は95.5 ± 2.5 Ma (誤差は2σ)を示す．

Fig. 4　Analytical data for detrital zircon grains from psammitic schists in the Miyakawa Formation in the Sambagawa Belt. (a) Concordia diagram for all data of the sample no. 20140521L3. (b) Probability density plot and histogram for concordia data of the sample no. 20140521L3. Inset is probability density plot and histogram for the Phanerozoic dataset. Peak age (weighted mean) of grains with the youngest cluster (N = 18) is 177.1 ± 1.6 Ma (2σ). (c) Concordia diagram for all data of the sample no. 20140522L5. (d) Probability density plot and histogram for concordia data of the sample no. 20140522L5. Inset is probability density plot and histogram for the Phanerozoic dataset. Peak age (weighted mean) of grains with the youngest cluster (N = 6) is 95.5 ± 2.5 Ma (2σ).

泥岩から *Stichocapsa fusiformis* Hinde，*Parvicingula* sp.，*Dictyomitrella* sp.の放散虫化石を見出し，その時代を中期ジュラ紀と考えている．この報告も，現時点で河内コンプレックスの付加年代を示す唯一の根拠となっている．河内コンプレックスの砂岩から今回得られた砕屑性ジルコンのU–Pb年代のうち，最若粒子集団のピーク年代（加重平均値）は183.4 ± 2.9 Ma（最若ジルコンの年代は174.0 ± 10.2 Ma）である．183.4 ± 2.9 Maは前期ジュラ紀中頃～前期ジュラ紀後半に相当し，本砂岩は少なくともその時代以降に堆積したといえる．したがって，都築・八尾（2006）が放散虫化石から判断した中期ジュラ紀という河内コンプレックスの付加年代は，今回の砕屑性ジルコン年代からも概ね支持できる．

4. 2　三波川帯

これまで本地域の三波川帯の泥質岩からは年代は報告されていない．本地域西隣（伊勢地域）ではTomiyoshi and Takasu（2010）によって，御荷鉾緑色岩類分布域中に産する泥質片岩から99.1 ± 2.5，97.1 ± 2.4及び93.2 ± 2.3 Ma（後期白亜紀初頭）の，また御荷鉾緑色岩類の北側に産する泥質片岩から84.2 ± 2.1と83.6 ± 2.1 Ma（後期白亜紀中頃）のフェンジャイトK–Ar年代がそれぞれ報告されている．

今回行った年代測定では，坂手島の砂質片岩の砕屑性ジルコンU–Pb年代（最若粒子集団のピーク年代）は95.5 ± 2.5 Ma（後期白亜紀前半）を示している．宮川層の変成度は四国三波川帯の緑泥石帯低温部に相当するため，沈み込み帯での変成作用でジルコンは生じていないと考えられる．また，ジルコン粒子の中心部を測定しているため，その年代は基本的に火成起源のジルコン年代を示すとみなせる．これらのことから，本試料のジルコン年代は砂質片岩の原岩の堆積年代に近似できる．すなわち，95 Ma以降に堆積した可能性を示す．これは，大藤ほか（2010）で示された紀伊半島西部の結果と同様である．そして，概ね同層準とみなせる伊勢地域の泥質片岩が示す99–83 MaのフェンジャイトK–Ar年代（Tomiyoshi and Takasu，2010）を参考にすれば，宮川層の付加年代は95 Ma（堆積年代）と99–83 Ma（変成・冷却年代）の間，すなわち後期白亜紀中頃とみなせる．

一方，鳴ヶ谷の砂質片岩の砕屑性ジルコンU–Pb年代（最若粒子集団のピーク年代）は177.1 ± 1.6 Ma（前期ジュラ紀後半）であり，本砂質片岩の原岩は177 Ma以降に堆積したといえる．しかし，坂手島の試料とは80 m.y.程度の有意な年代差がある．鳴ヶ谷の試料の一番若い砕屑性ジルコンでも157.9 ± 8.8 Ma（後期ジュラ紀前半）であり，やはり坂手島のものよりも有意に古い．両者の年代差について，鳴ヶ谷と坂手島の試料とが異なる堆積（付加）年代を示すのか，それとも鳴ヶ谷の試料が偶然白亜紀以降の砕屑性ジルコンを含んでいない（本研究では抽出できなかった）のか，あるいは他の原因によるものなのかは，現時点では不明である．ちなみに，坂手島と鳴ヶ谷の試料採取地点は宮川層中央部に存在する背斜軸の南翼に属しており（第1図），層準は異なるものの岩相には全く差異はない．また，両試料採取地点間に順序外スラストの存在など大きな構造変位を示す野外事実は認められていない．

今後，坂手島と鳴ヶ谷の試料の年代差について議論するために，鳴ヶ谷の試料あるいは同層準から更なる砕屑性ジルコンU–Pb年代測定やフェンジャイトK–Ar年代測定を行い，鳴ヶ谷試料の年代の妥当性を検証する必要がある．

5. まとめ

秩父累帯北帯逢坂峠コンプレックスの砂岩中ジルコンの最若粒子集団は204.4 ± 4.0 Ma（三畳紀末～ジュラ紀初頭）を示し，河内コンプレックスの砂岩中のジルコンの最若粒子集団は183.4 ± 2.9 Ma（前期ジュラ紀中頃～前期ジュラ紀後半）を示す．これらは放散虫化石から想定されている陸源性砕屑岩の堆積年代と矛盾しない．

三波川帯宮川層の砂質片岩中のジルコンの最若粒子集団は177.1 ± 1.6 Ma（前期ジュラ紀後半）と95.5 ± 2.5 Ma（後期白亜紀前半）を示す．後者は，周辺地域から得られているフェンジャイトK–Ar年代から想定される変成（冷却）年代と矛盾しない．しかし，前者は後者よりも有意に古い年代を示す結果となった．

謝辞：株式会社京都フィッション・トラックの檀原　徹氏及び岩野英樹氏には分析手法についての記述について意見をいただいた．原　英俊氏（地質情報研究部門）には砕屑性ジルコンU–Pb年代測定について情報をいただいた．査読者の野田　篤氏（地質情報研究部門）及び昆　慶明氏（地圏資源環境研究部門）と編集委員の高橋　浩氏（地質情報研究部門）には原稿改善に有益な指摘をいただいた．記して感謝の意を表する．

文　献

青木一勝・大藤　茂・柳井修一・丸山茂徳（2010）　三波川変成帯中の新たな独立した広域変成帯の存在－白亜紀から第三紀の日本における造山運動－．地学雑誌，**119**，313–332.

坂野靖行（1992）　紀伊半島東部，御荷鉾緑色岩類に伴う蛇紋岩礫岩中の青色片岩．岩鉱，**87**，207–220.

Gradstein, F. M., Ogg, J. G., Schmitz, M. D. and Ogg, G. M., eds.（2012）*The Geologic Time Scale 2012.* Elsevier, 1144p.

飯塚保五郎（1929）　7万5千分の1「鳥羽」図幅および同説明書．商工省地質調査所，28p.

磯﨑行雄・橋口孝泰・板谷徹丸（1992）　黒瀬川クリッペの検証．地質雑，**98**，917–941.

岩野英樹・折橋裕二・檀原　徹・平田岳史・小笠原正継（2012）　同一ジルコン結晶を用いたフィッション・トラックとU-Pbダブル年代測定法の評価－島根県川本花崗閃緑岩中の均質ジルコンを用いて－．地質雑，**118**，365–375.

Iwano, H., Orihashi, Y., Hirata, T., Ogasawara, M., Danhara, T., Horie, K., Hasebe, N., Sueoka, S., Tamura, A., Hayasaka, Y., Katsube, A., Ito, H., Tani, K., Kimura, J., Chang, Q., Kouchi, Y., Haruta, Y. and Yamamoto, K. (2013)　An inter-laboratory evaluation of OD-3 zircon for use as a secondary U–Pb dating standard. *Island Arc*, **22**, 382–394.

加藤武夫・杉　健一（1927）　日本西南部外帯の推し被せ構造（予報）．地質雑，**34**，249–252.

日下部吉彦・宮村 学（1958）　伊勢市南方の古生層について．地質雑，**64**，269–280.

Ludwig, K. R. (2008)　Isoplot 3.70: *Geochronological Toolkit for Microsoft Excel*. Berkeley Geochronology Center Special Publication, **4**, 77p.

Lukács, R., Harangi, S., Bachmann, O., Guillong, M., Danišík, M., Buret, Y., von Quadt, A., Dunkl, I., Fodor, L., Sliwinski J., Soós, I. and Szepesi, J. (2015)　Zircon geochronology and geochemistry to constrain the youngest eruption events and magma evolution of the Mid-Miocene ignimbrite flare-up in the Pannonian Basin, eastern central Europe. *Contributions to Mineralogy and Petrology*, **170**, 1–26.

Maruyama, S., Hattori, K., Hirata, T. and Danhara, T. (2016)　A proposed methodology for analyses of wide-ranged elements in volcanic glass shards in the Quaternary widespread tephras. *Quaternary International*, **397**, 267–280.

Nakamura, Y. (1971)　Petrology of the Toba ultrabasic complex, Mie Prefecture, Central Japan. *Jour. Fac. Sci. Univ. Tokyo, Sec. II*, **18**, 1–51.

大藤　茂・下条将徳・青木一勝・中間隆晃・丸山茂徳・柳井修一（2010）　砂質片岩中のジルコンの年代分布に基づく三波川帯再区分の試み．地学雑誌，**119**，333–346.

坂　幸恭（2009）　中・古生界，紀伊半島東部地域．日本地質学会編，日本地方地質誌5：近畿地方，朝倉書店，134–140.

坂　幸恭・手塚茂雄・岡田洋一・市川昌則・高木秀雄（1988）　蛇紋岩メランジュ帯としての志摩半島，五ヶ所–安楽島構造線．地質雑，**94**，19–34.

坂　幸恭・加藤　潔・津村善博・大場穂高（1999）　志摩半島の秩父帯と黒瀬川帯．日本地質学会第106年学術大会見学旅行案内書，163–186.

Sakata, S., Hattori, K., Iwano, H., Yokoyama, T. D., Danhara, T. and Hirata, T. (2014)　Determination of U-Pb ages for young zircons using laser ablation-ICP-mass spectrometry coupled with an ion detection attenuator device. *Geostand. Geoanal. Res*., **38**, 409–420.

Sláma, J., Košler, J., Condon, J. D. Crowley, J. L., Gerdes, A. Hanchar, J. M., Horstwood, M. S. A., Morris, G. A., Nasdala, L., Norberg, N., Schaltegger, U., Schoene, B., Tubrett, M. N. and Whitehouse, M. J (2008)　Plešovice zircon — A new natural reference material for U-Pb and Hf isotopic microanalysis. *Chemical Geology*, **249**, 1–35.

菅野耕三・中世古幸次郎・脇本礼子（1980）　志摩半島東部に分布する築地層群から産する放散虫化石について，大阪教育大紀要，Ⅲ，**28**，111–121.

Tomiyoshi, S. and Takasu, A. (2010)　K–Ar ages of lawsonite-bearing pelitic schists from the Sambagawa metamorphic belt in the Ise district, eastern Kii Peninsula, southwest Japan. *Earth Science (Chikyu Kagaku)*, **64**, 193–200.

都築　宏・八尾　昭（2006）　志摩半島東部地域の秩父北帯のジュラ紀付加コンプレックス．日本地質学会第113年学術大会講演要旨，45.

上野貴司（2001）　紀伊半島東部，伊勢地方三波川帯から産する含ローソン石泥質片岩．岩石鉱物科学，**30**，255–264.

Wiedenbeck, M., Allé, P., Corfu, F., Griffin, W. L., Meier, M., Oberli, F., von Quadt, A., Roddick, J. C. and Spiegel, W. (1995)　Three natural zircon standards for U–Th–Pb, Lu–Hf, trace element and REE analyses. *Geostand. Newslett*., **19**, 1–23.

山際延夫（2015）　三重県志摩半島産出のペルム紀前期四放珊瑚化石*Ivanovia*属の1種について．大阪教育大紀要，Ⅲ，**63**，23–29.

山際延夫・坂　幸恭（1967）　志摩半島東部の中・古生界．日本地質学会第74年年会地質見学案内書，24p.

Yokoyama, T. D., Suzuki, T., Kon, Y. and Hirata, T. (2011)　Determinations of rare earth element abundance and U-Pb age of zircons using multispot laser ablation-inductively coupled plasma mass spectrometry. *Anal. Chem*., **83**, 8892–8899.

（受 付：2016年7月25日；受 理：2017年1月30日）

付録

Zircon grains composing the youngest cluster of the sample no. 20140722L3, Osakatoge Complex

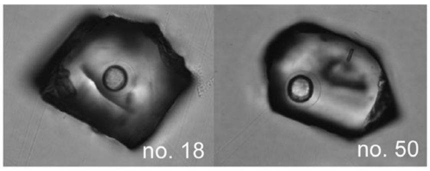

Laser spot diameter: 25 μm

Zircon grains composing the youngest cluster of the sample no. 20140722L1-1, Kochi Complex

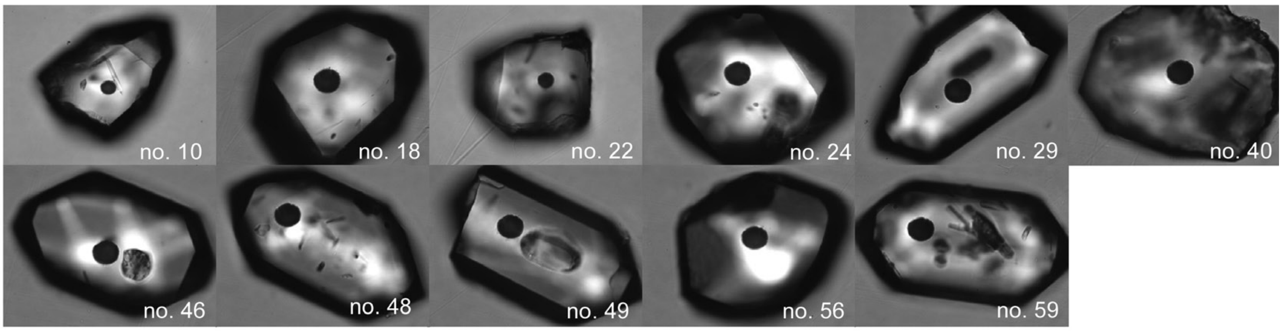

Laser spot diameter: 15 μm

Zircon grains composing the youngest cluster of the sample no. 20140521L3, Miyakawa Formation

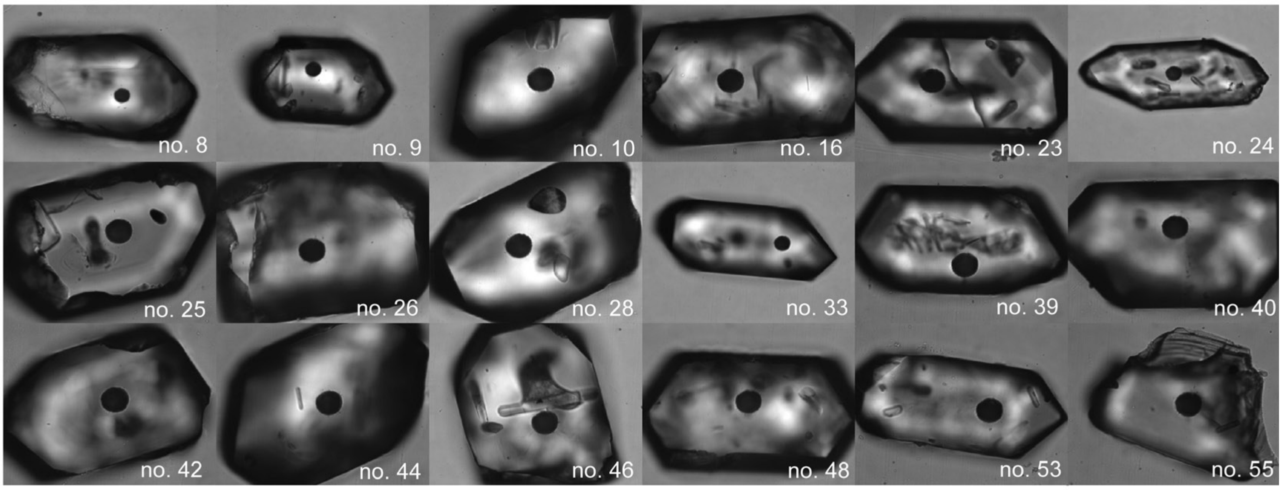

Laser spot diameter: 15 μm

Zircon grains composing the youngest cluster of the sample no. 20140522L5, Miyakawa Formation

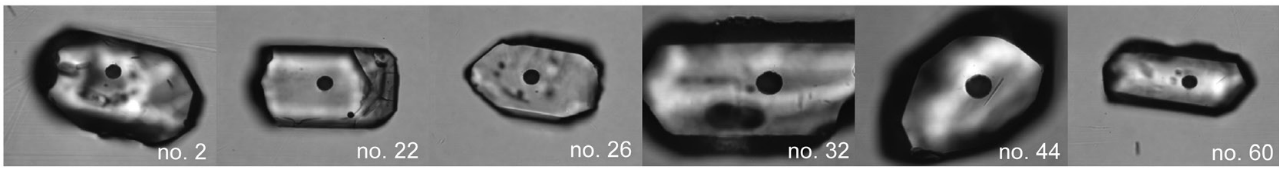

Laser spot diameter: 15 μm

付図1　レーザー照射位置を示した最若粒子集団を構成するジルコンの顕微鏡写真.

Figure A1　Photomicrographs of the zircon grains with laser radiation points composing the youngest cluster in each sample.

付表1　二重結合型LA-ICP-MSで測定した2次標準試料（OD-3及びPlešovice）のU-Pb同位体データ.

Table A1　U–Pb isotopic data for secondary zircon standards determined by LA-ICP-MS using a double-focusing sector field mass spectrometer.

Sample name	Isotopic ratios								Age (Ma)						U (ppm)	Th (ppm)	Th/U
	^{207}Pb/^{206}Pb	Error 2σ	^{206}Pb/^{238}U	Error 2σ	^{207}Pb/^{235}U	Error 2σ	^{208}Pb/^{232}Th	Error 2σ	^{206}Pb/^{238}U	Error 2σ	^{207}Pb/^{235}U	Error 2σ	^{208}Pb/^{232}Th	Error 2σ			
Plešovice (337 Ma): Sláma *et al*. (2008)																	
PSV 1-1	0.0547	± 0.0036	0.05086	± 0.00255	0.3894	± 0.0438	0.0159	± 0.0015	320	± 16	334	± 43	319	± 31	812	119	0.15
PSV 1-2	0.0507	± 0.0033	0.05242	± 0.00263	0.3722	± 0.0424	0.0162	± 0.0016	329	± 17	321	± 42	324	± 32	758	118	0.16
PSV 2-1	0.0522	± 0.0031	0.05259	± 0.00277	0.3772	± 0.0429	0.0156	± 0.0013	330	± 18	325	± 43	313	± 27	694	109	0.16
PSV 3-1	0.0527	± 0.0048	0.05228	± 0.00081	0.3602	± 0.0387	0.0156	± 0.0010	329	± 5	312	± 39	312	± 21	724	110	0.15
PSV 4-1	0.0513	± 0.0027	0.05330	± 0.00145	0.3643	± 0.0261	0.0155	± 0.0017	335	± 9	315	± 26	311	± 33	766	118	0.15
PSV 5-1	0.0529	± 0.0041	0.05538	± 0.00172	0.4006	± 0.0331	0.0164	± 0.0014	347	± 11	342	± 33	330	± 27	730	102	0.14
PSV 6-1	0.0529	± 0.0029	0.05200	± 0.00182	0.3851	± 0.0357	0.0162	± 0.0013	327	± 12	331	± 36	326	± 25	705	85	0.12
PSV 7-1	0.0546	± 0.0040	0.05204	± 0.00200	0.3926	± 0.0384	0.0142	± 0.0013	327	± 13	336	± 38	286	± 26	710	91	0.13
PSV 8-1	0.0558	± 0.0047	0.05125	± 0.00191	0.3849	± 0.0421	0.0163	± 0.0014	322	± 12	331	± 42	327	± 28	771	110	0.14
PSV 8-2	0.0549	± 0.0046	0.05142	± 0.00192	0.3798	± 0.0418	0.0162	± 0.0014	323	± 12	327	± 42	325	± 28	748	103	0.14
PSV 10-1	0.0573	± 0.0028	0.05277	± 0.00267	0.4049	± 0.0322	0.0163	± 0.0015	332	± 17	345	± 32	326	± 31	787	116	0.15
PSV 11-1	0.0556	± 0.0027	0.05324	± 0.00277	0.3945	± 0.0316	0.0148	± 0.0014	334	± 18	338	± 32	296	± 29	601	79	0.13
PSV 12-1	0.0536	± 0.0036	0.05257	± 0.00169	0.3787	± 0.0286	0.0157	± 0.0014	330	± 11	326	± 29	315	± 29	870	126	0.14
PSV 13-1	0.0555	± 0.0032	0.05267	± 0.00223	0.3926	± 0.0363	0.0156	± 0.0009	331	± 14	336	± 36	313	± 19	842	120	0.14
PSV 14-1	0.0544	± 0.0031	0.05252	± 0.00222	0.3834	± 0.0358	0.0160	± 0.0010	330	± 14	330	± 36	321	± 21	807	97	0.12
OD-3 (33 Ma): Iwano *et al*.(2012), Iwano *et al*.(2013), Lukács *et al*. (2015)																	
OD3 1-1	0.0498	± 0.0032	0.00520	± 0.00044	0.0363	± 0.0119	0.0017	± 0.0002	33	± 3	36	± 12	34	± 4	234	307	1.31
OD3 2-1	0.0445	± 0.0026	0.00466	± 0.00033	0.0285	± 0.0072	0.0014	± 0.0001	30	± 2	29	± 7	29	± 3	501	607	1.21
OD3 2-2	0.0582	± 0.0034	0.00506	± 0.00036	0.0405	± 0.0090	0.0014	± 0.0001	33	± 2	40	± 9	28	± 3	475	576	1.21
OD3 3-1	0.0471	± 0.0043	0.00490	± 0.00023	0.0302	± 0.0071	0.0014	± 0.0001	31	± 2	30	± 7	29	± 2	484	611	1.26
OD3 4-1	0.0430	± 0.0023	0.00526	± 0.00027	0.0301	± 0.0066	0.0014	± 0.0002	34	± 2	30	± 7	28	± 3	489	623	1.27
OD3 5-1	0.0522	± 0.0040	0.00507	± 0.00027	0.0362	± 0.0075	0.0015	± 0.0001	33	± 2	36	± 8	30	± 3	504	601	1.19
OD3 6-1	0.0437	± 0.0024	0.00521	± 0.00028	0.0319	± 0.0069	0.0016	± 0.0001	34	± 2	32	± 7	32	± 3	548	676	1.23
OD3 7-1	0.0454	± 0.0034	0.00501	± 0.00029	0.0314	± 0.0072	0.0017	± 0.0002	32	± 2	31	± 7	34	± 3	489	589	1.20
OD3 8-1	0.0484	± 0.0040	0.00522	± 0.00029	0.0340	± 0.0073	0.0016	± 0.0001	34	± 2	34	± 7	32	± 3	523	656	1.26
OD3 10-1	0.0535	± 0.0026	0.00544	± 0.00035	0.0390	± 0.0075	0.0017	± 0.0002	35	± 2	39	± 8	34	± 4	522	644	1.23
OD3 10-2	0.0358	± 0.0018	0.00520	± 0.00033	0.0249	± 0.0056	0.0016	± 0.0002	33	± 2	25	± 6	33	± 3	577	609	1.06
OD3 11-1	0.0481	± 0.0023	0.00517	± 0.00034	0.0332	± 0.0068	0.0017	± 0.0002	33	± 2	33	± 7	34	± 3	557	564	1.01
OD3 12-1	0.0521	± 0.0035	0.00519	± 0.00027	0.0363	± 0.0072	0.0015	± 0.0002	33	± 2	36	± 7	31	± 3	545	551	1.01
OD3 13-1	0.0463	± 0.0026	0.00525	± 0.00031	0.0326	± 0.0071	0.0015	± 0.0001	34	± 2	33	± 7	31	± 3	540	552	1.02
OD3 14-1	0.0423	± 0.0024	0.00524	± 0.00030	0.0298	± 0.0063	0.0014	± 0.0001	34	± 2	30	± 6	28	± 2	640	683	1.07

付表2　四重極型LA-ICP-MSで測定した2次標準試料（OD-3及びPlešovice）のU-Pb同位体データ.

Table A2　U–Pb isotopic data for secondary zircon standards determined by LA-ICP-MS using a quadrupole mass spectrometer.

Sample name	Isotopic ratios								Age (Ma)						U (ppm)	Th (ppm)	Th/U
	^{207}Pb/^{206}Pb	Error 2σ	^{206}Pb/^{238}U	Error 2σ	^{207}Pb/^{235}U	Error 2σ	^{208}Pb/^{232}Th	Error 2σ	^{206}Pb/^{238}U	Error 2σ	^{207}Pb/^{235}U	Error 2σ	^{208}Pb/^{232}Th	Error 2σ			
Plešovice (337 Ma): Sláma *et al*. (2008)																	
PSV 1-1	0.0549	± 0.0030	0.05322	± 0.00179	0.4032	± 0.0313	0.0174	± 0.0008	334	± 12	344	± 31	349	± 16	1549	177	0.11
PSV 1-2	0.0527	± 0.0029	0.05356	± 0.00180	0.3893	± 0.0302	0.0179	± 0.0008	336	± 12	334	± 30	359	± 17	1577	180	0.11
PSV 2-1	0.0536	± 0.0028	0.05383	± 0.00102	0.3979	± 0.0228	0.0164	± 0.0018	338	± 7	340	± 23	329	± 36	1057	150	0.14
PSV 2-2	0.0514	± 0.0027	0.05417	± 0.00102	0.3837	± 0.0220	0.0167	± 0.0018	340	± 7	330	± 22	334	± 37	1072	146	0.14
PSV 3-1	0.0521	± 0.0025	0.05397	± 0.00184	0.3879	± 0.0233	0.0155	± 0.0014	339	± 12	333	± 23	311	± 28	1557	231	0.15
PSV 3-2	0.0543	± 0.0027	0.05374	± 0.00183	0.4023	± 0.0245	0.0157	± 0.0014	337	± 12	343	± 25	314	± 28	1421	175	0.12
PSV 4-1	0.0543	± 0.0023	0.05396	± 0.00282	0.4041	± 0.0303	0.0159	± 0.0016	339	± 18	345	± 30	319	± 33	1050	166	0.16
PSV 4-2	0.0541	± 0.0023	0.05417	± 0.00283	0.4044	± 0.0303	0.0155	± 0.0016	340	± 18	345	± 30	310	± 32	1057	170	0.16
PSV 5-1	0.0535	± 0.0023	0.05397	± 0.00282	0.3983	± 0.0299	0.0161	± 0.0017	339	± 18	340	± 30	323	± 34	1033	155	0.15
PSV 5-2	0.0548	± 0.0023	0.05462	± 0.00286	0.4125	± 0.0310	0.0158	± 0.0016	343	± 18	351	± 31	318	± 33	1001	148	0.15
OD-3 (33 Ma): Iwano *et al*.(2012), Iwano *et al*.(2013), Lukács *et al*. (2015)																	
OD3 1-1	0.0468	± 0.0069	0.00509	± 0.00023	0.0329	± 0.0051	0.0014	± 0.0001	33	± 1	33	± 5	28	± 2	799	1149	1.44
OD3 2-1	0.0463	± 0.0086	0.00495	± 0.00021	0.0316	± 0.0059	0.0015	± 0.0002	32	± 1	32	± 6	30	± 4	317	309	0.98
OD3 3-1	0.0497	± 0.0054	0.00517	± 0.00021	0.0354	± 0.0040	0.0016	± 0.0001	33	± 1	35	± 4	32	± 3	1276	1745	1.37
OD3 4-1	0.0470	± 0.0051	0.00503	± 0.00028	0.0327	± 0.0040	0.0016	± 0.0002	32	± 2	33	± 4	33	± 3	898	1211	1.35
OD3 5-1	0.0428	± 0.0056	0.00509	± 0.00021	0.0300	± 0.0040	0.0016	± 0.0001	33	± 1	30	± 4	32	± 3	675	785	1.16

Bulletin of the Geological Survey of Japan, vol. 68 (2), p. 57–86, 2017

Report

Preliminary report on the radiolarian age of the Upper Cretaceous Matoya Group (Shimanto belt) in the Toba District, Mie Prefecture, Southwest Japan

Satoshi Nakae[1,*] and Toshiyuki Kurihara[2]

Satoshi Nakae and Toshiyuki Kurihara (2017) Preliminary report on the radiolarian age of the Upper Cretaceous Matoya Group (Shimanto belt) in the Toba District, Mie Prefecture, Southwest Japan. *Bull. Geol. Surv. Japan*, vol. 68 (2), p. 57–86, 3 figs, 2 tables, 3 plates.

Abstract: A detailed field mapping and radiolarian dating in the Toba District, the Shima Peninsula (eastern tip of the Kii Peninsula) have revealed Coniacian–Campanian mudstones of the Upper Cretaceous Matoya Group. This group belongs to the Shimanto belt (northern subbelt) that formed along the plate boundary where the Kula plate has been subducting beneath the paleo-Asian continent. Seven out of 51 radiolarian-bearing samples from different outcrops of mudstone yield relatively well-preserved radiolarian assemblages, which are concentrated in three age-groups: (i) Early Coniacian, (ii) Early Campanian or Middle Santonian–Middle Campanian, and (iii) Middle–Late Campanian. This evidence has a potential to chronologically and stratigraphically divide the Matoya Group into several units.

Keywords: radiolaria, Upper Cretaceous, Matoya Group, Shimanto belt, Toba, Shima, Mie Prefecture, Kii Peninsula, Southwest Japan

1. Introduction

The Matoya Group distributed in the eastern Kii Peninsula is an Upper Cretaceous accretionary complex in the Shimanto belt. Several previous studies on Albian to Campanian radiolarians, which mentioned to constrain the age of terrigenous clastic rocks of this group, have been published (Nakaseko *et al*., 1979; Nakaseko and Nishimura, 1981; Mizutani *et al*., 1982; Mizugaki, 1987; Obase, 1988; Tanabe and Kano, 1994; Yamanashi and Kashiwagi, 2010; Ohta *et al*., 2013). Nevertheless, in the Shima Peninsula (eastern tip of the Kii Peninsula) where the Toba District is located, the Matoya Group has been poorly dated because Yamagiwa (1957) and Obase (1988) did not list nor illustrate any radiolarians in their reports.

In this paper, the results of a biostratigraphical study on Early Coniacian to Late Campanian radiolarian-bearing mudstones in the Toba District is documented to provide age data, and will be used for the next issue of the regional stratigraphic investigation of the Matoya Group with more precise age determination. During the field survey, more than one hundred of rock sample for radiolarian dating in the Toba District were collected, and seven out of 51 radiolarian-bearing samples are treated for this preliminary report.

2. Geological setting

The Toba District is located in the Shima Peninsula (eastern tip of the Kii Peninsula), and occupies the area including a southern part of Toba City and a northern part of Shima City, Mie Prefecture (Fig. 1). In the Shima Peninsula, a thick sedimentary sequence called the Matoya Group (Yamagiwa, 1957) is dominated by terrigenous clastic rocks such as mudstone and sandstone associated with minor pelagic chert. This group formed as an accretionary complex in the Shimanto belt: Late Cretaceous subduction zone where the Kula plate has been subducting beneath the paleo-Asian continent. This group contacts with the Tsuiji Complex (Jurassic accretionary complex in the Chichibu belt) by the Butsuzo Tectonic Line to the northwest, and faces Ise Bay (Enshunada Sea) to the southeast. The structure of this group is relatively simple: NE–SW strike with moderate dip to NW.

3. Materials and method

The radiolarians examined in this study occur in mudstones. The rock samples were crushed, individually soaked in 5% HF solution for 10 to 15 hours, and washed through a 62 μm mesh sieve (235#). The resulting residue was boiled with 30% HCl and HNO_3 admixture for more

[1] AIST, Geological Survey of Japan, Research Institute of Geology and Geoinformation

[2] Graduate School of Science and Technology, Niigata University, Ikarashi 2, Nishi-ku, Niigata 950-2181, Japan

*Corresponding author: S.Nakae,Central 7,1-1-1 Higashi, Tsukuba, Ibaraki 305-8567, Japan. Email: nakae-satoshi@aist.go.jp

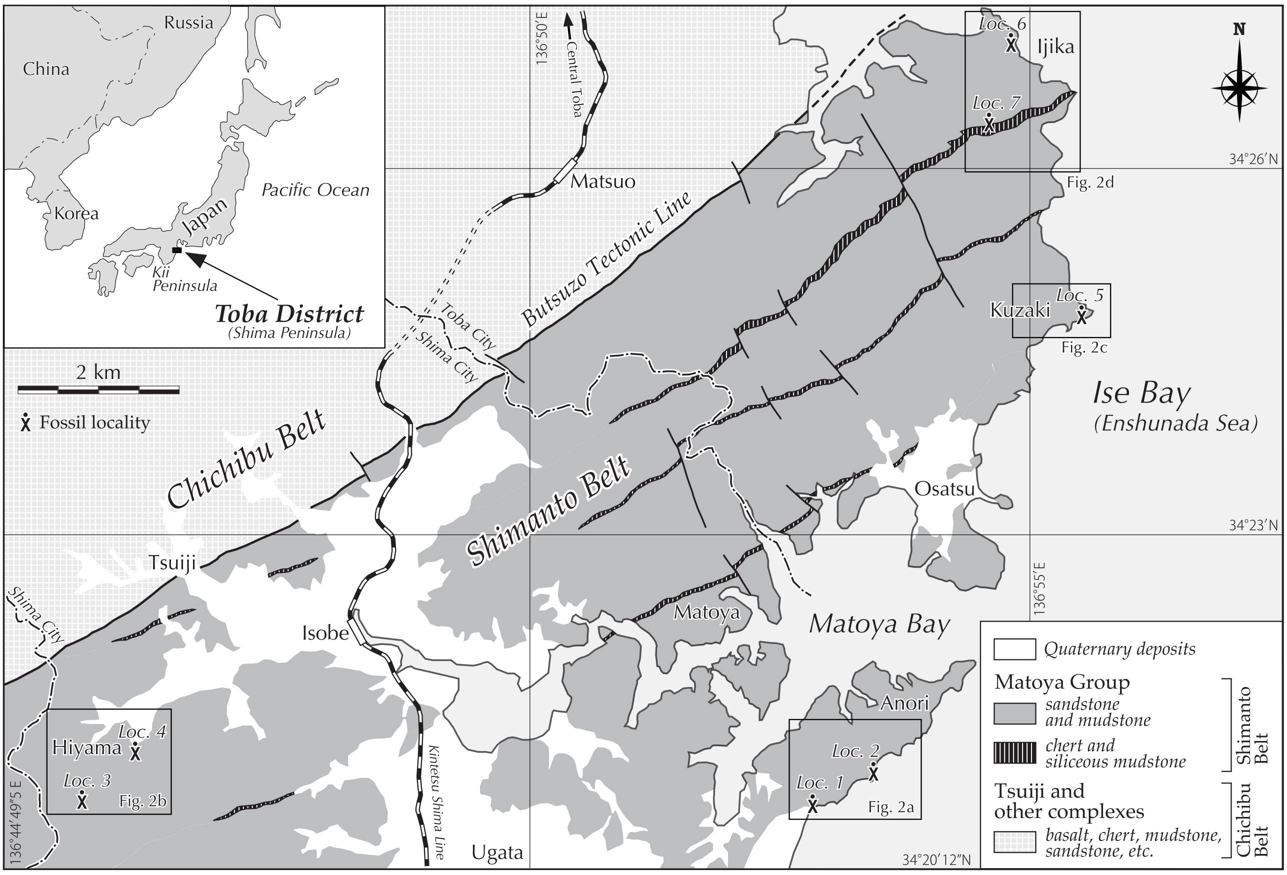

Fig. 1 Location map and geological sketch map of the Matoya Group in the Toba District.
The Toba District is located at the Shima Peninsula (eastern tip of the Kii Peninsula). The Matoya Group belonging to the Shimanto belt, is distributed along the coastline of Enshunada Sea, and contacts with Jurassic complexes in the Chichibu belt through the Butsuzo Tectonic Line. Detailed radiolarian localities with symbols are given in Fig. 2. Loc.: Locality.

than 20 minutes, sieved again and left to dry. The residue of each processed sample was then examined under a stereomicroscope and radiolarian remains were picked by hand with an ink brush for examination by scanning electronic microscope (SEM).

4. Localities and radiolarian assemblages

The sample localities (Locs. 1–7) are plotted on topographic maps published on the website of the Geospatial Information Authority of Japan (Fig. 2), and their outcrops are shown in Fig. 3. Identified radiolarian species are listed in Table 1 and given on Plates 1, 2 and 3. The outcrops are mostly composed of silty mudstones; they are not only laminated but also locally intercalated with sandstone beds. Well-preserved radiolarians are rarely included in all examined samples (Fig. 3h). Below is a description of the radiolarian assemblage of each locality.

4. 1. Locality 1 (Figs. 2a and 3a)
Location: 1.8 km southwest of Anori, Shima City. (34°20′43.8″ N/136°52′54.4″ E)
Sample number: TB 31-06.
Lithology: Black, slaty foliated mudstone.
Assemblage: *Dactyliosphaera* sp. aff. *D. silviae* Squinabol, *Orbiculiforma sacramentoensis* Pessagno, *Pseudoaulophacus praefloresensis* Pessagno, *Archaeospongoprunum hueyi* Pessagno, *Patellula planoconvexa* (Pessagno), *Rhopalosyringium magnificum* Campbell and Clark, *Cryptamphorella macropora* Dumitrică, *Diacanthocapsa* sp. cf. *D. ovoidea* Dumitrică, *Dictyomitra densicostata* Pessagno, *Amphipternis stocki* (Campbell and Clark), *Stichomitra manifesta* Foreman (Plate 1).

4. 2. Locality 2 (Figs. 2a and 3b)
Location: 900 m southwest of Anori, Shima City. (34°20′59.0″ N/136°53′31.2″ E)
Sample number: TB 31-03.
Lithology: Dark gray, weakly slaty foliated, silty mudstone, with fine-grained sandstone interbeds.
Assemblage: *Orbiculiforma* sp. cf. *O. railensis* Pessagno, *Alievium gallowayi* (White), *Pseudoaulophacus* sp. cf. *P. lenticulatus* (White), *Archaeospongoprunum hueyi* Pessagno,

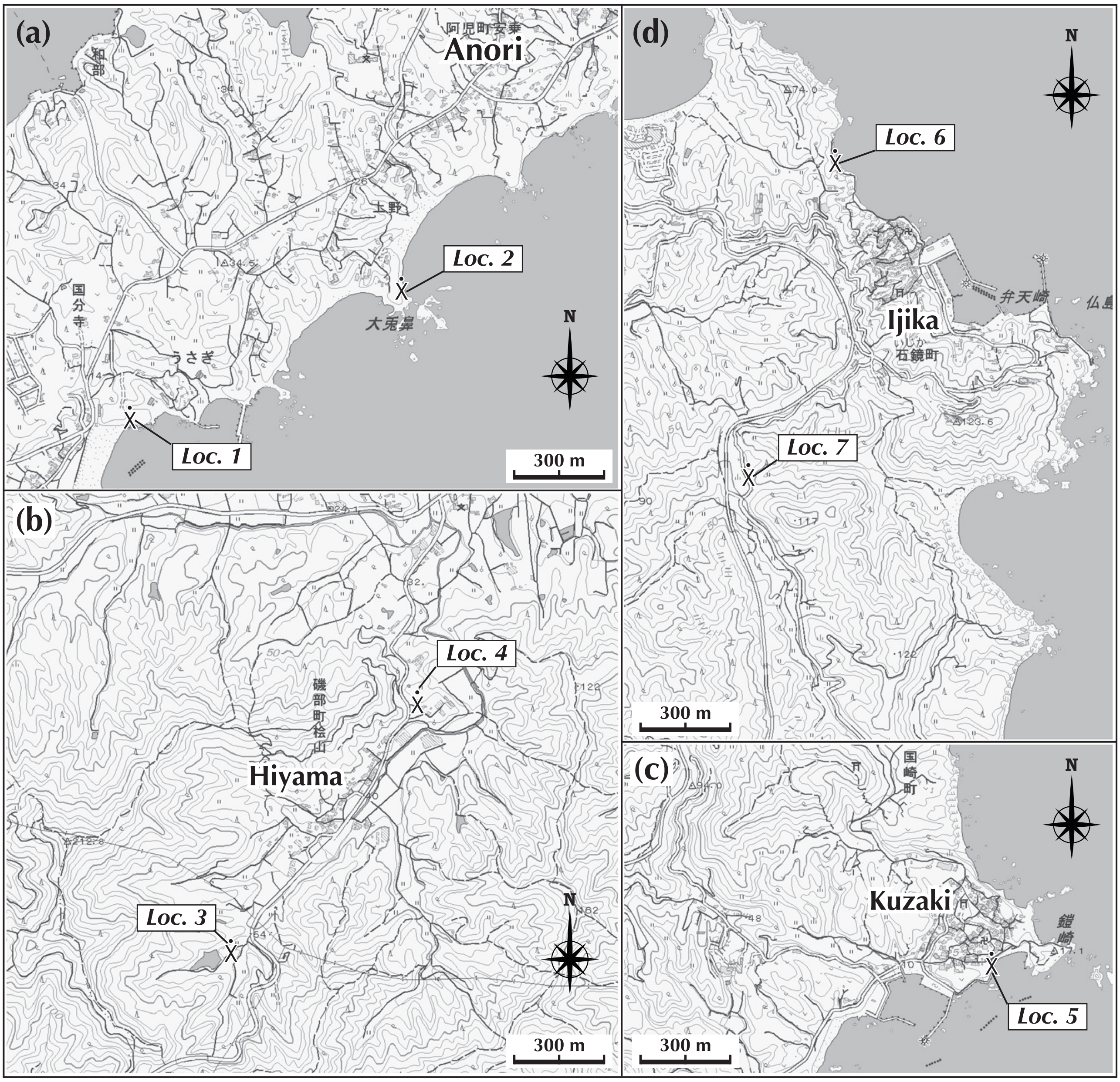

Fig. 2 Radiolarian localities.
Topographic maps are downloaded from the website of Geospatial Information Authority of Japan. URL of each map is as follows: (a) http://maps.gsi.go.jp/#16/34.351488/136.888393/ &base=std &ls=std&disp=1&vs=c1j0l0u0f1, (b) http://maps.gsi.go.jp/#16/34.348565/ 136.763424/&base= std&ls=std&disp=1&vs=c1j0l0u0f1, (c) http://maps.gsi.go.jp/#16/ 34.414690/136.922296/&bas e=std&ls=std&disp=1&vs=c1j0l0u0f1, (d) http://maps.gsi.go.jp/#17/34.444393/136.917077/&b ase=std&ls=std&disp=1&vs=c1j0l0u0f1. Loc.: Locality.

Rhopalosyringium magnificum Campbell and Clark, *Cryptamphorella sphaerica* (White), *Cryptamphorella* sp. B sensu Bąk (1996), *Eastonerius* sp. aff. *E. acuminatus* (Dumitrică), *Dictyomitra multicostata* Zittel, *Dictyomitra densicostata* Pessagno, *Thanarla* sp. aff. *T. veneta* (Squinabol), *Amphipternis stocki* (Campbell and Clark), *Amphipyndax tylotus* Foreman, *Amphipyndax* sp. cf. *A. tylotus* Foreman, *Xitus spicularius* (Aliev), (Plate 1).

4. 3. Locality 3 (Figs. 2b and 3c)
Location: 780 m southwest of Hiyama, Shima City. (34°20′37.9″ N/136°45′34.6″ E)
Sample number: TB 20-03.
Lithology: Dark to light gray, slaty foliated mudstone,

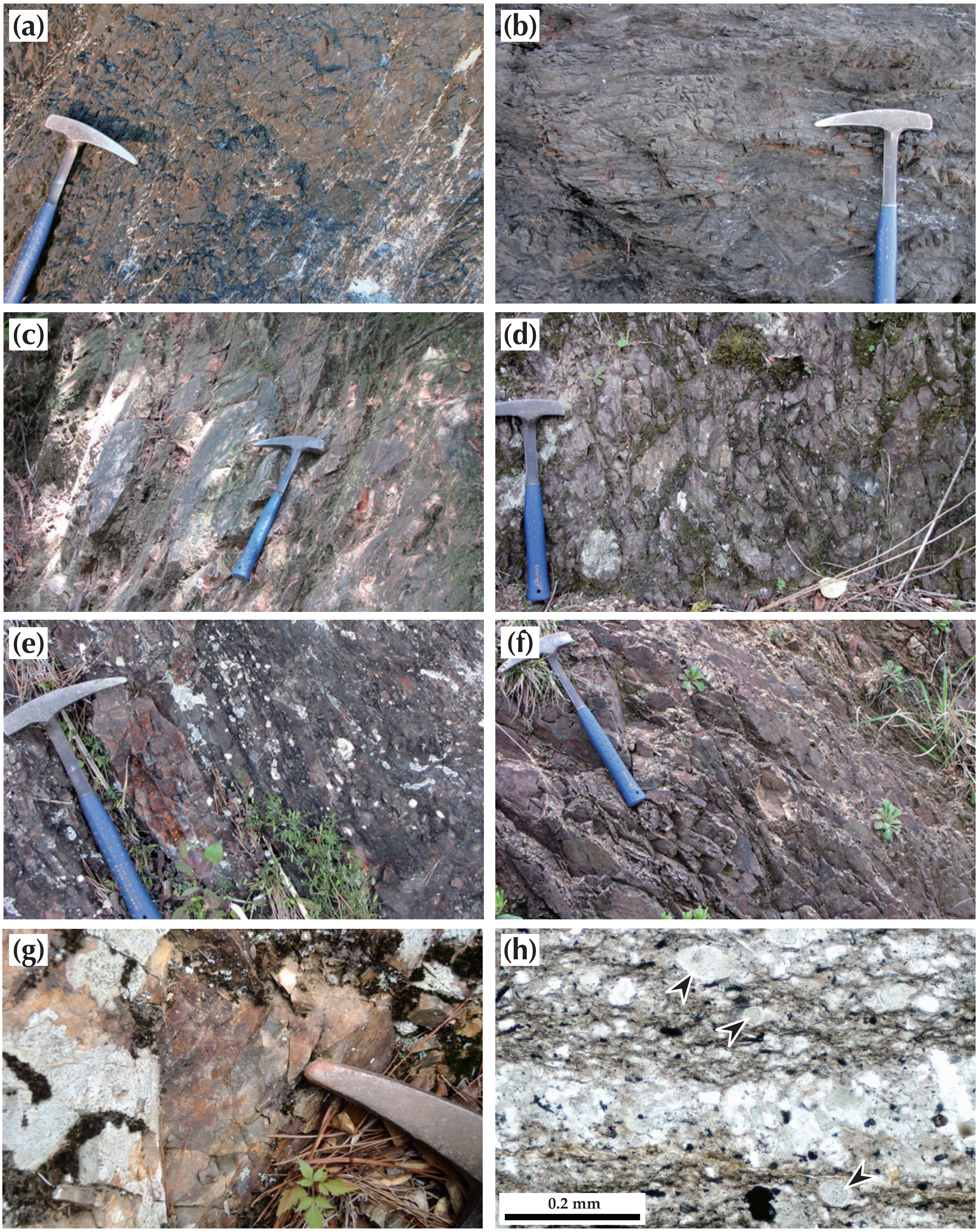

Fig. 3 Outcrop of radiolarian localities and a thin section of the mudstone.
(a) Locality 1 (TB31-06): Black slaty mudstone, southwest of Anori, (b) Locality 2 (TB31-03): Dark gray silty mudstone with fine-grained sandstone interbeds, southwest of Anori, (c) Locality 3 (TB20-03): Dark to light gray slaty mudstone, with planar lamination, southwest of Hiyama. (d) Locality 4 (TB20-02): Pale to dark gray silty mudstone, northeast of Hiyama, (e) Locality 5 (TB05-12): Dark gray silty mudstone with fine-grained sandstone interbeds at Kuzaki, (f) Locality 6 (TB01-04): Black silty mudstone with sandstone interbeds, northwest of Ijika, (g) Locality 7 (TB01-02a): Dark gray massive mudstone, southwest of Ijika, (h): Thin section of a representative silty mudstone, with radiolarian remains (arrows).

Table 1 List of radiolarian species detected from the Matoya Group in the Toba District.

	Radiolarian Species	7	6	5	4	3	2	1
	Locality Number (Loc.) / Sample Number	TB01-02a	TB01-04	TB05-12	TB20-02	TB20-03	TB31-03	TB31-06
Spumellaria	*Archaeocenosphaera*? *mellifera* O'Dogherty 1994		+					
	Conocaryomma universa (Pessagno 1976)	+						
	Conocaryomma californiaensis (Pessagno 1976)		+					
	Dactyliosphaera sp. aff. *D. silviae* Squinabol 1904							+
	Orbiculiforma sacramentoensis Pessagno 1973							+
	Orbiculiforma sp. cf. *O. railensis* Pessagno 1977						+	
	Alievium gallowayi (White 1928)						+	
	Alievium sp. cf. *A. gallowayi* (White 1928)			+	+			
	Alievium sp. cf. *A. praegallowayi* Pessagno 1972	+	+					
	Pseudoaulophacus lenticulatus (White 1928)			+	+			
	Pseudoaulophacus sp. cf. *P. lenticulatus* (White 1928)						+	
	Pseudoaulophacus praefloresensis Pessagno 1972							+
	Pseudoaulophacus sp. cf. *P. praefloresensis* Pessagno 1972	+						
	Pseudoaulophacus floresensis Pessagno 1963			+	+	+		
	Pseudoaulophacus pargueraensis Pessagno 1963	+						
	Pseudoaulophacus sp. cf. *P. pargueraensis* Pessagno 1963					+		
	Archaeospongoprunum sp. cf. *A. stocktonensis* Pessagno 1973					+		
	Archaeospongoprunum sp. aff. *A. andersoni* Pessagno 1973		+					
	Archaeospongoprunum hueyi Pessagno 1973						+	+
	Pyramispongia glascockensis Pessagno 1973	+						
	Patellula planoconvexa (Pessagno 1963)							+
	Patellula verteroensis (Pessagno 1963)	+	+		+	+		
Nassellaria	*Rhopalosyringium magnificum* Campbell and Clark 1944				+		+	+
	Rhopalosyringium sp. A sensu Bandini *et al*. 2008	+						
	Cryptamphorella sphaerica (White 1928)				+		+	
	Cryptamphorella macropora Dumitrică 1970					+		+
	Cryptamphorella sp. aff. *C. gilkeyi* (Dumitrica 1973)		+					
	Cryptamphorella wogiga Empson-Morin 1981			+				
	Cryptamphorella sp. B sensu Bąk 1996						+	
	Hemicryptocapsa polyhedra Dumitrică 1970		+					
	Theocampe urna (Foreman 1971)			+				
	Theocampe salillum Foreman 1971	+			+	+		
	Diacanthocapsa ovoidea Dumitrică 1970					+		
	Diacanthocapsa sp. cf. *D. ovoidea* Dumitrică 1970							+
	Diacanthocapsa sp. cf. *D. ancus* (Foreman 1968) sensu Dumitrică 1970					+		
	Eastonerius sp. aff. *E. acuminatus* (Dumitrică 1970)						+	
	Archaeodictyomitra squinaboli Pessagno 1976	+						
	Dictyomitra undata Squinabol 1904			+				
	Dictyomitra sp. cf. *D. gracilis* (Squinabol 1903)	+						
	Dictyomitra formosa Squinabol 1904	+	+					
	Dictyomitra duodecimcostata (Squinabol 1903) sensu Foreman (1975)			+				
	Dictyomitra multicostata Zittel 1876	+	+			+	+	
	Dictyomitra densicostata Pessagno 1976				+		+	+
	Dictyomitra sp. aff. *D. densicostata* Pessagno 1976	+						
	Dictyomitra koslovae Foreman 1975			+	+	+		
	Dictyomitra andersoni (Campbell and Clark 1944)	+						
	Thanarla sp. aff. *T. veneta* (Squinabol 1903)						+	
	Amphipternis stocki (Campbell and Clark 1944)	+	+		+	+	+	+
	Amphipyndax tylotus Foreman 1978						+	
	Amphipyndax sp. aff. *A tylotus* Foreman 1978						+	
	Xitus spicularius (Aliev 1965)						+	
	Torculum sp. aff. *T. bastetani* O'Dogherty 1994		+					
	Pseudodictyomitra tiara (Holmes 1900)	+	+					
	Pseudoeucyrtis sp. cf. *P. spinosa* (Squinabol 1903)	+						
	Stichomitra communis Squinabol 1903	+						
	Stichomitra manifesta Foreman 1978	+			+			+
	Stichomitra asymbatos Foreman 1968	+			+			
	Stichomitra sp. aff. *S. asymbatos* Foreman 1968					+		
	Stichomitra sp. cf. *S. conicus* (Nakaseko and Nishimura 1981)				+			

with planar lamination.
Assemblage: *Pseudoaulophacus floresensis* Pessagno, *Pseudoaulophacus* sp. cf. *P. pargueraensis* Pessagno, *Archaeospongoprunum* sp. cf. *A. stocktonensis* Pessagno, *Patellula verteroensis* (Pessagno), *Cryptamphorella macropora* Dumitrică, *Theocampe salillum* Foreman, *Diacanthocapsa ovoidea* Dumitrică, *Diacanthocapsa* sp. cf. *D. ancus* (Foreman) sensu Dumitrică (1970), *Dictyomitra multicostata* Zittel, *Dictyomitra koslovae* Foreman, *Amphipternis stocki* (Campbell and Clark), *Stichomitra* sp. cf. *S. asymbatos* Foreman (Plate 2).

4. 4. Locality 4 (Figs. 2b and 3d)
Location: 280 m northeast of Hiyama, Shima City. (34°21′5.3″ N/136°45′59.2″ E)
Sample number: TB 20-02.
Lithology: Pale to dark gray, weakly slaty foliated, silty mudstone.
Assemblage: *Alievium* sp. cf. *A. gallowayi* (White), *Pseudoaulophacus lenticulatus* (White), *Pseudoaulophacus floresensis* Pessagno, *Patellula verteroensis* (Pessagno), *Rhopalosyringium magnificum* Campbell and Clark, *Cryptamphorella sphaerica* (White), *Theocampe salillum* Foreman, *Dictyomitra densicostata* Pessagno, *Dictyomitra koslovae* Foreman, *Amphipternis stocki* (Campbell and Clark), *Stichomitra manifesta* Foreman, *Stichomitra asymbatos* Foreman, *Stichomitra* sp. cf. *S. conicus* (Nakaseko and Nishimura) (Plate 2).

4. 5. Locality 5 (Figs. 2c and 3e)
Location: Kuzaki, Toba City. (34°24′46.3″ N/136°55′31.9″ E)
Sample number: TB 05-12.
Lithology: Dark gray, silty mudstone, with fine-grained sandstone interbeds.
Assemblage: *Alievium* sp. cf. *A. gallowayi* (White), *Pseudoaulophacus lenticulatus* (White), *Pseudoaulophacus floresensis* Pessagno, *Cryptamphorella wogiga* Empson-Morin, *Theocampe urna* (Foreman), *Dictyomitra undata* Squinabol, *Dictyomitra duodecimcostata* (Squinabol), *Dictyomitra koslovae* Foreman (Plate 2).

4. 6. Locality 6 (Figs. 2d and 3f)
Location: 520 m northwest of Ijika, Toba City. (34°27′2.1″ N/136°54′53.5″ E)
Sample number: TB 01-04.
Lithology: Black, silty mudstone, with sandstone interbeds.
Assemblage: *Archaeocenosphaera*? *mellifera* O'Dogherty, *Conocaryomma californiaensis* (Pessagno), *Alievium* sp. cf. *A. praegallowayi* Pessagno, *Archaeospongoprunum* sp. aff. *A. andersoni* Pessagno, *Patellula verteroensis* (Pessagno), *Cryptamphorella* sp. aff. *C. gilkeyi* (Dumitrica), *Hemicryptocapsa polyhedra* Dumitrică, *Dictyomitra formosa* Squinabol, *Dictyomitra multicostata* Zittel, *Amphipternis stocki* (Campbell and Clark), *Torculum* sp. aff. *T. bastetani* O'Dogherty, *Pseudodictyomitra tiara* (Holmes), (Plate 3).

4. 7. Locality 7 (Figs. 2d and 3g)
Location: 910 m southwest of Ijika, Toba City. (34°26′25.4″ N/136°54′42.3″ E)
Sample number: TB 01-02a.
Lithology: Dark gray, massive mudstone.
Assemblage: *Conocaryomma universa* (Pessagno), *Alievium* sp. cf. *A. praegallowayi* Pessagno, *Pseudoaulophacus* sp. cf. *P. praefloresensis* Pessagno, *Pseudoaulophacus pargueraensis* Pessagno, *Pyramispongia glascockensis* Pessagno, *Patellula verteroensis* (Pessagno), *Rhopalosyringium* sp. A sensu Bandini *et al*. (2008), *Theocampe salillum* Foreman, *Archaeodictyomitra squinaboli* Pessagno, *Dictyomitra* sp. cf. *D. gracilis* (Squinabol), *Dictyomitra formosa* Squinabol, *Dictyomitra multicostata* Zittel, *Dictyomitra* sp. aff. *D. densicostata* Pessagno, *Dictyomitra andersoni* (Campbell and Clark), *Amphipternis stocki* (Campbell and Clark), *Pseudodictyomitra tiara* (Holmes), *Pseudoeucyrtis* sp. cf. *P. spinosa* (Squinabol), *Stichomitra communis* Squinabol, *Stichomitra manifesta* Foreman, *Stichomitra asymbatos* Foreman (Plate 3).

5. Age determination

In order to determine the age of radiolarian assemblages extracted from the mudstone samples in the Toba District, the biostratigraphic ranges of each species and the existing Upper Cretaceous zonations (e.g., Dumitrică, 1970; Foreman, 1975; Pessagno, 1976, 1977; Taketani, 1982; Sanfilippo and Riedel, 1985; Thurow, 1988; Hollis and Kimura, 2001; Hashimoto *et al*., 2015) are primarily used. Nevertheless, there are considerable problem that the ranges of some species are not compatible among the above authors, as pointed out by Bandini *et al*. (2008). For dating the radiolarian assemblages, this paper follows essentially the same approach as Bandini *et al*. (2008); a maximum range of each species, which is obtained by combining the ranges of each species from the above authors, is established.

Consequently, an age of the radiolarian assemblage from each sample can be determined based on the co-occurrence of included species, which range from the Coniacian to Campanian.

TB 31-06 (Locality 1)

Although several species having a wide range in age from Cenomanian to Early Maastrichtian, the occurrence of *Orbiculiforma sacramentoensis* gives a late Middle–early Late Campanian age.

TB 31-03 (Locality 2)

The co-occurrence of *Amphipyndax tylotus* and *Xitus spicularius* suggests a late Middle Campanian age.

TB 20-03 (Locality 3)

The co-occurrence of *Pseudoaulophacus floresensis*, *Patellula verteroensis* and *Diacanthocapsa ovoidea* gives a Middle Santonian–Early Campanian age.

Table 2 Biostratigraphic ranges of radiolarian species from the Matoya Group in the Toba District.

Lower Creta.	Upper Cretaceous																		Paleogene
	Cenomanian			Turonian			Coniacian			Santonian			Campanian			Maastrichtian			
	Lower	Mid	Upper	Lower	Middle	Upper	Lower	Mid	Upper	L	M	Upper	Lower	Middle	Uppr	Lower	Upper		

Sample	Locality	Species
TB 01-02a	(Loc. 7)	*Conocaryomma universa*
		Alievium sp. cf. *A. praegallowayi*
		Pseudoaulophacus sp. cf. *P. praefloresensis*
		Pseudoaulophacus pargueraensis
		Pyramispongia glascockensis
		Patellula verteroensis
		Rhopalosyringium sp. A sensu Bandini *et al*. 2008
		Theocampe salillum Foreman
		Archaeodictyomitra squinaboli
		Dictyomitra sp. cf. *D. gracilis*
		Dictyomitra formosa
		Dictyomitra multicostata
		Dictyomitra sp. aff. *D. densicostata*
		Dictyomitra andersoni
		Amphipternis stocki
		Pseudodictyomitra tiara
		Pseudoeucyrtis sp. cf. *P. spinosa*
		Stichomitra communis
		Stichomitra manifesta
		Stichomitra asymbatos
TB 01-04	(Loc. 6)	*Archaeocenosphaera? mellifera*
		Conocaryomma californiaensis
		Alievium sp. cf. *A. praegallowayi*
		Archaeospongoprunum sp. aff. *A. andersoni*
		Patellula verteroensis
		Cryptamphorella sp. aff. *C. gilkeyi*
		Hemicryptocapsa polyhedra
		Dictyomitra formosa
		Dictyomitra multicostata
		Amphipternis stocki
		Torculum sp. aff. *T. bastetani*
		Pseudodictyomitra tiara
TB 05-12	(Loc. 5)	*Alievium* sp. cf. *A. gallowayi*
		Pseudoaulophacus lenticulatus
		Pseudoaulophacus floresensis
		Cryptamphorella wogiga
		Theocampe urna
		Dictyomitra undata
		Dictyomitra duodecimcostata sensu Foreman (1975)
		Dictyomitra koslovae
TB 20-02	(Loc. 4)	*Alievium* sp. cf. *A. gallowayi*
		Pseudoaulophacus lenticulatus
		Pseudoaulophacus floresensis
		Patellula verteroensis
		Rhopalosyringium magnificum
		Cryptamphorella sphaerica
		Theocampe salillum
		Dictyomitra densicostata
		Dictyomitra koslovae
		Amphipternis stocki
		Stichomitra manifesta
		Stichomitra asymbatos
		Stichomitra sp. cf. *S. conicus*
TB 20-03	(Loc. 3)	*Pseudoaulophacus floresensis*
		Pseudoaulophacus sp. cf. *P. pargueraensis*
		Archaeospongoprunum sp. cf. *A. stocktonensis*
		Patellula verteroensis
		Cryptamphorella macropora
		Theocampe salillum
		Diacanthocapsa ovoidea
		Diacanthocapsa sp. cf. *D. ancus* sensu Dumitrică 1970
		Dictyomitra multicostata
		Dictyomitra koslovae
		Amphipternis stocki
		Stichomitra sp. aff. *S. asymbatos*
TB 31-03	(Loc. 2)	*Orbiculiforma* sp. cf. *O. railensis*
		Alievium gallowayi
		Pseudoaulophacus sp. cf. *P. lenticulatus*
		Archaeospongoprunum hueyi
		Rhopalosyringium magnificum
		Cryptamphorella sphaerica
		Cryptamphorella sp. B sensu Bąk 1996
		Eastonerius sp. aff. *E. acuminatus*
		Dictyomitra multicostata
		Dictyomitra densicostata
		Thanarla sp. aff. *T. veneta*
		Amphipternis stocki
		Amphipyndax tylotus
		Amphipyndax sp. aff. *A. tylotus*
		Xitus spicularius
TB 31-06	(Loc. 1)	*Dactyliosphaera* sp. aff. *D. silviae*
		Orbiculiforma sacramentoensis
		Pseudoaulophacus praefloresensis
		Archaeospongoprunum hueyi
		Patellula planoconvexa
		Rhopalosyringium magnificum
		Cryptamphorella macropora
		Diacanthocapsa sp. cf. *D. ovoidea*
		Dictyomitra densicostata
		Amphipternis stocki
		Stichomitra manifesta

TB 20-02 (Locality 4)

The co-occurrence of *Patellula verteroensis* and *Rhopalosyringium magnificum* suggests an Early Campanian age.

TB 05-12 (Locality 5)

The co-occurrence of *Pseudoaulophacus floresensis* and *Theocampe urna* suggests a Middle Santonian–middle Middle Campanian age.

TB 01-04 (Locality 6)

The co-occurrence of *Conocaryomma californiaensis* and *Pseudodictyomitra tiara* gives in an Early Coniacian age.

TB 01-02a (Locality 7)

The co-occurrence of *Pseudoaulophacus pargueraensis*, *Theocampe salillum*, *Pseudodictyomitra tiara*, *Stichomitra communis* and *Stichomitra manifesta* gives an Early Coniacian age.

The Matoya Group in the Toba District is currently assumed to be Early Coniacian to Late Campanian in age, and is probably divided into three age-groups: (i) Early Coniacian, (ii) Early Campanian (or Middle Santonian–middle Middle Campanian), and (iii) late Middle–early Late Campanian (Table 2). On the basis of the comparison between the sample localities and their age, it is revealed that localities 6 (TB01-04) and 7 (TB01-02a) of the oldest age-group (i) are situated at an upper horizon of the Matoya Group, whereas localities 1 (TB 31-06) and 2 (TB 31-03) of the youngest age-group (iii) at a lower horizon (See Fig. 1). This evidence has a potential to chronologically and stratigraphically divide the Matoya Group into several units.

6. Conclusion

This study preliminarily shows that the radiolarian assemblages from the Matoya Group in the Toba District are assigned in age to three age-groups: Early Coniacian, Early Campanian (or Middle Santonian–Middle Campanian) and Middle–Late Campanian. This result associated with the sample localities is possible to provide significant biostratigraphic and stratigraphic control in the Matoya Group; it will be divided into several units in a regional stratigraphic investigation in the near future.

7. Systematic Paleontology

Subclass **RADIOLARIA** Müller 1858
Order **SPUMELLARIA** Ehrenberg 1875

Family **XIPHOSTYLIDAE** Haeckel 1881,
emend. De Wever *et al*. 2001

Genus ***Archaeocenosphaera*** Pessagno and Yang in Pessagno *et al*. 1989

Archaeocenosphaera*? *mellifera O'Dogherty 1994
(Plate 3, fig. 1)

1984 *Cenosphaera*? sp. A – Empson-Morin, pl. 1, fig. 6.
1988 *Hemicryptocapsa polyhedra* Dumitrică – Thurow, p. 401, pl. 1, fig. 1.
1988 *Hemicryptocapsa* sp. cf. *H. polyhedra* Dumitrică – Thurow, p. 401, pl. 5, fig. 2.
1992 *Hemicryptocapsa* sp. A. – Marcucci Passerini and Gardin, fig. 3.l.
1994 *Archaeocenosphaera*? *mellifera* n. sp. – O'Dogherty, p. 375–376, pl. 67, figs. 1–5.
1997 *Archaeocenosphaera*? *mellifera* O'Dogherty – Sýkora *et al*., pl. III, fig. 5.
1998 *Archaeocenosphaera*? *mellifera* O'Dogherty – Salvini and Marcucci Passerini, fig. 7o.
2001 *Archaeocenosphaera*? *mellifera* O'Dogherty – Bragin *et al*., figs. 4.5–4.6.
2007 *Archaeocenosphaera*? *mellifera* O'Dogherty – Bragina *et al*., p. 318, pl. I, fig. 7.
2011 *Archaeocenosphaera mellifera* O'Dogherty – Smrečková, pl. I, fig. 4.
2012 *Archaeocenosphaera*? *mellifera* O'Dogherty – Moez *et al*., pl. 4, fig. 12.
2015 *Archaeocenosphaera*? *mellifera* O'Dogherty – Bragina and Bragin, pl. III, fig. 12.

Remarks: Archaeocenosphaera? *mellifera* first described by O'Dogherty (1994) consists of spherical cortical shell with symmetrical meshwork and a polygonal surface.

Family **CONOCARYOMMIDAE** Lipman 1969,
emend. De Wever *et al*. 2001

Genus ***Conocaryomma*** Lipman 1969

Conocaryomma universa (Pessagno 1976)
(Plate 3, fig. 13)

1976 *Praeconocaryomma universa* n. sp. – Pessagno, p. 42, pl. 6, figs. 14–16.
1981 *Conocaryomma universa* (Pessagno) – Empson-Morin, p. 260, pl. 3, fig. 5.
1982 *Praeconocaryomma universa* Pessagno – Taketani, p. 47, pl. 1, figs. 3a–3b, 4; pl. 9, fig. 4.
1982 *Praeconocaryomma universa* Pessagno – Mizutani *et al*., p. 63, pl. 5, fig. 11.
1988 *Conocaryomma universa* (Pessagno) – Thurow, p. 169, pl. 3, fig. 7.
1988 *Conocaryomma universum* (Pessagno) – De Wever *et al*., p. 398–399, pl. 2, fig. 18.
1992 *Praeconocaryomma californiaensis* Pessagno – Okamura, pl. 35, fig. 20; pl. 39, fig. 11.
1994 *Conocaryomma universa* (Pessagno) – Yamasaki and Tsujii, pl.II, fig. 7.
2005 *Praeconocaryomma universa* Pessagno – Popova-Goll *et al*., p. 20, pl. 1, figs. 19–20; pl. 6, fig. 14.
2008 *Praeconocaryomma universa* Pessagno – Bandini

et al., p. 17, pl. 1, figs. 8, 19; pl. 4, fig. 8.
2012 *Praeconocaryomma universa* Pessagno – Asis and Jasin, pl. 3, fig. 1.

Remarks: Cortical shell of the obtained specimen is composed of hemispherical nodes (mamma) and lattice of pore frames. Each mamma is surrounded by small circular pores.

Range: Coniacian to Middle Campanian (Pessagno, 1976), Coniacian to Middle Santonian (Taketani, 1982), Turonian to Upper Campanian (Thurow, 1988), and Coniacian? to lowermost Maastrichtian (Hollis and Kimura, 2001).

Conocaryomma californiaensis (Pessagno 1976)
(Plate 3, figs. 2)
1976 *Praeconocaryomma californiaensis* n. sp. – Pessagno, p. 41, pl. 7, figs. 1–8.
1982 *Praeconocaryomma californiaensis* Pessagno – Taketani, p. 47, pl. 9, figs. 1–2.
1992 *Praeconocaryomma californiaensis* Pessagno – Okamura, pl. 32, figs. 1–3.

Remarks: This specimen differs from *Conocaryomma universa* by having large ellipsoidal pores surrounding each mamma.

Range: Coniacian (Pessagno, 1976), Lower to Middle Coniacian or to Lower Campanian? (Taketani, 1982).

Family **DACTYLIOSPHAERIDAE** Squinabol 1904

Genus ***Dactyliosphaera*** Squinabol 1904

Dactyliosphaera* sp. aff. *D. silviae Squinabol 1904
(Plate 1, fig. 2)

Remarks: The examined specimen consists of a large circular disc-like test with pentagonal pore frames, and possesses probably twelve short spines that radiate from the periphery of the disc. But, it differs from *Dactyliosphaera silviae* in having smaller central convex area.

Family **HAGIASTRIDAE** Riedel 1971

Genus ***Orbiculiforma*** Pessagno 1973

Orbiculiforma sacramentoensis Pessagno 1976
(Plate 1, fig. 1)
1976 *Orbiculiforma sacramentoensis* n. sp. – Pessagno, p. 36–37, pl. 11, fig. 8.
1986 *Orbiculiforma sacramentoensis* Pessagno – Iwata and Tajika, pl. 5, figs. 6, 10.
1997 *Orbiculiforma* sp. – Yamasaki and Sakamoto, pl. III, fig. 12.

Remarks: This specimen consists of a disc-like test with meshwork of tetragonal to pentagonal pore frame, and possesses convex portion in the central area. It differs from other species of *Orbiculiforma* by having hexagonal outline.

Range: Upper Middle to lower Upper Campanian (Pessagno, 1976).

Orbiculiforma* sp. cf. *O. railensis Pessagno 1977
(Plate 1, fig. 14)

Remarks: The examined specimen is similar to *Orbiculiforma railensis* in having a circular disc-like test and central convex area surrounded by a narrow and deep groove, but slightly different by more than six short spines radiating from periphery of the test.

Family **PSEUDOAULOPHACIDAE** Riedel 1967, *emend*. Dumitrica 1997

Genus ***Alievium*** Pessagno 1972

Alievium gallowayi (White 1928)
(Plate 1, fig. 16)
1928 *Baculogypsina*? *gallowayi* n. sp. – White, p. 305, pl. 41, figs. 9–10.
1962 *Aulophacus gallowayi* (White). – Pessagno, p. 364, pl. 3, figs. 5–6.
1963 *Pseudoaulophacus gallowayi* (White) – Pessagno, p. 202, pl. 2, figs. 1, 3, 6; pl. 4, figs. 2, 5, 7; pl. 7, figs. 2, 4.
1972 *Alievium gallowayi* (White) – Pessagno, p. 299–300, pl. 25, figs. 4–6; pl. 26, fig. 5; pl. 31, figs. 2–3.
1976 *Alievium gallowayi* (White) – Pessagno, p. 27, pl. 8, figs. 13, 14; pl. 9, fig. 1.
1981 *Alievium gallowayi* (White) – Nakaseko and Nishimura, p. 142, pl. 2, fig. 3.
1982 *Alievium gallowayi* (White) – Taketani, p. 50–51, pl. 10, fig. 7.
1985 *Alievium gallowayi* (White) – Sanfilippo and Riedel, p. 594, fig. 6.1.
1988 *Alievium gallowayi* (White) – Thurow, p. 396–397, pl. 2, fig. 3.
1997 *Alievium gallowayi* (White) – Hashimoto and Ishida, pl. 3, fig. 21.
1998 *Alievium gallowayi* (White) – Ishida and Hashimoto, pl. 2, fig. 22.
2008 *Alievium gallowayi* (White) – Bandini *et al*., p. 16, pl. 1, fig.1; pl. 2, fig. 7; pl. 3, figs. 9, 25.
2015 *Alievium gallowayi* (White) – Hashimoto *et al*., p. 43, pl. 2, fig. 25.

Range: Santonian to Upper Campanian (Pessagno, 1976), Middle Campanian to lowermost Maastrichtian (Sanfilippo and Riedel, 1985), Campanian to Upper Maastrichtian (Thurow, 1988), uppermost Santonian to lowermost Maastrichtian (Hollis and Kimura, 2001), and Middle Campanian? to lowermost Maastrichtian (Hashimoto *et al*., 2015).

Alievium* sp. cf. *A. gallowayi (White 1928)
(Plate 2, figs. 15, 28)

Remarks: Although spines are lacked, the obtained specimens are similar to *Alievium gallowayi* in having subtriangular test with coarse meshwork.

Alievium* sp. cf. *A. preagallowayi Pessagno 1972
(Plate 3, figs. 3, 14)
Remarks: The obtained specimens are composed of more inflated subtriangular test than *Alievium gallowayi*, and similar to *Alievium praegallowayi* in having the nodes (situated at the vertices of triangular frames), which are aligned in curved row.

Genus ***Pseudoaulophacus*** Pessagno 1963

Pseudoaulophacus lenticulatus (White 1928)
(Plate 2, figs. 16, 29)
1928 *Baculogypsina*? *lenticulata* n. sp. – White, p. 306, pl. 41, figs. 9, 11.
1962 *Aulophacus lenticulatus* (White) – Pessagno, p. 364, pl. 6, figs. 1–2.
1963 *Pseudoaulophacus lenticulatus* (White) – Pessagno, p. 202, pl. 2, figs. 8–9.
1976 *Pseudoaulophacus lenticulatus* (White) – Pessagno, p. 28, pl. 9, figs. 11–12.
1981 *Pseudoaulophacus lenticulatus* (White) – Nakaseko and Nishimura, p. 158, pl. 2, figs. 7a–7b.
1982 *Pseudoaulophacus lenticulatus* (White) – Taketani, p. 51, pl. 10, fig. 11.
1982 *Pseudoaulophacus lenticulatus* (White) – Mizutani *et al*., p. 59, pl. 7, figs. 7a–7b; pl. 8, fig. 3.
1985 *Pseudoaulophacus lenticulatus* (White) – Sanfilippo and Riedel, p. 596, figs. 6.4a–6.4b.
1988 *Pseudoaulophacus lenticulatus* (White) – Thurow, p. 404, pl. 2, fig. 6.
1988 *Pseudoaulophacus lenticulatus* (White) – De Wever *et al*., p. 170, pl. 1, fig. 1.
1992 *Pseudoaulophacus lenticulatus* (White) – Iwata *et al*., pl. 1, fig. 12.
1992 *Pseudoaulophacus lenticulatus* (White) – Okamura, pl. 29, fig. 12.
1998 *Pseudoaulophacus lenticulatus* (White) – Salvini and Marcucci Passerini, fig. 8.d.
2008 *Pseudoaulophacus lenticulatus* (White) – Bandini *et al*., p. 18, pl. 1, figs. 22–23.
2015 *Pseudoaulophacus lenticulatus* (White) – Hashimoto *et al*., p. 46, pl. 1, fig. 23.
2015 *Pseudoaulophacus lenticulatus* (White) – Kopaevich *et al*., pl. VI, fig. 9.
Range: Coniacian to Upper Campanian (Pessagno, 1976), Coniacian to Lower Campanian? (Taketani, 1982), Lower to Middle Campanian (Sanfilippo and Riedel, 1985), Uppermost Coniacian to Upper Campanian (Thurow, 1988), Coniacian? to lowermost Maastrichtian (Hollis and Kimura, 2001), and Middle Campanian? to Lower Maastrichtian (Hashimoto *et al*., 2015).

Pseudoaulophacus* sp. cf. *P. lenticulatus (White 1928)
(Plate 1, fig. 15)
Remarks: This specimen is similar to *Pseudoaulophacus lenticulatus* in having a circular shell with central convex portion, short spines which occur from periphery of the shell.

Pseudoaulophacus preafloresensis Pessagno 1972
(Plate 1, fig. 3)
1972 *Pseudoaulophacus preafloresensis* n. sp. – Pessagno, p. 309–310, pl. 27, figs. 2–6.
1982 *Pseudoaulophacus preafloresensis* Pessagno – Yamauchi, pl. 3, fig. 5; pl. 4, fig. 17.
1994 *Pseudoaulophacus floresensis* Pessagno – Yamasaki and Tsujii, pl. II, fig. 9.
2007 *Pseudoaulophacus preafloresensis* Pessagno – Bragina *et al*., pl. II, fig. 1.
Remarks: This species is different from *Pseudoaulophacus lenticulatus* by its subangular shell and from *Pseudoaulophacus floresensis* by having a shell which is concave around its central convex portion.
Range: Coniacian to Upper Campanian (Pessagno, 1976) and Middle Santonian to lowermost Maastrichtian (Hollis and Kimura, 2001).

Pseudoaulophacus* sp. cf. *P. preafloresensis Pessagno 1972
(Plate 3, fig. 15)
Remarks: This specimen resembles *Pseudoaulophacus preafloresensis* in having a subtriangular shell and centreal convex area surrounded by slight concave.

Pseudoaulophacus floresensis Pessagno 1963
(Plate 2, figs. 1, 17, 30)
1963 *Pseudoaulophacus floresensis* n. sp. – Pessagno, p. 200, pl. 2, figs. 2, 5; pl. 4, fig. 6; pl. 7, figs. 1, 5.
1972 *Pseudoaulophacus floresensis* Pessagno – Pessagno, p. 304, pl. 26, fig. 6; pl. 28, figs. 4–6; pl. 29, figs. 1–2; pl. 31, fig. 1.
1976 *Pseudoaulophacus floresensis* Pessagno – Pessagno, p. 28, pl. 9, fig. 6.
1981 *Pseudoaulophacus floresensis* Pessagno – Nakaseko and Nishimura, p. 158, pl. 2, fig. 4.
1982 *Pseudoaulophacus* sp. cf. *P. floresensis* Pessagno – Taketani, p. 51, pl. 10, figs. 10–11.
1982 *Pseudoaulophacus floresensis* Pessagno – Mizutani *et al*., p. 60, pl. 8, fig. 2; pl. 8, fig. 3.
1985 *Pseudoaulophacus floresensis* Pessagno – Sanfilippo and Riedel, p. 595–596, figs. 6.3a–6.3b.
1988 *Pseudoaulophacus floresensis* Pessagno – Thurow, p. 404, pl. 2, fig. 5.
1992 *Pseudoaulophacus floresensis* Pessagno – Iwata *et al*., pl. 1, fig. 11.
1992 *Pseudoaulophacus floresensis* Pessagno – Okamura, pl. 33, figs. 8–10; pl. 36, figs. 3–5.
2005 *Pseudoaulophacus floresensis* Pessagno – Popova-Goll *et al*., p. 22, pl. 1, fig. 13; pl. 8, fig. 11.
2008 *Pseudoaulophacus floresensis* Pessagno – Bandini *et al*., p. 18, pl. 1, figs. 20–21.
Range: Middle Santonian to Upper Campanian (Pessagno, 1976), Lower Campanian to lowermost Maastrichtian (Sanfilippo and Riedel, 1985), Lower Campanian to Upper Maastrichtian (Thurow, 1988), Middle Santonian

to lowermost Maastrichtian (Hollis and Kimura, 2001), and Lower Campanian to Lower Maastrichtian (Hashimoto *et al*., 2015).

Pseudoaulophacus pargueraensis Pessagno 1963
(Plate 3, fig. 16)
- 1963 *Pseudoaulophacus pargueraensis* n. sp. – Pessagno, p. 204, pl. 2, figs. 4, 7; pl.6, figs. 4–5.
- 1972 *Pseudoaulophacus pargueraensis* Pessagno – Pessagno, p. 309, pl. 30, fig. 4.
- 1982 *Pseudoaulophacus pargueraensis* Pessagno – Taketani, p. 51, pl. 10, fig. 12.
- 1981 *Pseudoaulophacus pargueraensis* Pessagno – Nakaseko and Nishimura, p. 158 pl. 2, fig. 5.
- 1982 *Pseudoaulophacus pargueraensis* Pessagno – Mizutani *et al*., p. 59–60, pl. 7, fig. 8.
- 1982 *Pseudoaulophacus pargueraensis* Pessagno – Yamauchi, pl. 3, fig. 8.
- 1985 *Pseudoaulophacus pargueraensis* Pessagno – Sanfilippo and Riedel, p. 596, figs. 6.5a–6.5d.
- 1988 *Pseudoaulophacus pargueraensis* Pessagno – Thurow, p. 404, pl. 2, fig. 7.
- 2008 *Pseudoaulophacus pargueraensis* Pessagno – Bandini *et al*., p. 18, pl. 1, figs. 24–25.

Remarks: *Pseudoaulophacus pargueraensis* consists of a circular shell with lobate periphery, which is a most differentiated character from other species of *Pseudoaulophacus*.
Range: Lower Santonian to Lower Campanian (Pessagno, 1972), Lower to Middle Campanian (Sanfilippo and Riedel, 1985), Lower to Upper Campanian (Thurow, 1988), and Coniacian? to lowermost Maastrichtian (Hollis and Kimura, 2001).

Pseudoaulophacus* sp. cf. *P. pargueraensis Pessagno 1963
(Plate 2, fig. 2)
Remarks: This poorly-preserved specimen is similar to *Pseudoaulophacus pargueraensis* in having a weakly-developed lobate periphery.

Family **ARCHAEOSPONGOPRUNIDAE** Pessagno 1973

Genus ***Archaeospongoprunum*** Pessagno 1973

Archaeospongoprunum* sp. cf. *A. stocktonensis Pessagno 1973
(Plate 2, fig. 4)
Remarks: This specimen consists of ellipsoidal shell with two polar spines, one of which is broken. It is similar to *Archaeospongoprunum stocktonensis* rather than *Archaeospongoprunum rumseyensis* Pessagno based on the outline of the shell.

Archaeospongoprunum* sp. aff. *A. andersoni Pessagno 1973
(Plate 3, fig. 4)
Remarks: This specimen resembles *Archaeospongoprunum andersoni* by having an elongate cylindrical test with fine meshwork comprised of tetragonal to pentagonal pore frames, but differs from it by having three indistinct lobe. *Archaeospongoprunum bipartitum* also consists of an elongate cylindrical test with two lobes, but meshwork of its test is much coarser than this specimen.

Archaeospongoprunum hueyi Pessagno 1973
(Plate 1, figs. 4, 17–18)
- 1973 *Archaeospongoprunum hueyi* n. sp. – Pessagno, p. 61–62, pl. 13, fig. 1.
- 1976 *Archaeospongoprunum hueyi* Pessagno – Pessagno, p. 33, pl. 11, fig. 5.
- 1992 *Archaeospongoprunum hueyi* Pessagno – Okamura, pl. 34, figs. 5, 18.
- 1997 *Archaeospongoprunum hueyi* Pessagno – Hashimoto and Ishida, pl. 3, fig. 25.
- 2015 *Archaeospongoprunum hueyi* Pessagno – Hashimoto *et al*., p. 44, pl. 1, fig. 18.

Remarks: Test is elongate and ellipsoidal with two polar spines and with spongy meshwork. Each spine consists of four longitudinal grooves and ridges, which are arranged not spirally but straight.
Range: Lower Campanian (Pessagno, 1973), lower upper Campanian (Pessagno, 1976), Campanian to Lower Maastrichtian (Hollis and Kimura, 2001), and Middle Campanian to Upper Maastrichtian (Hashimoto *et al*., 2015).

Family **PYRAMISPONGIIDAE** Kozur and Mostler 1978, *emend.* De Wever *et al*. 2001

Genus ***Pyramispongia*** Pessagno 1973

Pyramispongia glascockensis Pessagno 1973
(Plate 3, fig. 17)
- 1973 *Pyramispongia glascockensis* n. sp. – Pessagno, p. 79–80, pl. 21, figs. 2–5.
- 1976 *Pyramispongia glascockensis* Pessagno – Pessagno, p. 37, pl. 1, fig. 9.
- 1982 *Pyramispongia glascockensis* Pessagno – Taketani, p. 51, pl. 10, fig. 12.
- 1982 *Pyramispongia glascockensis* Pessagno – Yamauchi, pl. 2, fig. 9.
- 1988 *Pyramispongia glascockensis* Pessagno – Thurow, p. 405, pl. 2, fig. 23.
- 1992 *Pyramispongia glascockensis* Pessagno – Marcucci Passerini and Gardin, fig. 3o.
- 1998 *Pyramispongia glascockensis* Pessagno – Salvini and Marcucci Passerini, pl. 8, fig. i.
- 2004 *Pyramispongia glascockensis* Pessagno – Bąk, figs. 5.15–5.16.

Range: Cenomanian to Coniacian (Pessagno, 1976), Middle Cenomanian to Lower Santonian (Taketani, 1982), Lower Cenomanian to Middle Turonian (Thurow, 1988), and Lower Cenomanian to Turonian? (O’Dogherty, 1994).

Family **SPONGURIDAE** Haeckel 1862

Genus ***Patellula*** Kozlova in Petrushevskaya and Kozlova 1972

Patellula planoconvexa (Pessagno 1963)
(Plate 1, fig. 5)
1963 *Stylospongia planoconvexa* n. sp. – Pessagno, p. 199, pl. 3, figs. 4–6; pl. 6, fig. 1.
1972 *Patellula planoconvexa* (Pessagno) – Petrushevskaya and Kozlova, p. 527, pl. 3, fig. 13.
1979 *Patellula planoconvexa* (Pessagno) – Nakaseko *et al*., pl. 8, fig. 1.
1994 Patellula planoconvexa (Pessagno) – Yamasaki and Tsujii, pl. II, fig. 13.

Patellula verteroensis (Pessagno 1963)
(Plate 2, figs. 3, 18; Plate 3, figs. 5, 18)
1963 *Stylospongia verteroensis* n. sp. – Pessagno, p. 199, pl. 3, figs. 1–3; pl. 6, figs. 2–3; pl. 7, figs. 3, 6.
1972 *Patellula verteroensis* (Pessagno) – Petrushevskaya and Kozlova, p. 527, pl. 3, figs. 8–9.
1981 *Patellula verteroensis* (Pessagno) – Empson-Morin, p. 257, pl. 2, figs. 1–5.
1988 *Patellula verteroensis* (Pessagno) – Thurow, p. 403, pl. 2, figs. 19–20.
1989 *Patellula verteroensis* (Pessagno) – Tumanda, p. 34–35, pl. 9, figs. 15–16.
1994 *Patellula verteroensis* (Pessagno) – O'Dogherty, p. 328–329, pl. 60, figs. 25–26.
1994 *Patellula verteroensis* (Pessagno) – Yamasaki and Tsujii, pl. II, fig. 14.
1998 *Patellula verteroensis* (Pessagno) – Erbacher, p. 370, pl. 1, fig. 24.
2004 *Patellula verteroensis* (Pessagno) – Bąk, pl. 7, fig. 13.
Range: Probably Lower Campanian (Pessagno, 1963), and Middle Cenomanian to Lower Turonian? (O'Dogherty, 1994).

Order **NASSELLARIA** Ehrenberg 1875

Family **CANNOBOTRYIDAE** Haeckel 1881

Genus ***Rhopalosyringium*** Campbell and Clark 1944

Rhopalosyringium magnificum Campbell and Clark 1944
(Plate 1, figs. 6, 19–20; Plate 2, fig. 19)
1944 *Rhopalosyringium magnificum* n. sp. – Campbell and Clark, p. 30, pl. 7, figs. 16–17.
1968 *Rhopalosyringium*? *magnificum* Campbell and Clark – Foreman, p. 55, pl. 6, figs. 7a–7b.
1981 *Rhopalosyringium magnificum* Campbell and Clark – Empson-Morin, p. 265, pl. 8, figs. 1A–1D.
1982 *Rhopalosyringium magnificum* Campbell and Clark – Yamauchi, pl. 5, fig. 1.
1992 *Rhopalosyringium* sp. – Okamura, pl. 38, fig. 23.
1998 *Rhopalosyringium magnificum* Campbell and Clark – Ishida and Hashimoto, pl. 2, fig. 20.
2006 *Rhopalosyringium magnificum* Campbell and Clark – Musavu-Moussavou and Danelian, p. 154, pl. 2, figs. 3–5.
2015 *Rhopalosyringium magnificum* Campbell and Clark – Hashimoto *et al*., pl. 1, fig. 14.
Range: Campanian to Lower Maastrichtian (Hollis and Kimura, 2001), and Middle? to Upper Campanian (Hashimoto *et al*., 2015).

***Rhopalosyringium* sp. A** sensu Bandini *et al*. 2008
(Plate 3, fig. 19)
2006 *Rhopalosyringium*? sp. – Denyer and Baumgartner, fig. 7P.
2008 *Rhopalosyringium* sp. A – Bandini *et al*., pl. 1, fig. 10; pl. 3, fig. 19.
Description: Test, lacking strictures, is spindle-shaped, rounded apically, and is composed of two segments; cephalis minute, hemispherical and thorax cylindrical without aperture ring. Seven to eight edged costae are visible in a lateral view, which arise near the apex and extend distally on the thorax. Thoracic pores are arranged longitudinally but irregularly, forming single or double rows between adjacent costae.
Remarks: This species is similar to *Rhopalosyringium scissum*, but distinguished from it in having edged costae and lack of the cephlo-thoracic stricture.
Occurrence: Coniacian–Santonian chert of the Nicoya Complex (Denyer and Baumgartner, 2006) and turbiditic sequence of the Berrugate and Sabana Grande formations (Bandini *et al*., 2008) in Costa Rica.

Family **WILLIRIEDELLIDAE** Dumitrică 1970

Genus ***Cryptamphorella*** Dumitrică 1970

Cryptamphorella sphaerica (White 1928)
(Plate 1, fig. 21; Plate 2, fig. 20)
1928 *Baculogypsina*? *sphaerica* n. sp. – White, p. 306, pl. 41, figs. 12–13.
1962 *Aulonia sphaerica* (White) – Pessagno, p. 366, pl. 6, fig. 3.
1963 *Holocryptocapsa*? *sphaerica* (White) – Pessagno, p. 206, pl. 1, fig. 3; pl. 5, figs. 1–2.
1970 *Cryptamphorella sphaerica* (White) – Dumitrică, p. 82, pl. XII, figs. 73a–73b, 74a–74c, 75a–75b, 77; pl. XX, figs. 133a–133b.
1981 *Cryptamphorella sphaerica* (White) – Nakaseko and Nishimura, p. 149, pl. 5, figs. 1–2.
1989 *Cryptamphorella sphaerica* (White) – Tumanda, p. 36, pl. 7, fig. 18; pl. 10, fig. 15.
1998 *Cryptamphorella sphaerica* (White) – Ishida and Hashimoto, fig. 3.20.
2005 *Cryptamphorella sphaerica* (White) – Popova-Goll *et al*., p. 11–12, pl. 1, fig. 16; pl. 6, fig. 11.
2015 *Cryptamphorella sphaerica* (White) – Hashimoto

et al., p. 44–45, pl. 1, fig. 26.
Range: Middle Santonian to lowermost Maastrichtian (Hollis and Kimura, 2001), and Campanian? to Lower Maastrichtian (Hashimoto *et al*., 2015).

Cryptamphorella macropora Dumitrică 1970
(Plate 1, fig. 7; Plate 2, fig. 5)
1970 *Cryptamphorella macropora* n. sp. – Dumitrică, p. 81, pl. X, figs. 64a–64b, 65; p. XI, figs. 67, 69–72a–72b; pl. XX, fig. 132; pl. XXI, figs. 137, 140a–140b, 141.
1981 *Cryptamphorella macropora* Dumitrică – Nakaseko and Nishimura, p. 149, pl. 4, figs. 6–7; pl. 14, fig. 6.
1988 *Cryptamphorella macropora* Dumitrică – Thurow, p. 400, pl. 1, fig. 3.
1997 *Cryptamphorella macropora* Dumitrică – Hashimoto and Ishida, pl. 3, fig. 11.
1998 *Cryptamphorella macropora* Dumitrică – Ishida and Hashimoto, pl. 2, fig. 18.
Range: Coniacian? to lowermost Maastrichtian (Hollis and Kimura, 2001).

Cryptamphorella* sp. aff. *C. gilkeyi (Dumitrica 1973)
(Plate 3, fig. 6)
Remarks: This specimen is similar to *Cryptamphorella gilkeyi*, which was originally described as *Wiliriedellum*? *gilkeyi* by Dumitrica (1973), in its subspherical test with three segments, third of which is completely covered by triangular or polygonal depressions limited by sharp crests. Nevertheless, it differs from *Cryptamphorella gilkeyi* by lacking of a large sutural pore and having six (or much more) small pores in each depression. The radiolarian assemblage suggests a much younger age (early Coniacian) is given to this specimen, whereas an Aptian or Albian age was assigned to *Cryptamphorella gilkeyi* by Dumitrica (1973) and O'Dogherty (1994). On the basis of these morphology and age, they seem to be different species.

Cryptamphorella wogiga Empson-Morin 1981
(Plate 2, fig. 31)
1981 *Cryptamphorella wogiga* n. sp. – Empson-Morin, p. 266, pl. 12, figs. 3A–3D.
Remarks: Pores on abdomen are recessed into ridged pentagonal to hexagonal pore frames, which interlock to form irregular polygonal network.

***Cryptamphorella* sp. B** sensu Bąk 1996
(Plate 1, fig. 22)
1996 *Cryptamphorella* sp. B – Bąk, p. 100, fig. 9D.
Remarks: This specimen consists of three segments. It differs from *Cryptamphorella conara* by having an oval abdomen and from *Cryptamphorella macropora* by lacking a large sutural pore.
Occurrence: The Macelowa Marl Member in the Pieniny Klippen belt, Polish Carpathians (Bąk 1996).

Genus ***Hemicryptocapsa*** Tan 1927

Hemicryptocapsa polyhedra Dumitrică 1970
(Plate 3, fig. 7)
1970 *Hemicryptocapsa polyhedra* n. sp. – Dumitrică, p. 72, pl. XIV, figs. 85a–85c.
1981 *Hemicryptocapsa polyhedra* Dumitrică – Nakaseko and Nishimura, p. 153, pl. 4, fig. 2; pl. 14, fig. 5.
1992 *Hemicryptocapsa polyhedra* Dumitrică – Marcucci Passerini and Gardin, fig. 3f.
2006 *Hemicryptocapsa polyhedra* Dumitrică – Denyer and Baumgartner, fig. 7Q.
2008 *Hemicryptocapsa polyhedra* Dumitrică – Bandini *et al*., pl. 1, fig. 17; p. 3, fig. 15.
Remarks: *Hemicryptocapsa polyhedra* is similar to *Hemicryptocapsa prepolyhedra* in general features, especially having a subspherical test with polygonal facets, but is distinguished from it by lacking of perforate ridges which limit polygonal facets.
Range: Lower Cenomanian to Middle Coniacian (Taketani, 1982).

Family **ARTOSTROBIIDAE** Riedel 1967

Genus ***Theocampe*** Haeckel 1887

Theocampe urna (Foreman 1971)
(Plate 2, fig. 32)
1970 Artostrobiid gen. et sp. indet – Kling, pl. 7, fig. 8.
1971 *Artostrobium urna* n. sp. – Foreman, p. 1677–1678, pl. 4, figs. 1–2.
1973b *Theocampe urna* (Foreman) – Foreman, pl. 15, fig. 21.
1974 *Artostrobium urna* (Foreman) – Riedel and Sanfilippo, p. 775, pl. 11, figs. 4, 6.
1981 *Artostrobium urna* Foreman – Nakaseko and Nishimura, p. 148, pl. 17, fig. 10.
1982 *Theocampe urna* (Foreman) – Taketani, p. 53, pl. 2, fig. 12.
1988 *Theocampe tina* (Foreman) – Thurow, p. 407, pl. 1, fig. 6.
1985 *Theocampe urna* (Foreman) – Sanfilippo and Riedel, p. 606, figs. 7a–7c.
1987 *Artostrobium urna* Foreman – Yamasaki, pl. 2, fig. 16.
1992 *Artostrobium tina* Foreman – Okamura, pl. 39, fig. 1.
1992 *Artostrobium urna* Foreman – Okamura, pl. 39, fig. 2.
1998 *Artostrobium urna* Foreman – Ishida and Hashimoto, pl. 1, fig. 21.
Remarks: This species has a wide range of variation in the external form and ornamentation, and resembles to *Theocampe tina*. However, this species is distinguished from the latter by having a more constricted test and short and inflated abdomen as pointed out by O'Dogherty (1994) and Hollis and Kimura (2001). The examined specimen

also possesses a prominent apertural ring.
Range: Lower Coniacian to Lower Campanian? (Taketani, 1982), Middle Coniacian to Middle Campanian (Sanfilippo and Riedel, 1985), Turonian to Middle Campanian (Thurow, 1988), and Coniacian? to Middle Campanian (Hollis and Kimura, 2001).

Theocampe salillum Foreman 1971
(Plate 2, figs. 6, 21; Plate 3, fig. 20)
1970 *Theocampe salillum* sp. – Kling, pl. 7, figs. 1, 5.
1971 *Theocampe salillum* n. sp. – Foreman, p. 1678–1679, pl. 4, fig. 5.
1973a *Theocampe salillum* Foreman – Foreman, p. 430, pl. 13, fig. 2.
1973b *Theocampe salillum* Foreman – Foreman, pl. 15, fig. 12.
1974 *Theocampe salillum* Foreman – Riedel and Sanfilippo, p. 780, pl. 11, figs. 8–10.
1981 *Theocampe salillum* Foreman – Empson-Morin, p. 263, pl. 5, figs. 4A–4C.
1981 *Theocampe salillum* Foreman – Nakaseko and Nishimura, p. 164, pl. 13, figs. 4, 7.
1982 *Theocampe salillum* Foreman – Taketani, p. 53, pl. 2, fig. 14.
1985 *Theocampe salillum* Foreman – Sanfilippo and Riedel, p. 605, figs. 4a–4c.
1988 *Theocampe salillum* Foreman – De Wever *et al*., p. 171, pl. 1, fig. 8.
1998 *Theocampe salillum* Foreman – Ishida and Hashimoto, pl. 1, fig. 17.
2012 *Theocampe salillum* Foreman – Asis and Jasin, pl. 2, fig. 10.
Range: Santonian to Upper Campanian (Sanfilippo and Riedel, 1985), and Lower Coniacian to Lower Campanian? (Taketani, 1982).

Family **CARPOCANIIDAE** Haeckel 1881, *emend*. De Wever *et al*. 2001

Genus ***Diacanthocapsa*** Squinabol 1903

Diacanthocapsa ovoidea Dumitrică 1970
(Plate 2, fig. 7)
1970 *Diacanthocapsa ovoidea* n. sp. – Dumitrică, p. 63, pl. V, fig. 25a; pl. VI, figs. 26–28b.
1982 *Diacanthocapsa ovoidea* Dumitrică – Mizutani *et al*., p. 72, pl. 5, fig. 6.
1987 *Diacanthocapsa ovoidea* Dumitrică – Yamasaki, pl. 2, fig. 8.
1992 *Diacanthocapsa ovoidea* Dumitrică – Iwata *et al*., pl. 2, fig. 10; pl. 3, figs. 9–10.
1994 *Diacanthocapsa ovoidea* Dumitrică – O'Dogherty, p. 220, pl. 37, figs. 1–16
1998 *Diacanthocapsa ovoidea* Dumitrică – Salvini and Marcucci Passerini, p. 269, fig. 9o.
2007 *Diacanthocapsa ovoidea* Dumitrică – Musavu-Moussavou *et al*., p. 269, pl. 3, fig. 4.
Range: Middle Cenomanian to Lower Turonian? (O'Dogherty, 1994), and Lower Campanian (Dumitrică, 1970).

Diacanthocapsa* sp. cf. *D. ovoidea Dumitrică 1970
(Plate 1, fig. 8)
Remarks: This specimen is broken, but almost similar to *Diacanthocapsa ovoidea* in having a lengthened-oval outline and in having small circular pores on the test surface, which are arranged irregularly in apical portion and longitudinally in distal portion.

Diacanthocapsa* sp. cf. *D. ancus (Foreman 1968) sensu Dumitrică 1970
(Plate 2, fig. 8)
1968 *Theocapsomma ancus* n. sp. – Foreman, p. 32–33, pl. 4, fig. 3.
1970 *Diacanthocapsa* sp. cf. *D. ancus* (Foreman) – Dumitrică, p. 64–65, pl. VI, figs. 35a–35b; pl. VII, fig. 40; pl. XX, fig. 125.
1992 *Diacanthocapsa* sp. – Okamura, pl. 38, fig. 5.
1997 *Diacanthocapsa* sp. cf. *D. ancus* (Foreman) – Hashimoto and Ishida, pl. 2, fig. 13.
1998 *Diacanthocapsa* sp. cf. *D. ancus* (Foreman) – Ishida and Hashimoto, pl. 2, fig. 9.

Genus ***Eastonerius*** Empson-Morin 1981

Eastonerius* sp. aff. *E. acuminatus (Dumitrică 1970)
(Plate 1, fig. 23)
1982 *Diacanthocapsa acuminata* Dumitrică – Matsuyama *et al*., pl. IV, fig. 15.
1997 *Diacanthocapsa acuminata* Dumitrică – Hashimoto and Ishida, pl. 3, fig. 22.
1998 *Diacanthocapsa acuminata* Dumitrică – Ishida and Hashimoto, pl. 2, fig. 10.
Remarks: *Eastonerius acuminatus*, which was emended from *Diacanthocapsa acuminata* by Empson-Morin (1981), consists of oval three-segmented test with a rounded apical end, and possesses a short inverted conical abdomen. Although not always well-visible, sutural pores are recognized. The present specimen is similar to *Eastonerius acuminatus* in having oval test and external ornamentations, but different from it by probably consisting of four segments.

Family **ARCHAEODICTYOMITRIDAE** Pessagno 1976

Genus ***Archaeodictyomitra*** Pessagno 1976

Archaeodictyomitra squinaboli Pessagno 1976
(Plate 3, fig. 21)
1976 *Archaeodictyomitra squinaboli* n. sp. – Pessagno, p. 50, pl. 5, figs. 2–8.
1981 *Archaeodictyomitra squinaboli* Pessagno – Nakaseko and Nishimura, p. 147, pl. 6, fig. 7; pl. 15, fig. 1.

1989 *Archaeodictyomitra squinaboli* Pessagno – Tumanda, p. 36, pl. 7, fig. 7.
1992 *Dictyomitra* sp.– Okamura, pl. 37, fig. 6.
1997 *Archaeodictyomitra squinaboli* Pessagno – Hashimoto and Ishida, pl. 1, fig. 4.

Remarks: This species consists of elongated conical test with eight or nine segments and without distinct constrictions. 11 to 12 longitudinal costae are visible in a lateral view. *Dictyomitra multicostata* is similar to *Archaeodictyomitra squinaboli* in their outline, which is elongated conical, but different from the latter by having shallow strictures between post-abdominal segments.
Range: Cenomanian? to Upper Campanian (Pessagno, 1976), and Campanian (Hollis and Kimura, 2001).

Genus ***Dictyomitra*** Zittel 1876, *emend*. Pessagno 1976

Dictyomitra undata Squinabol 1904
(Plate 2, fig. 34)
1904 *Dictyomitra undata* n. sp. – Squinabol, p. 231, pl. 10, fig. 2.
1997 *Dictyomitra undata* Squinabol – Sýkora *et al*., pl. V, fig. 8.
2004 *Dictyomitra undata* Squinabol – Bąk, fig. 4.3.
2008 *Dictyomitra undata* Squinabol – Bandini *et al*., pl. 4, fig. 5.
2011 *Archaeodictyomitra undata* (Squinabol) – Bandini *et al*., p. 20, pl. 11, fig. 1.

Dictyomitra* sp. cf. *D. gracilis (Squinabol 1903)
(Plate 3, fig. 22)
Remarks: This specimen resembles to *Dictyomitra gracilis* in possessing a spindle-shape test with longitudinally extending costae, but differs by possessing slightly intense constriction.

Dictyomitra formosa Squinabol 1904
(Plate 3, figs. 8, 23)
1904 *Dictyomitra formosa* n. sp. – Squinabol, p. 232, pl. 10, fig. 4.
1973a *Dictyomitra torquata* Foreman – Foreman, p. 430, pl. 13, fig. 7.
1976 *Dictyomitra formosa* Squinabol – Pessagno, p. 51–52, pl. 8, figs. 10–12.
1982 *Dictyomitra formosa* Squinabol – Mizutani *et al*., p. 66, pl. 9, fig. 1.
1982 *Dictyomitra formosa* Squinabol – Taketani, p. 58, pl. 4, figs. 6a–6b; pl. 11, fig. 13.
1988 *Dictyomitra formosa* Squinabol – Thurow, p. 400, pl. 1, fig. 23.
1992 *Dictyomitra formosa* Squinabol – Okamura, pl. 28, fig. 2; pl. 36, fig. 33; pl. 37, figs. 2–3.
1992 *Dictyomitra formosa* Squinabol – Iwata *et al*., pl. 5, fig. 5.
1994 *Dictyomitra formosa* Squinabol – O'Dogherty, p. 80–81, pl. 4, figs. 8–12.
1997 *Dictyomitra formosa* Squinabol – Hashimoto and Ishida, pl. 2, fig. 15.
2008 *Dictyomitra formosa* Squinabol – Bandini *et al*., p. 16–17, pl. 2, fig. 23; pl. 3, fig. 13; pl. 4, fig. 3.
2009 *Dictyomitra formosa* Squinabol – Djerić *et al*., fig. 8.11.
2011 *Dictyomitra formosa* Squinabol – Smrečková, pl. 1, fig. 17.
2015 *Dictyomitra formosa* Squinabol – Hashimoto *et al*., p. 45, pl. 2, fig. 2.

Remarks: As mentioned by Pessagno (1976) and O'Dogherty (1994), test of this species is moderately or markedly lobulate in outline with continuously arranged longitudinal costae, and post-abdominal segments are separated by relatively deep strictures. It is distinguished from *Dictyomitra duodecimcostata* and D*ictyomitra multicostata* as described below.
Range: Coniacian to Lower Campanian (Pessagno, 1976), Coniacian to Santonian (Taketani, 1982), Middle Turonian to Lower Campanian (Thurow, 1988), Upper Albian to Lower Turonian? (O'Dogherty, 1994), Middle Coniacian? to Upper Campanian (Hollis and Kimura, 2001), and Middle Coniacian? to Upper Campanian (Hashimoto *et al*., 2015).

Dictyomitra duodecimcostata (Squinabol 1903) sensu Foreman (1975)
(Plate 2, fig. 35)
1903 *Lithostrobus duodecimcostatus* n. sp. – Squinabol, p. 438, pl. X, fig. 21.
1972 *Dictyomitra duodecimcostata* (Squinabol) group – Petrushevskaya and Kozlova, p. 550, pl. 2, figs. 10–115.
1973b *Dictyomitra torquata* Foreman – Foreman, pl. 15, figs. 9–11.
1975 *Dictyomitra duodecimcostata* (Squinabol) – Foreman, p. 614, pl. 1G, fig. 5; pl. 7, fig. 8.
1978 *Dictyomitra duodecimcostata duodecimcostata* (Squinabol) – Foreman, p. 746, pl. 4, figs. 8–9.
1981 *Dictyomitra formosa* Squinabol – Nakaseko and Nishimura, p. 150–151, pl. 8, figs. 7–8; pl. 16, figs. 4, 11.
1997 *Dictyomitra duodecimcostata* (Squinabol) – Yamasaki and Sakamoto, pl. 1, fig. 6.
2008 *Dictyomitra formosa* Squinabol – Bandini *et al*., p. 16–17, pl. 1, figs. 5, 15; pl. 2, fig. 10.

Remarks: According to the original description by Squinabol (1904), *Dictyomitra duodecimcostata* consists of pyramidal test. Foreman (1975) also mentioned that the expanded segments after the initial conical ones increase distally in size. The obtained specimen of *Dictyomitra duodecimcostata* is different from *Dictyomitra formosa* in having the pyramidal-shaped test with discontinuous costae, which are thicker than those of the latter species. Test generally consists of eight segments. Post-abdominal segments are inflated and separated by extremely deep strictures.

Dictyomitra multicostata Zittel 1876
(Plate 1, figs. 24; Plate 2, figs. 10–11; Plate 3, figs. 9, 24)
1876 *Dictyomitra multicostata* n. sp. – Zittel, p. 81, pl. 2, figs. 2–4.
1944 *Dictyomitra multicostata* Zittel – Campbell and Clark, p. 39–40, pl. 8, figs. 22–24, 35–42.
1968 *Dictyomitra multicostata* Zittel – Foreman, p. 63–65, pl. 7, figs. 4a–4b.
1968 *Dictyomitra lamellicostata* n. sp. – Foreman, p. 65–66, pl. 7, figs. 8a–8b.
1968 *Dictyomitra* sp. cf. *D. multicostata* Zittel – Foreman, p. 63–65, pl. 7, figs. 9a–9b.
1973b *Dictyomitra torquata* Foreman – Foreman, pl. 10, fig. 8c.
1976 *Dictyomitra multicostata* Zittel – Pessagno, p. 52–53, pl. 14, figs. 4–9.
1981 *Dictyomitra multicostata* Zittel – Nakaseko and Nishimura, p. 151, pl. 8, fig. 1; pl. 16, fig. 1.
1987 *Dictyomitra multicostata* Zittel – Yamasaki, pl. 1, fig. 16.
1994 *Dictyomitra multicostata* Zittel – O'Dogherty, p. 82–83, pl. 4, figs. 17–19.
1997 *Dictyomitra multicostata* Zittel – Hashimoto and Ishida, pl. 2, fig. 1.
2007 *Dictyomitra multicostata* Zittel – Musavu-Moussavou *et al*., p. 267–268, pl. 2, figs. 12–13.
2008 *Dictyomitra multicostata* Zittel – Bandini *et al*., p. 17, pl. 4, fig. 4.
2015 *Dictyomitra multicostata* Zittel – Hashimoto *et al*., p. 45, pl. 1, fig. 5.

Remarks: This species is similar to *Dictyomitra formosa*, but different by having a slender spindle-shaped or elongate mildly lobulate test with widely spaced costae (Pessagno, 1976; O'Dogherty, 1994).
Range: Middle Campanian to Lower Maastrichtian (Pessagno, 1976), and Turonian to Maastrichtian (Thurow, 1988).

Dictyomitra densicostata Pessagno 1976
(Plate 1, figs. 9–10, 25; Plate 2, fig. 23)
1976 *Dictyomitra densicostata* n. sp. – Pessagno, p. 51, pl. 14, figs. 10–14, 16.
1992 *Dictyomitra formosa* Squinabol – Okamura, pl. 31, fig. 5.
1997 *Dictyomitra densicostata* Pessagno – Hashimoto and Ishida, pl. 1, fig. 19; pl. 2, fig. 4.
1998 *Dictyomitra densicostata* Pessagno –Ishida and Hashimoto, pl. 1, fig. 18.
2007 *Dictyomitra* sp. cf. *D. densicostata* Pessagno – Musavu-Moussavou *et al*., p. 268, pl. 2, figs. 14–15.
2015 *Dictyomitra densicostata* Pessagno – Hashimoto *et al*., p. 45, pl. 1, fig. 6.

Remarks: Test of this species is distinctly lobulate with finely costae throughout. It differs from *Dictyomitra multicostata* by costae on post-abdominal segments which are spaced closely than those of the latter species.
Range: Upper Coniacian to Campanian (Pessagno, 1976), Middle Coniacian? to Lower Maastrichtian (Hollis and Kimura, 2001), and Middle Campanian? to Lower Maastrichtian (Hashimoto *et al*., 2015).

Dictyomitra* sp. aff. *D. densicostata Pessagno 1976
(Plate 3, fig. 26)
Remarks: This specimen resembles to *Dictyomitra densicostata*, but slightly differs by its short test having less post-abdominal segments than those of the latter species.

Dictyomitra koslovae Foreman 1975
(Plate 2, figs. 9, 22, 33)
1971 *Dictyomitra* sp. – Foreman, p. 1677, pl. 3, fig. 5.
1975 *Dictyomitra koslovae* n. sp. – Foreman, p. 614, pl. 7, fig. 4.
1978 *Dictyomitra koslovae* Foreman – Foreman, p. 746–747, pl. 4, fig. 10.
1981 *Dictyomitra koslovae* Foreman – Nakaseko and Nishimura, p. 151, pl. 8, figs. 2–5; pl. 16, figs. 2–3.
1982 *Dictyomitra koslovae* Foreman – Mizutani *et al*., p. 67–68, pl. 9, figs. 5–8.
1985 *Dictyomitra koslovae* Foreman – Sanfilippo and Riedel, p. 599–600, figs. 7.4a–7.4b, 7.4d–7.4e.
1987 *Dictyomitra koslovae* Foreman – Yamasaki, pl. 1, fig. 22.
1989 *Dictyomitra koslovae* Foreman – Iwata and Tajika, pl. 2, fig. 7.
1992 *Dictyomitra koslovae* Foreman – Iwata *et al*., pl. 1, fig. 1.
1994 *Dictyomitra koslovae* Foreman – Yamasaki and Tsujii, pl. 1, figs. 3–5.
2008 *Dictyomitra koslovae* Foreman – Bandini *et al*., p. 17, pl. 1, fig. 16; pl. 2, figs. 11, 24; pl. 3, fig. 14.
2009 *Dictyomitra koslovae* Foreman – Djerić *et al*., fig. 8.6.
2015 *Dictyomitra koslovae* Foreman – Hashimoto *et al*., p. 45, pl. 1, fig. 3.

Remarks: *Dictyomitra koslovae* is distinctly different from other species of *Dictyomitra* by having the fourth segment which is markedly wider than the next one or two segments (Foreman, 1975).
Range: Middle Coniacian to Lower Campanian? (Taketani, 1982), Middle to Upper Campanian (Sanfilippo and Riedel, 1985), Middle to Upper Campanian (Thurow, 1988), Upper Coniacian to Lower Maastrichtian (Hollis and Kimura, 2001), and Middle? to Upper Campanian (Hashimoto *et al*., 2015).

Dictyomitra andersoni (Campbell and Clark 1944)
(Plate 3, fig. 25)
1944 *Lithocampe andersoni* n. sp. – Campbell and Clark, p. 42–43, pl. 8, fig. 25.
1968 *Dictyomitra andersoni* (Campbell and Clark) – Foreman, p. 68, pl. 7, figs. 6a–6d.
1971 *Dictyomitra andersoni* (Campbell and Clark) –

Foreman, p. 1677, pl. 3, fig. 8.
1978 *Dictyomitra andersoni* (Campbell and Clark) – Foreman, p. 746, pl. 4, fig. 6.
1981 *Dictyomitra* sp. A – Nakaseko and Nishimura, p. 151, pl. 8, fig. 6.
1982 *Dictyomitra urakawensis* n. sp. – Taketani, p. 59, pl. 4, figs. 8a–8b; pl. 11, fig. 16.
1987 *Dictyomitra tiara* Campbell and Clark – Yamasaki, pl. 1, fig. 18.
1989 *Dictyomitra urakawensis* Taketani – Tumanda, p. 36, pl. 8, figs. 4–5.
1992 *Dictyomitra urakawensis* Taketani – Okamura, pl. 35, fig. 5.
1997 *Dictyomitra urakawensis* Taketani – Hashimoto and Ishida, pl. 1, fig. 21.
1997 *Dictyomitra tiara* Campbell and Clark – Hashimoto and Ishida, pl. 2, fig. 2.
1997 *Dictyomitra andersoni* (Campbell and Clark) – Hollis, p. 69, pl. 16, figs. 11–16.
2015 *Dictyomitra andersoni* (Campbell and Clark) – Hashimoto *et al*., p. 45, pl. 1, fig. 4.

Remarks: As mentioned by Hollis (1997), *Dictyomitra urakawensis* described by Taketani (1982) is a synonym of this species.
Range: Middle Coniacian? to Lower Maastrichtian or to Paleocene (Hollis and Kimura, 2001), and Middle Campanian? to Maastrichtian or to Paleocene? (Hashimoto *et al*., 2015).

Genus ***Thanarla*** Pessagno 1977

Thanarla* sp. aff. *T. veneta (Squinabol 1903)
(Plate 1, fig. 26)
Description: Test is elongate and conical to campanulate, and is composed of seven segments; Cephalothorax is conical and relatively short, inflated abdomen shows an annular form. Post-abdominal segments is cylindrical, narrower than proximal segments, gradually increasing in width as added. Final post-abdominal segment is slightly narrower. Constrictions are weakly developed, but markedly distinct between the annular abdomen and first post-abdominal segment. Edged costae are developed throughout, converging apically and widely spaced on the post-abdominal segments (ten costae are visible in lateral view).
Remarks: The examined specimen is similar to *Thanarla veneta* in general form, but distinguished by having an elongate test with seven segments (*Thanarla veneta* consists of four segments). *Dictyomitra koslovae* resembles to this species, but differs by lacking costae on its apical portion.

Family **AMPHIPYNDACIDAE** Riedel 1967

Genus ***Amphipternis*** Foreman 1973b

Amphipternis stocki (Campbell and Clark 1944)
(Plate 1, figs. 11–12, 28–29; Plate 2, figs. 12–13, 24; Plate 3, figs. 11, 30)
1944 *Stichocapsa*? *stocki* n. sp. – Campbell and Clark, p. 44, pl. 8, figs. 31–33.
1968 *Amphipyndax stocki* (Campbell and Clark) – Foreman, p. 78, pl. 8, figs. 12a–12c.
1972 *Amphipyndax stocki* (Campbell and Clark) – Petrushevskaya and Kozlova, p. 545, pl. 8, figs. 16–17.
1973a *Amphipyndax stocki* (Campbell and Clark) – Foreman, p. 430, pl. 13, fig. 5.
1975 *Amphipyndax stocki* (Campbell and Clark) – Pessagno, p. 1016, pl. 4, figs. 6–8.
1978 *Amphipyndax stocki* (Campbell and Clark) – Foreman, p. 745, pl. 4, fig. 4.
1981 *Amphipyndax stocki* (Campbell and Clark) – Nakaseko and Nishimura, p. 145, pl. 12, fig. 5.
1982 *Amphipyndax stocki* (Campbell and Clark) – Taketani, p. 52, pl. 2, fig. 9a–9b; pl. 10, figs. 13–14.
1982 *Protostichocapsa stocki* (Campbell and Clark) – Empson-Morin, p. 516–517, pl. 4, figs. 1–12.
1994 *Stichomitra stocki* (Campbell and Clark) – O'Dogherty, p. 147–150, pl. 18, figs. 9–15.
1998 *Stichomitra stocki* (Campbell and Clark) – Erbacher, p. 370–371, pl. 2, fig. 1.
2006 *Stichomitra stocki* (Campbell and Clark) – Musavu-Moussavou and Danelian, p. 155, pl. 2, figs. 11–13.
2007 *Stichomitra stocki* (Campbell and Clark) – Musavu-Moussavou *et al*., p. 273, pl. 4, figs. 9–12.
2015 *Amphipyndax stocki* (Campbell and Clark) – Hashimoto *et al*., p. 43, pl. 1, fig. 10.
2016 *Amphipternis stocki* (Campbell and Clark 1944) – Noda and Kurihara, pl. 1, figs. 6, 11, 18; pl. 2, fig. 4.

Remarks: *Amphipternis stocki* shows a wide range of morphological variation in the proximal portion of the test (O'Dogherty, 1994), and resembles to *Stichomitra mediocris*. However, they are distinguishable; *Amphipternis stocki* is composed of externally constricted test with smaller pores, larger numbers of rows of pores per segment, and is also marked by a large sutural pore on first post-abdominal segment.
Range: Middle Cenomanian to Turonian? (O'Dogherty, 1994), and Middle Coniacian? to Lower Maastrichtian (Hollis and Kimura, 2001).

Genus ***Amphipyndax*** Foreman 1966

Amphipyndax tylotus Foreman 1978
(Plate 1, fig. 30)
1978 *Amphipyndax tylotus* n. sp. – Foreman, p. 745, pl. 4, figs. 1–2.
1981 *Amphipyndax tylotus* Foreman – Nakaseko and Nishimura, p. 145, pl. 12, figs. 11a–11b; pl. 17, fig. 13.

1982 *Amphipyndax tylotus* Foreman – Empson-Morin, p. 512, pl. 3, figs. 1–7.
1985 *Amphipyndax tylotus* Foreman – Sanfilippo and Riedel, p. 598, figs. 7.2a–7.2b.
1987 *Amphipyndax tylotus* Foreman – Yamasaki, pl. 1, fig. 3.
1997 *Amphipyndax tylotus* Foreman – Hashimoto and Ishida, pl. 3, fig. 8.
1998 *Amphipyndax tylotus* Foreman – Ishida and Hashimoto, pl. 2, fig. 3.
2015 A*mphipyndax tylotus* Foreman – Hashimoto *et al*., p. 43–44, pl. 1, fig. 9.

Remarks: This species was first described to belong to genus *Amphipyndax* by Foreman (1978), whose sense has been followed by numerous succeeding literatures.
Range: Middle Campanian to Maastrichtian (Sanfilippo and Riedel, 1985; Thurow, 1988; Hashimoto *et al*., 2015), and Middle Campanian to Lower Maastrichtian (Hollis and Kimura, 2001).

Amphipyndax* sp. aff. *A. tylotus (Foreman 1978)
(Plate 1, figs. 31–32)
Remarks: The obtained specimens are similar to *Amphipyndax tylotus* in general form. Nevertheless, it is probably doubtful that these specimens belong to genus *Amphipyndax*, because their cephalis are small and conical, not knob-like.

Family **XITIDAE** Pessagno 1977

Genus ***Xitus*** Pessagno 1977

Xitus spicularius (Aliev 1965)
(Plate 1, fig. 27)
1965 *Dictyomitra spicularia* n. sp. – Aliev, p. 39, pl. 6, fig. 9; pl. 14, fig. 4.
1977 *Xitus antelopensis* n. sp. – Pessagno, p. 55, pl. 9, figs. 10, 20, 25; pl. 12, fig. 16.
1977 *Xitus plenus* n. sp. – Pessagno, p. 55, pl. 9, figs. 15, 21, 26; pl. 12, fig. 15.
1977 *Xitus spicularius* (Aliev) – Pessagno, p. 56, pl. 9, fig. 7; pl. 10, fig. 5.
1986 *Xitus*? sp. B – Iwata and Tajika, p. 408, pl. 3, fig. 3.
1988 *Xitus spicularius* (Aliev) – Thurow, p. 408, pl. 3, fig. 19; pl. 7, fig. 1.
1994 *Xitus spicularius* (Aliev) – O'Dogherty, p. 127–129, pl. 3, fig. 19; pl. 7, fig. 1.
2007 *Xitus spicularius* (Aliev) – Musavu-Moussavou *et al*., p. 275–276, pl. 4, figs. 17–18.
2008 *Xitus spicularius* (Aliev) – Bandini *et al*., p. 408, pl. 3, fig. 24.
2012 *Xitus spicularius* (Aliev) – Asis and Jasin, pl. 1, fig. 15.

Range: Berriasian to Cenomanian (Thurow, 1988), and Middle Coniacian to Middle Campanian (Hollis and Kimura, 2001).

Genus ***Torculum*** O'Dogherty 1994

Torculum* sp. aff. *T. bastetani O'Dogherty 1994
(Plate 3, fig. 12)
2004 *Stichomitra communis* Squinabol – Bąk, figs. 4.12–4.13.

Description: Test is multi-segmented and large conical, having seven post-abdominal segments with distinct strictures. Cephalis is conical and smooth without apical horn. Thorax and abdomen are trapezoidal and sparsely perforated. Post-abdominal segments consist of circular to polygonal pore frames, showing somewhat spongy meshwork. First and second post-abdominal segments are externally characterized by a ring of relatively large tubercles. Remaining post-abdominal segments constantly increase in width as added.
Remarks: *Torculum bastetani* proposed by O'Dogherty (1994) is more elongate conical to cylindrical in outline and covered by somewhat spongy meshwork. *Stichomitra communis* is similar to the examined specimen in having circular to polygonal pore frames and relatively deep strictures, but distinguished by lacking of large tubercles.

Family **PSEUDODICTYOMITRIDAE** Pessagno 1977

Genus ***Pseudodictyomitra*** Pessagno 1977

Pseudodictyomitra tiara (Holmes 1900)
(Plate 3, figs. 10, 27)
1900 *Dictyomitra tiara* n. sp. – Holmes, p. 701, pl. 38, fig. 4.
1977 *Pseudodictyomitra* sp. B – Pessagno, p. 52, pl. 9, fig. 3.
1982 *Pseudodictyomitra nakasekoi* n. sp. – Taketani, p. 60–61, pl. 12, figs. 4–6.
1982 *Pseudodictyomitra nakasekoi* Taketani – Mizutani *et al*., p. 70, pl. 4, figs. 8–9.
1989 *Pseudodictyomitra nakasekoi* Taketani – Tumanda, p. 39, pl. 9, fig. 3.
1992 *Pseudodictyomitra nakasekoi* Taketani – Okamura, pl. 25, fig. 3; pl. 27, figs. 2–3.
1994 *Pseudodictyomitra tiara* (Holmes) – O'Dogherty, p. 109–110, pl. 8, figs. 9–11.
1998 *Pseudodictyomitra tiara* (Holmes) – Salvini and Marcucci Passerini, fig. 6n.
2006 *Pseudodictyomitra nakasekoi* Taketani – Bragina and Bragin, pl. II, fig. 8.
2006 *Pseudodictyomitra nakasekoi* Taketani – Denyer and Baumgartner, fig. 7T.
2007 *Pseudodictyomitra tiara* (Holmes) – Musavu-Moussavou *et al*., p. 109–110, pl. 3, fig. 274.

Range: Middle Cenomanian to Lower Coniacian (Taketani, 1982), Cenomanian to Turonian (Thurow, 1988), and Lower to Upper Cenomanian (O'Dogherty, 1994).

Family **EUCYRTIDIIDAE** Ehrenberg 1847

Genus ***Pseudoeucyrtis*** Pessagno 1977

Pseudoeucyrtis* sp. cf. *P. spinosa (Squinabol 1903)
(Plate 3, fig. 28)
Remarks: Test of this specimen consists of a large spherical portion (post-abdominal segments) with a long robust apical horn and a long terminal cylindrical tube, main part of which is broken. On the basis of these external features, it probably belongs to *Pseudoeucyrtis spinosa*, but slightly different by lacking spines on the spherical portion.

Genus ***Stichomitra*** Cayeux 1897

Stichomitra communis Squinabol 1903
(Plate 3, fig. 29)
1903 *Stichomitra communis* n. sp. – Squinabol, p. 141, pl. 8, fig. 40.
1981 *Stichomitra communis* Squinabol – Nakaseko and Nishimura, p. 162, pl. 11, fig. 11; pl. 16, fig. 14.
1982 *Stichomitra communis* Squinabol – Taketani, p. 54–55, pl. 3, fig. 9; pl. 11, fig. 5.
1989 *Stichomitra communis* Squinabol – Tumanda, p. 40, pl. 7, fig. 7.
1992 *Stichomitra communis* Squinabol – Okamura, pl. 37, fig. 28.
1994 *Stichomitra communis* Squinabol – O'Dogherty, p. 144–145, pl. 17, figs. 6–16.
1997 *Stichomitra communis* Squinabol – Hashimoto and Ishida, pl. 1, fig. 3.
1997 *Stichomitra communis* Squinabol – Sýkora *et al*., pl. V, fig. 7.
1998 *Stichomitra communis* Squinabol – Salvini and Marcucci Passerini, fig. 8j.
1998 *Stichomitra communis* Squinabol – Erbacher, pl. 1, fig. 12.
2001 *Stichomitra communis* Squinabol – Bragin *et al*., figs. 6.15–6.17.
2006 *Stichomitra communis* Squinabol – Musavu-Moussavou and Danelian, p. 155, pl. 2, fig. 15.
2007 *Stichomitra communis* Squinabol – Musavu-Moussavou *et al*, p. 271–272, pl. 4, figs. 7–8.
2012 *Stichomitra communis* Squinabol – Asin and Jasin, pl. 2, fig. 2.
2015 *Stichomitra compsa* Foreman – Hashimoto *et al*., p. 47, pl. 1, fig. 13.
Range: Lower Cenomanian? to Lower Coniacian (Taketani, 1982), and Lower Aptian to Lower Turonian? (O'Dogherty, 1994).

Stichomitra manifesta Foreman 1978
(Plate 1, fig. 13; Plate 2, fig. 25; Plate 3, fig. 31)
1972 *Diacanthocapsa* sp. B – Petrushevskaya and Kozlova, p. 536, pl. 7, fig. 5.
1978 *Stichomitra manifesta* n. sp. – Foreman, p. 748, pl. 5, fig. 4.
1982 *Stichomitra manifesta* Foreman – Taketani, p. 55–56, pl. 3, figs. 8a–8b; pl. 11, figs. 7–8.
1992 *Stichomitra manifesta* Foreman – Iwata *et al*., pl. 3, fig. 9.
1997 *Stichomitra manifesta* Foreman – Hashimoto and Ishida, pl. 3, fig. 2.
1998 *Stichomitra manifesta* Foreman – Ishida and Hashimoto, pl. 2, fig. 7.
2008 *Lithocampe manifesta* (Foreman) – Bandini *et al*., pl. 3, fig. 16; pl. 4, fig. 6.
2012 *Lithocampe manifesta* (Foreman) – Asis and Jasin, pl. 2, fig. 11.
Remarks: According to Foreman (1978), *Stichomitra manifesta* is distinguished from other species of *Stichomitra* by having a large hemispherical thorax greater in length than the succeeding segments, and in the usual case, test is composed of four or five segments, but rarely of seven. The examined specimens possess four segments, except for the specimen illustrated in plate 3, fig. 31 which has seven segment.
Range: Coniacian to Lower Campanian? (Taketani, 1982), and Middle Coniacian? to Lower Maastrichtian (Hollis and Kimura, 2001).

Stichomitra asymbatos Foreman 1968
(Plate 2, fig. 27; Plate 3, fig. 32)
1968 *Stichomitra asymbatos* n. sp. – Foreman, p. 73–75, pl. 8, figs. 10a–10c.
1972 *Stichocapsa asymbatos* (Foreman) – Petrushevskaya and Kozlova, p. 546, pl. 8, figs. 1–3.
1974 *Stichomitra asymbatos* Foreman group – Riedel and Sanfilippo, p. 780, pl. 10, figs. 1–7.
1978 *Stichomitra asymbatos* Foreman group – Foreman, p. 748, pl. 4, fig. 15.
1982 *Stichomitra asymbatos* Foreman – Taketani, p. 54, pl. 4, fig. 13; pl. 11, figs. 3–4.
1982 *Stichomitra asymbatos* Foreman – Yamauchi, pl. 5, fig. 8.
1987 *Stichomitra asymbatos* Foreman – Yamasaki, pl. 1, fig. 15.
1992 *Stichomitra asymbatos* Foreman – Iwata *et al*., pl. 5, fig. 9.
1997 *Stichomitra asymbatos* Foreman – Hashimoto and Ishida, pl. 3, fig. 17.
1998 *Stichomitra asymbatos* Foreman – Ishida and Hashimoto, pl. 2, fig. 4.

Stichomitra* sp. aff. *S. asymbatos Foreman 1968
(Plate 2, fig. 14)
Remarks: This specimen is probably different from *Stichomitra asymbatos* by having a more inflated test with five segments.

Stichomitra* sp. cf. *S. conicus (Nakaseko and Nishimura 1981)
(Plate 2, fig. 26)
Remarks: This specimen resembles to *Stichomitra* conicus in having a test which is proximally conical and distally subcylindrical shape, but slightly differs by having transverse rows of pores which are smaller in size.

Acknowledgements

This preliminary report is based on results of the study "Geology of the Toba District" which has been conducted by the Geological Survey of Japan, AIST. We acknowledge our reviewer, Dr. C. Kurimoto for his constructive comments on the manuscript. Dr. T. Uchino (GSJ) is also thanked for his advice to improve the manuscript.

References

Aliev, K. S., (1965) *Radiolyarii nizhnemelovykh otlozhenii Severo-Vostochnogo Azerbaidzhana i ikh stratigraficheskoe znachenie*. Izdatel'stvo Akademii Nauk, Azerbaidzhanskoi SSR, Baku, 124p.

Asis, J. and Jasin, B. (2012) Aptian to Turonian radiolaria from the Darvel Bay Ophiolite Complex, Kunak, Sabah. *Bulletin of Geological Society of Malaysia*, **58**, 89–96.

Bąk, M. (1996) Cretaceous Radiolaria from Niedzica succession of the Pieniny klippen belt in Polish Carpathians. *Acta Palaeontologica Polonica*, **41**, 91–110.

Bąk, M. (2004) Radiolarian biostratigraphy of the Upper Cenomanian–Lower Turonian deposits in the Subsilesian Nappe (outer western Carpathians). *Geologica Carpathica*, **55**, 239–250.

Bandini, A. N., Flores, K., Baumgartner, P. O., Jackett, S.-J. and Denyer, P. (2008) Late Cretaceous and Paleogene Radiolaria from the Nicoya Peninsula, Costa Rica: a tectonostratigraphic application. *Stratigraphy*, **5**, 3–21.

Bandini, A. N., Baumgartner, P. O., Flores, K., Dumitrica, P. and Jackett, S.-J. (2011) Early Jurassic to early Late Cretaceous radiolarians from the Santa Rosa accretionary complex (northwestern Costa Rica). *Ofioliti*, **36**, 1–35.

Bragin, N., Bragina, L., Tunoglu, C. and Tekin, U. K. (2001) The Cenomanian (Late Cretaceous) radiolarians from the Tomalar Formation, central Pontides, northern Turkey. *Geologica Carpathica*, **52**, 349–360.

Bragina, L. and Bragin, N. (2006) Stratigraphy and radiolarians of Upper Cretaceous sedimentary cover of the Arakapas ophiolite massif (Cyprus). *Stratigraphy and Geological Correlation*, **14**, 507–523.

Bragina, L. and Bragin, N. (2015) New data on Albian–Coniacian radiolarians from the Kelevudag Section (Northeastern Azerbaijan). *Stratigraphy and Geological Correlation*, **23**, 45–56.

Bragina, L., Agarkov, Yu. and Bragin, N. (2007) Radiolarians of the Upper Cenomanian and Lower Turonian from deposits of the Ananuri Formation, the Western Caucasus (Lazarevskoe area). *Stratigraphy and Geological Correlation*, **15**, 310–320.

Campbell, A. S. and Clark, B. L. (1944) Radiolaria from Upper Cretaceous of middle California. *Geological Society of America, Special Papers*, no. 57, 61p.

Cayeux, L. (1897) Contribution a l'étude micrographique des terrains sédimentaires. 1. – Etude de quelques depots siliceux secondaires et tertiaires du Basin de Paris et de la Belgique. 2. – Craie du Basin de Paris. *Mémoires de la Societe Geologique du Nord*, **4**, 1–591.

Denyer, P. and Baumgartner, P. O. (2006) Emplacement of Jurassic–Lower Cretaceous radiolarites of the Nicoya Complex (Costa Rica). *Geologica Acta*, **4**, 203–218.

De Wever, P., Dumitrica, P., Caulet, J. P., Nigrini, C. and Caridroit, M. (1988) Radiolaires Sénoniens la nappe de Samail (Oman). *Revue de Micropaléontologie*, **31**, 166–179.

De Wever, P., Dumitrica, P., Caulet, J. P., Nigrini, C. and Caridroit, M. (2001) *Radiolarians in the sedimentary record*. Gordon and Breach Science Publishers, 533p.

Djerić, N., Gerzina, N., Gajić, V. and Vasić, N. (2009) Early Senonian radiolarian microfauna and biostratigraphy from the western Vardar zone (western Serbia). *Geologica Carpathica*, **60**, 35–41.

Dumitrică, P. (1970) Cyrtocephalic and cyrtothracic Nassellaria in some Mesozoic deposits of Romania. *Revue Roumaine de Géologie, Géophysique et Géographie (série de Géolgie)*, **14**, 45–124.

Dumitrica, P. (1973) Cretaceous and Quaternary Radiolaria in deep sea sediments from the Northwest Atlantic Ocean and Mediterranean Sea. *In* Ryan, W. B. F., Hsü, K. J. *et al*., eds., *Initial reports of the Deep Sea Drilling Project*, **13**, US Government Printing Office, Washington D. C., 829–901.

Dumitrica, P. (1997) On the status of the Lower Cretaceous radiolarian species *Alievium helenae* Schaaf and of the other related species. *Revue de Micropaléontologie*, **40**, 211–226.

Ehrenberg, C. G. (1847) Über die mikroskopischen kieselschaligen Polycystinen als mächtige Gebirgsmasse von Barbados und über das Verhaltniss der aus mehr als 300 neuen Arten bestehenden ganz eigenthumlichen Formengruppe jener Felsmasse zu den jetzt lebenden Thieren und zur Kreidebildung Eine neue Anregung zur Erforschung des Erdlebens. *Bericht der königlichen preussischen Akademie der Wissenschaften zu Berlin*, Abhandlungen, Jahre 1847, 40–60.

Ehrenberg, C. G. (1875) Fortsetzung der mikrogeologischen Studien als Gesammt-Ubersichtder der mikroskopischen Palaontologie gleichartig analysirter Gebirgsarten der Erde, mit specieller Rucksicht auf den Polycystinen-Mergel von Barbados. *Bericht der königlichen preussischen Akademie Wissenschaften zu Berlin*, Abhandlungen, Jahre 1875, 1–225.

Empson-Morin, K. (1981) Campanian Radiolaria from DSDP Site 313, Mid-Pacific Mountains. *Micropaleontology*, **27**, 1–13.

Empson-Morin, K. (1982) Reexamination of the Late Cretaceous radiolarian genus *Amphipyndax* Foreman.

Journal of Paleontology, **56**, 507–519.

Empson-Morin, K. (1984) Depth and latitude distribution of radiolaria in Campanian (Late Cretaceous) tropical and subtropical oceans. *Micropaleontology*, **30**, 87–115.

Erbacher, J. (1998) Mid-Cretaceous radiolarians from the eastern equatorial Atlantic and their paleoceanography. *In* Mascle, J., Lohmann, G. P. and Moullade, M. eds, *Proceedings of the Ocean Drilling Program*, *Scientific Results*, **159**, 363–373.

Foreman, H. (1966) Two Cretaceous radiolarian genera. *Micropaleontology*, **12**, 355–359.

Foreman, H. (1968) *Upper Maastrichtian Radiolaria of California*. The Paleontological Association, Special Papers in Paleontology, London, no. 3, 82p.

Foreman, H. (1971) Cretaceous Radiolaria, Leg 7, DSDP. *In* Winterer, E. L., Riedel, W. R. *et al*., eds, *Initial reports of the Deep Sea Drilling Project*, **7**, US Government Printing Office, Washington D. C., 1673–1693.

Foreman, H. (1973a) Radiolaria of Leg. 10 with systematics and ranges for the families Amphipyndacidae, Artostrobiidae, and Theoperidae. *In* Worzel, J. L., Bryant, W. *et al*., eds, *Initial reports of the Deep Sea Drilling Project*, **10**, US Government Printing Office, Washington D. C., 407–474.

Foreman, H. (1973b) Radiolaria from DSDP Leg. 20. *In* Heezen, B. C., MacGregor, I. D. *et al*., eds, *Initial reports of the Deep Sea Drilling Project*, **20**, US Government Printing Office, Washington D. C., 249–305.

Foreman, H. (1975) Radiolaria from the North Pacific, Deep Sea Drilling Project, Leg 32. *In* Larson, R. L., Moberly, R. *et al*., eds, *Initial reports of the Deep Sea Drilling Project*, **32**, US Government Printing Office, Washington D. C., 579–676.

Foreman, H. (1978) Mesozoic Radiolaria in the Atlantic Ocean off the northwest coast of Africa, Deep Sea Drilling Project, Leg 41. *In* Lancelot, Y., Seibold, E., *et al*., eds., *Initial reports of the Deep Sea Drilling Project*, **41**, US Government Printing Office, Washington D. C., 739–761.

Haeckel, E. (1862) *Die Radiolarien (Rhizopoda Radiaria)*. Eine Monographie, Reimer, Berlin, 572p.

Haeckel, E. (1881) Entwurf eines Radiolarien-ystems auf Grund von Studien der Challenger-Radiolarien. *Jenaische Zeitschrift für Naturwussebschaft*, **15**, 418–472.

Haeckel, E. (1887) Report on the Radiolaria collected by H.M.S. Challenger during the years 1873–1876. *Report on the Scientific Results of the Voyage of the H.M.S. Challenger*, *Zoology*, **18**, 1803p.

Hashimoto, H. and Ishida, K. (1997) Correlation of selected radiolarian assemblages of the Upper Cretaceous Izumi and Sotoizumi groups and Shimanto Supergroup, in Shikoku. *News of Osaka Micropaleontologists, special volume*, no. 10, 245–257. (in Japanese with English abstract)

Hashimoto, H., Ishida, K., Yamasaki, T., Tsujino, Y. and Kozai, T. (2015) Revised radiolarian zonation of the Upper Cretaceous Izumi inter-arc basin (SW Japan). *Revue de micropaléontology*, **58**, 29–50.

Hollis, C. J. (1997) Cretaceous–Paleogene Radiolaria from eastern Marlborough, New Zealand. *Institute of Geological and Nuclear Sciences Monograph*, **17**, 152p.

Hollis, C. J. and Kimura, K. (2001) A unified radiolarian zonation for the Late Cretaceous and Paleogene of Japan. *Micropaleontology*, **47**, 235–255.

Holmes, W. M. (1900) On Radiolaria from the Upper Chalk at Coulsdon (Surrey). *Quarterly Journal of Geological Society of Landon*, **56**, 694–704.

Ishida, K. and Hashimoto, H. (1998) Upper Cretaceous radiolarian biostratigraphy in selected chert–clastic sequences of the North Shimanto terrane, East Shikoku. *News of Osaka Micropaleontologists, special volume*, no. 11, 211–225. (in Japanese with English abstract)

Iwata, K. and Tajika, J. (1986) Late Cretaceous radiolarians of the Yubetsu Group, Tokoro belt, northeast Hokkaido. *Journal of Faculty of Science, Hokkaido Univ., series IV*, **21**, 619–644.

Iwata, K. and Tajika, J. (1989) Jurassic and Cretaceous radiolarians from the pre-Tertiary system in the Hidaka belt, Maruseppu region, northeast Hokkaido. *Journal of Faculty of Science, Hokkaido Univ., series IV*, **22**, 453–466.

Iwata, K., Watanabe, Y. and Tajika, J. (1992) Radiolarian biostratigraphic study of the Hakobuchi Group in the Nakatonbetsu area, north Hokkaido. *Report of Geological Survey of Hokkaido*, no. 63, 1–21.

Kling, S. A. (1970) Radiolaria: Leg 6 of the Deep Sea Drilling Project. *In* Heezen, E. C. *et al*., eds., *Initial Reports of Deep Sea Drilling Project*, **6**, US Government Printing Office, Washington D. C., 1069–1117.

Kopaevich, L. F., Beniamovskii, V. N. and Bragina, L. G. (2015) Upper Albian–Turonian foraminifers and radiolarians from the Kelevudag Section, northwestern Azerbaijan. *Stratigraphy and Geological Correlation*, **23**, 580–599.

Kozur, H. and Mostler, H. (1978) Beiträge zur Erforschung der mesozoischen Radiolarien Teil II: Oberfamilie Trematodiscacea Haeckel 1862 emend. und Beschreibung ihrer triassischen Vertreter. *Geologisch-Paläontologische Mitteilungen Innsbruck*, **8**, 123–182.

Lipman, R. Kh. (1969) Novyy rod I novyye vidy eotsenovykh radiolyariy SSSR. *Vses.Nauchno-Issled. Geol. Inst (VSEGEI), Trudy, n.s*., **130**, 181–200.

Marcucci Passerini, M. and Gardin, S. (1992) The Fosso Cupo Formation (northern Latium, Italy): redefinition and new age data from radiolarian and calcareous nannofossil biostratigraphy. *Cretaceous Research*, **13**, 549–563.

Matsuyama, H., Kumon, F. and Nakajo, K. (1982) Cretaceous radiolarian fossils from he Hidakagawa Group in the Shimanto belt, Kii Peninsula, Southwest Japan. *News of Osaka Micropaleontologists, special volume*, no. 5, 371–382. (in Japanese with English abstract)

Mizugaki, K. (1987) Mesozoic radiolarians in conglomerate of the Shimanto Supergroup in the Sazare-ura area, eastern Kii Peninsula, central Japan. *Bulletin of Nagoya Univ. Museum*, no. 3, 19–69.

Mizutani, S., Nishiyama, H. and Ito, T. (1982) Radiolarian biostratigraphic study of the Shimanto Group in the Nanto–Nansei area, Mie Prefecture, Kii Peninsula, central Japan. *Journal of Earth Sciences, Nagoya Univ*., **30**, 31–107. (in Japanese with English abstract)

Moez, B. F., Mohamed, S., Taher, Z., Mohsen, L., Ahlem, A. and Mohamed, Y. (2012) Radiolarian age constraints of Mid-Cretaceous black shales in northern Tunisia. *In* Dar, I. A. ed., *Earth Sciences*, InTech Europe, Rijieka, 599 – 618.

Müller, J. (1858) Einige neue bei St. Tropez am Mittelmeer beobachtete Polycystinen und Acanthometren. *Königliche Preussichen Akademie der Wissenschaften zu Berlin, Monatsberichte*, Jahrgang 1858, 154–155.

Musavu-Moussavou, B. and Danelian, T. (2006) The radiolarian biotic response to Oceanic Anoxic Event 2 in the southern part of the Northern proto-Atlantic (Demerara Rise, ODP Leg 207). *Revue de Micropaléontologie*, **49**, 141–163.

Musavu-Moussavou, B., Danelian, T., Baudin, F., Coccioni, R. and Fröhlich, F. (2007) The radiolarian biotic response during OAE2. A high-resolution study across the Bonarelli level at Bottaccione (Gubbio, Italy). *Revue de Micropaléontologie*, **50**, 253–287.

Nakaseko, K. and Nishimura, A. (1981) Upper Jurassic and Cretaceous radiolaria from the Shimanto Group, in Southwest Japan. *Science Report*, *Collage of General Education*, *Osaka Univ*., **30**, 133–203.

Nakaseko, K., Nishimura, A. and Sugano, K. (1979) Cretaceous radiolaria in the Shimanto belt, Japan. *News of Osaka Micropaleontologists, Special Volume*, no. 2, 1–49. (in Japanese)

Noda, A. and Kurihara, T. (2016) Late Cretaceous radiolarian assemblages obtained from the Izumi Group in the Kan-onji district, eastern Shikoku, Japan. *Bulletin of Geological Survey of Japan*, **67**, 119–131. (in Japanese with English abstract)

Obase, M. (1988) The Shimanto superbelt. *Regional Geology Japan Part 5 Chubu II*, Kyoritsu Shuppan, Tokyo, 73–75. (in Japanese)

O'Dogherty, L. (1994) Biochronology and paleontology of Mid-Cretaceous radiolarians from northern Apennines (Italy) and Betic Cordillera (Spain). *Mémoires de Géologie (Lausanne)*, no. 21, Lausanne, Switzerland, 1–415.

Okamura, M. (1992) Cretaceous radiolaria from Shikoku, Japan (Part 1). *Mem. Faculty of Science, Kochi Univ., Series E, Geology*, **13**, 21–164.

Ohta, T., Ohtake, N., Morita, N., Kamimura, T., Takahashi, N., Koumi, S. and Saka, Y. (2013) Radiolarian biostratigraphy of the Matoya Complex in the Northern Shimanto Belt, eastern Kii Peninsula, Southwest Japan. *Academic studies and scientific research. Natural science, Waseda Univ*., **61**, 9–29. (in Japanese with English abstract)

Pessagno, E. A., Jr. (1962) The Upper Cretaceous stratigraphy and micropaleontology of south-central Puerto Rico. *Micropaleontology*, **8**, 349–368.

Pessagno, E. A., Jr. (1963) Upper Cretaceous radiolaria from Puerto Rico. *Micropaleontology*, **9**, 197–214.

Pessagno, E. A., Jr. (1972) Cretaceous radiolaria. *Bulletins of American Paleontology*, **61**, 269–328.

Pessagno, E. A., Jr. (1973) Upper Cretaceous Spumellariina from the Great Valley Sequence, California Coast Ranges. *Bulletins of American Paleontology*, **63**, 49–102.

Pessagno, E. A., Jr. (1975) Upper Cretaceous Radiolaria from DSDP Site 275. *In* Kennett, J. P., Houtz, R. E. *et al*., eds., *Initial Reports of Deep Sea Drilling Project*, **29**, US Government Printing Office, Washington D. C., 1011–1029.

Pessagno, E. A., Jr. (1976) Radiolarian zonation and stratigraphy of the Upper Cretaceous portion of the Great Valley Sequence, California Coast Ranges. *Micropaleontology Special Publication*, no. 2, 1–95.

Pessagno, E. A., Jr. (1977) Lower Cretaceous radiolarian biostratigraphy of the Great Valley Sequence and Franciscan Complex, California Coast Ranges. *Cushman Foundation for Foraminiferal Research, Special Publication*, no. 15, 5–87.

Pessagno, E. A., Jr., Six, W. and Yang, Q. (1989) Xiphostylidae Haeckel and Parvivaccidae, n. fam., (Radiolaria) from the North American Jurassic. *Micropaleontology*, **35**, 193–255.

Petrushevskaya, M. G. and Kozlova, G. E. (1972) Radiolaria: Leg 14, Deep Sea Drilling Project. *In* Hayes, D. E., Pimm, A. C. *et al*., eds, *Initial reports of the Deep Sea Drilling Project*, **14**, US Government Printing Office, Washington D. C., 495–648.

Popova-Goll, I., Vishnevskaya, V. and Baumgartner, P. O. (2005) Upper Cretaceous (Santonian–Campanian) radiolarians from Voronesh anticline, southwestern Russia. *Micropaleontology*, **51**, 1–37.

Riedel, W. R. (1967) Some new families of Radiolaria. *Geological Society of London, Proceedings*, no. 1640, 148–149.

Riedel, W. R. (1971) Systematic classification of Polycystine Radiolaria. *In* Funnell, B. M. and Riedel, W. R., eds., *The micropaleontology of the oceans*, Cambridge University Press, Cambridge, 649–661.

Riedel, W. R. and Sanfilippo, A. (1974) Radiolaria from the southwestern Indian Ocean, DSDP Leg 26. *In* Davies, T. A., Luyendyk, B. P. *et al*., eds., *Initial reports of the Deep Sea Drilling Project*, **26**, US

Government Printing Office, Washington D. C., 503–575.
Salvini, G. and Marcucci Passerini, M. (1998) The radiolarian assemblages of the Bonarelli Horizon in the Umbria–Marche Apennines and southern Alps, Italy. *Cretaceous Research*, **19**, 777–804.
Sanfilippo, A. and Riedel, W. (1985) Cretaceous radiolaria. *In* Bolli, H. M., Saunders, J. B. and Perch-Nielsen, K. eds., *Plankton stratigraphy*, 573–630, Cambridge Univ. Press.
Smrečková, M. (2011) Lower Turonian radiolarians from the Červená skala section (Pieniny Klippen belt, western Carpathians). *Mineralia Slovaca*, **43**, 31–38.
Squinabol, S. (1903) Le Radiolarie dei Noduli selciosi nella Scaglia degli Euganei. *Rivista Italiana di Paleontologia*, **9**, 105–451.
Squinabol, S. (1904) Radiolarie cretacee degli Euganei. *Atti e memorie dell'Accademia di scienze, lettere ed arti, Padova, new series*, **20**, 171–244.
Sýkora, M., Ožvoldová, L. and Boorova, D. (1997) Turonian silicified sediments in the Czorsztyn Succession of the Pieniny Klippen belt (western Carpathians, Slovakia). *Geologica Carpathica*, **48**, 243–261.
Taketani, Y. (1982) Cretaceous radiolarian biostratigraphy of the Urakawa and Obira areas, Hokkaido. *Tohoku Univ*., *Science Reports*, *2nd series (Geology)*, **52**, 1–76.
Tan, S. H. (1927) Over de samenstelling en het onstaan van krijt- en mergel-gesteenten van de Molukken. *In* Brouwer, H. A. ed., *Jaarboek van het mijnwezen in Nederlandsch Oost-Indie, verhandelingen 3rd gedeelte*, **55**, 5–165.
Tanabe, H. and Kano, K. (1994) Upper Cretaceous strata in the Shimanto belt of the Miyama area, eastern Kii Peninsula, Southwest Japan. *Geoscience Reports, Shizuoka Univ*., **21**, 1–10. (in Japanese with English abstract)
Thurow, J. (1988) Cretaceous radiolarians of the North Atlantic Ocean: ODP Leg 103 (Sites 638, 640, and 641) and DSDP Leg 93 (Site 603) and 47B (Site 398). *Proceedings of the Ocean Drilling Program*, *Scientific results*, **103**, 379–418.
Tumanda, F. P. (1989) Cretaceous radiolarian biostratigraphy in the Esashi mountain area, northern Hokkaido, Japan. *Science Reports of Institute of Geoscience, Uni. Tsukuba*, *sec. B*., **10**, 1–44.
White, M. P. (1928) Some index Foraminifera of the Tampico Embayment area of Mexico (Part II). *Journal of Paleontology*, **2**, 280–317.
Yamagiwa, N. (1957) Stratigraphy and geological structures of the eastern area of Shima Peninsula. *Journal of Geological Society of Japan*, **63**, 263–273.
Yamanashi, T. and Kashiwagi, K. (2010) Radiolarian ages and geological structures of the Shimanto belt in the Kisei–Ouchiyama area of the eastern Kii Peninsula, Southwest Japan. *Memoir of Fukui Prefectural Dinosaur Museum*, **9**, 9–40. (in Japanese with English abstract)
Yamasaki, T. (1987) Radiolarian assemblages of the Izumi Group in Shikoku and western Awaji Island, Southwest Japan. *Journal of Geological Society of Japan*, **93**, p. 403–417. (in Japanese with English abstract)
Yamasaki, T. and Sakamoto, S. (1997) Radiolarian fossils of the Cretaceous Shimanto Group in the Izumi area, Hiromi Town, Ehime Prefecture. *Bulletin of Faculty of Education, Ehime Univ., Natural Science*, **18**, 9–17. (in Japanese with English abstract)
Yamasaki, T. and Tsujii, O. (1994) Radiolarians from the northern margin of the Izumi Group in Shikoku, Part II. *Memoirs of Faculty of Education*, *Ehime Univ., Natural Science*, **15**, 41–53. (in Japanese with English abstract)
Yamauchi, M. (1982) Upper Cretaceous radiolarians from the Northern Shimanto belt along the course of Shimanto River, Kochi Prefecture, Japan. *News of Osaka Micropaleontologists, special volume*, no. 5, 383–397. (in Japanese with English abstract)
Zittel, K. A. (1876) Über einige fossile Radiolarien aus der norddeutschen Kreide. *Zeitschrift der Deutschen Geolgischen Gesellschaft*. **28**, 75–86.

Recieved October 12, 2016
Accepted January 30, 2017

Plate 1 SEM images of Upper Cretaceous radiolarians from the Matoya Group in the Toba District.

TB31-06 (Locality 1, southwest of Anori, Shima City)
1: *Orbiculiforma sacramentoensis* Pessagno
2: *Dactyliosphaera* sp. aff. *D. silviae* Squinabol
3: *Pseudoaulophacus praefloresensis* Pessagno
4: *Archaeospongoprunum hueyi* Pessagno
5: *Patellula planoconvexa* (Pessagno)
6: *Rhopalosyringium magnificum* Campbell and Clark
7: *Cryptamphorella macropora* Dumitrică
8: *Diacanthocapsa* sp. cf. *D. ovoidea* Dumitrică
9,10: *Dictyomitra densicostata* Pessagno
11,12: *Amphipternis stocki* (Campbell and Clark)
13: *Stichomitra manifesta* Foreman

TB31-03 (Locality 2, southwest of Anori, Shima City)
14: *Orbiculiforma* sp. cf. *O. railensis* Pessagno
15: *Pseudoaulophacus* sp. cf. *P. lenticulatus* (White)
16: *Alievium gallowayi* (White)
17,18: *Archaeospongoprunum hueyi* Pessagno
19,20: *Rhopalosyringium magnificum* Campbell and Clark
21: *Cryptamphorella sphaerica* (White)
22: *Cryptamphorella* sp. B sensu Bąk (1996)
23: *Eastonerius* sp. aff. *E. acuminatus* (Dumitrică)
24: *Dictyomitra multicostata* Zittel
25: *Dictyomitra densicostata* Pessagno
26: *Thanarla* sp. aff. *T. veneta* (Squinabol)
27: *Xitus spicularius* (Aliev)
28,29: *Amphipternis stocki* (Campbell and Clark)
30: *Amphipyndax tylotus* Foreman
31,32: *Amphipyndax* sp. aff. *A. tylotus* Foreman

All scale bars are equal to 0.1 mm.

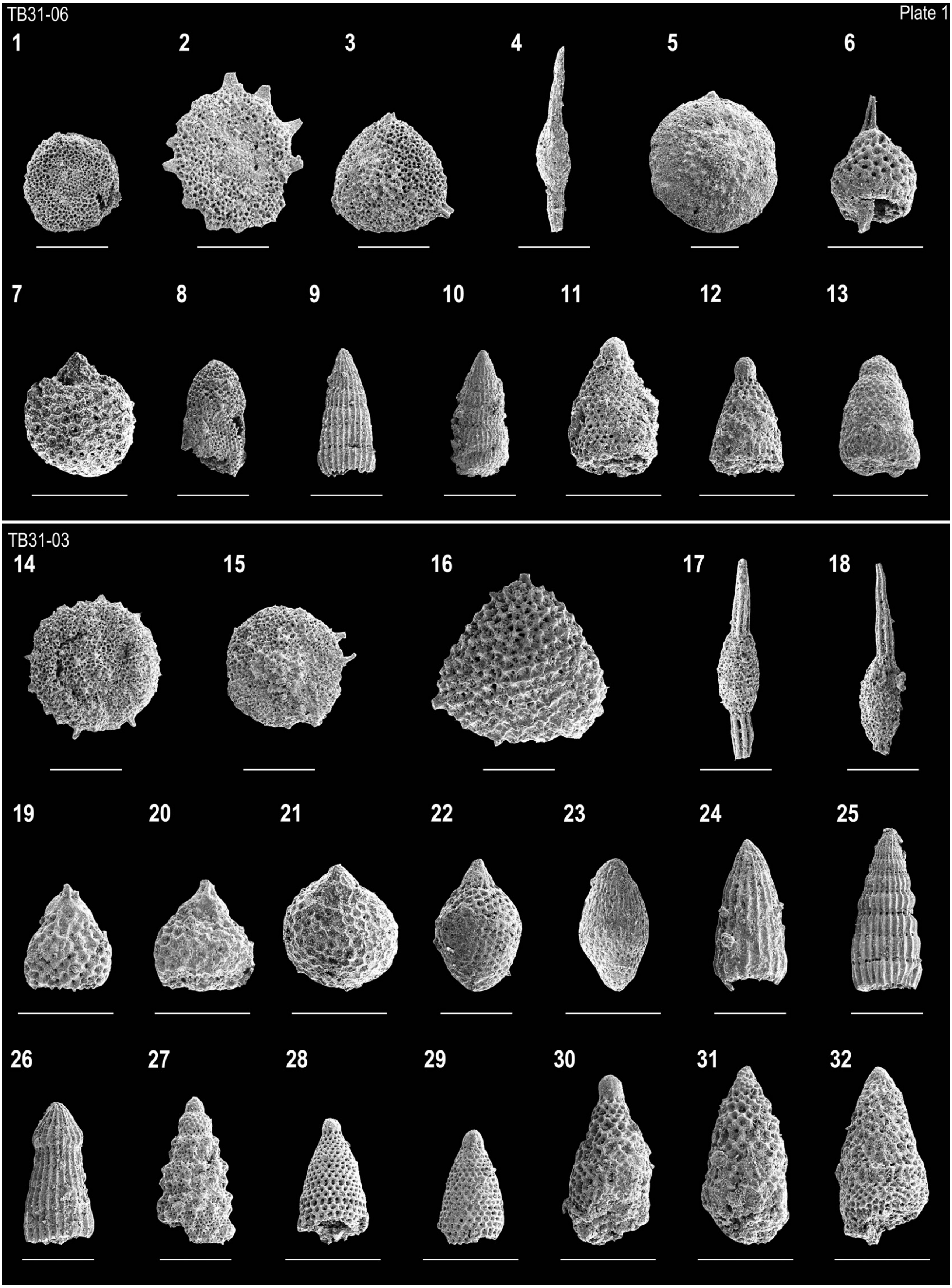
TB31-06
Plate 1
1
2
3
4
5
6
7
8
9
10
11
12
13
TB31-03
14
15
16
17
18
19
20
21
22
23
24
25
26
27
28
29
30
31
32

Plate 2 SEM images of Upper Cretaceous radiolarians from the Matoya Group in the Toba District.

TB20-03 (Locality 3, southwest of Hiyama, Shima City)
1: *Pseudoaulophacus floresensis* Pessagno
2: *Pseudoaulophacus* sp. cf. *P. pargueraensis* Pessagno
3: *Patellula verteroensis* (Pessagno)
4: *Archaeospongoprunum* sp. cf. *A. stocktonensis* Pessagno
5: *Cryptamphorella macropora* Dumitrică
6: *Theocampe salillum* Foreman
7: *Diacanthocapsa ovoidea* Dumitrică
8: *Diacanthocapsa* sp. cf. *D. ancus* (Foreman) sensu Dumitrică (1970)
9: *Dictyomitra koslovae* Foreman
10,11: *Dictyomitra multicostata* Zittel
12,13: *Amphipternis stocki* (Campbell and Clark)
14: *Stichomitra* sp. aff. *S. asymbatos* Foreman

TB20-02 (Locality 4, northeast of Hiyama, Shima City)
15: *Alievium* sp. cf. *A. gallowayi* (White)
16: *Pseudoaulophacus lenticulatus* (White)
17: *Pseudoaulophacus floresensis* Pessagno
18: *Patellula verteroensis* (Pessagno)
19: *Rhopalosyringium magnificum* Campbell and Clark
20: *Cryptamphorella sphaerica* (White)
21: *Theocampe salillum* Foreman
22: *Dictyomitra koslovae* Foreman
23: *Dictyomitra densicostata* Pessagno
24: *Amphipternis stocki* (Campbell and Clark)
25: *Stichomitra manifesta* Foreman
26: *Stichomitra* sp. cf. *S. conicus* (Nakaseko and Nishimura)
27: *Stichomitra asymbatos* Foreman

TB05-12 (Locality 5, Kuzaki, Toba City)
28: *Alievium* sp. cf. *A. gallowayi* (White)
29: *Pseudoaulophacus lenticulatus* (White)
30: *Pseudoaulophacus floresensis* Pessagno
31: *Cryptamphorella wogiga* Empson-Morin
32: *Theocampe urna* (Foreman)
33: *Dictyomitra koslovae* Foreman
34: *Dictyomitra undata* Squinabol
35: *Dictyomitra duodecimcostata* (Squinabol) sensu Foreman (1975)

All scale bars are equal to 0.1 mm.

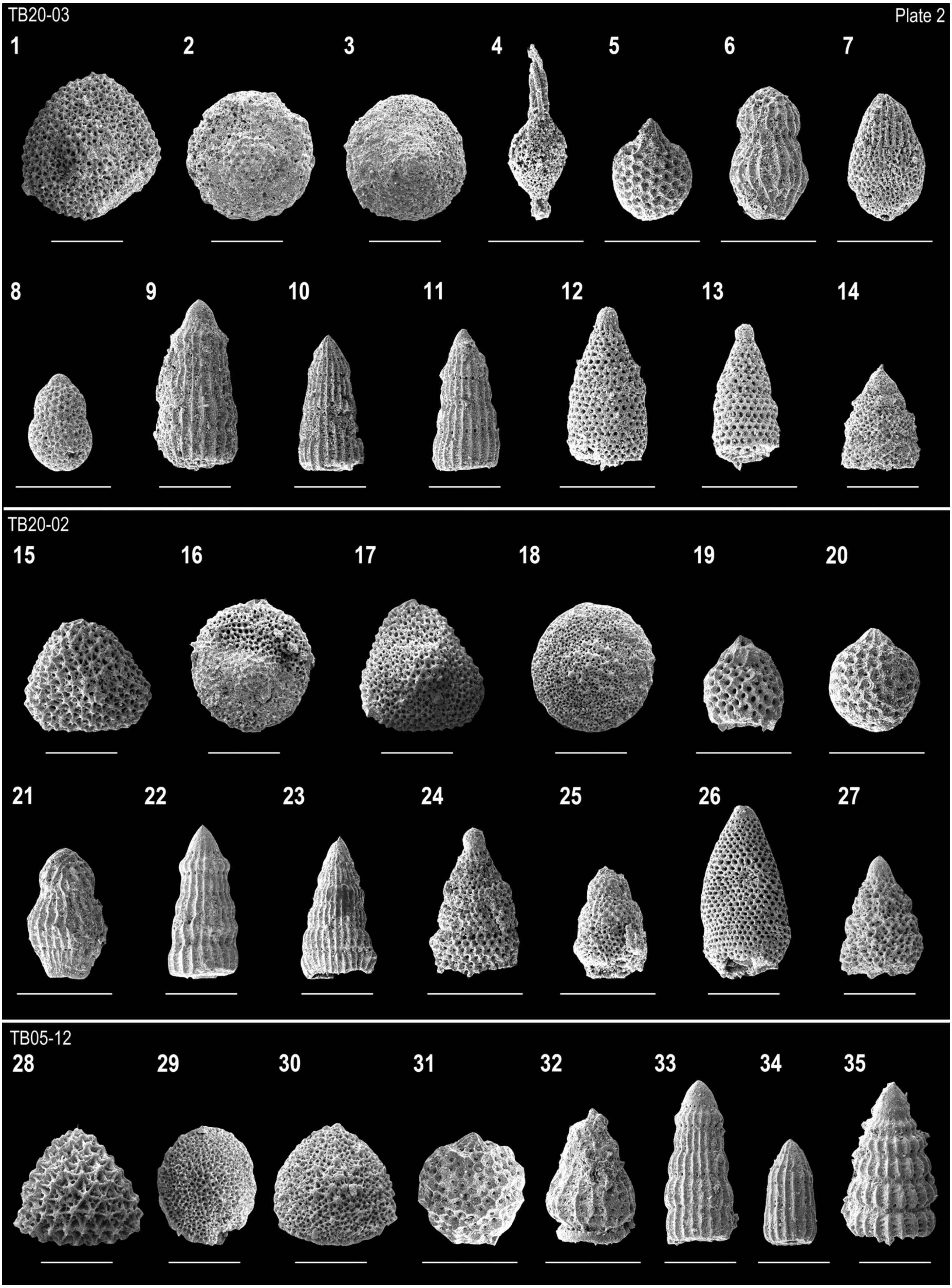

TB20-03
Plate 2
1
2
3
4
5
6
7
8
9
10
11
12
13
14
TB20-02
15
16
17
18
19
20
21
22
23
24
25
26
27
TB05-12
28
29
30
31
32
33
34
35

Plate 3 SEM images of Upper Cretaceous radiolarians from the Matoya Group in the Toba District.

TB01-04 (Locality 6, northwest of Ijika, Toba City)
1: *Archaeocenosphaera*? *mellifera* O'Dogherty
2: *Conocaryomma californiaensis* (Pessagno)
3: *Alievium* sp. cf. *A. praegallowayi* Pessagno
4: *Archaeospongoprunum* sp. aff. *A. andersoni* Pessagno
5: *Patellula verteroensis* (Pessagno)
6: *Cryptamphorella* sp. aff. *C. gilkeyi* (Dumitrica)
7: *Hemicryptocapsa polyhedra* Dumitrică
8: *Dictyomitra formosa* Squinabol
9: *Dictyomitra multicostata* Zittel
10: *Pseudodictyomitra tiara* (Holmes)
11: *Amphipternis stocki* (Campbell and Clark)
12: *Torculum* sp. aff. *T. bastetani* O'Dogherty

TB01-02a (Locality 7, southwest of Ijika, Toba City)
13: *Conocaryomma universa* (Pessagno)
14: *Alievium* sp. cf. *A. praegallowayi* Pessagno
15: *Pseudoaulophacus* sp. cf. *P. praefloresensis* Pessagno
16: *Pseudoaulophacus pargueraensis* Pessagno
17: *Pyramispongia glascockensis* Pessagno
18: *Patellula verteroensis* (Pessagno)
19: *Rhopalosyringium* sp. A sensu Bandini *et al*. (2008)
20: *Theocampe salillum* Foreman
21: *Archaeodictyomitra squinaboli* Pessagno
22: *Dictyomitra* sp. cf. *D. gracilis* (Squinabol)
23: *Dictyomitra formosa* Squinabol
24: *Dictyomitra multicostata* Zittel
25: *Dictyomitra andersoni* (Campbell and Clark)
26: *Dictyomitra* sp. aff. *D. densicostata* Pessagno
27: *Pseudodictyomitra tiara* (Holmes)
28: *Pseudoeucyrtis* sp. cf. *P. spinosa* (Squinabol)
29: *Stichomitra communis* Squinabol
30: *Amphipternis stocki* (Campbell and Clark)
31: *Stichomitra manifesta* Foreman
32: *Stichomitra asymbatos* Foreman

All scale bars are equal to 0.1 mm.

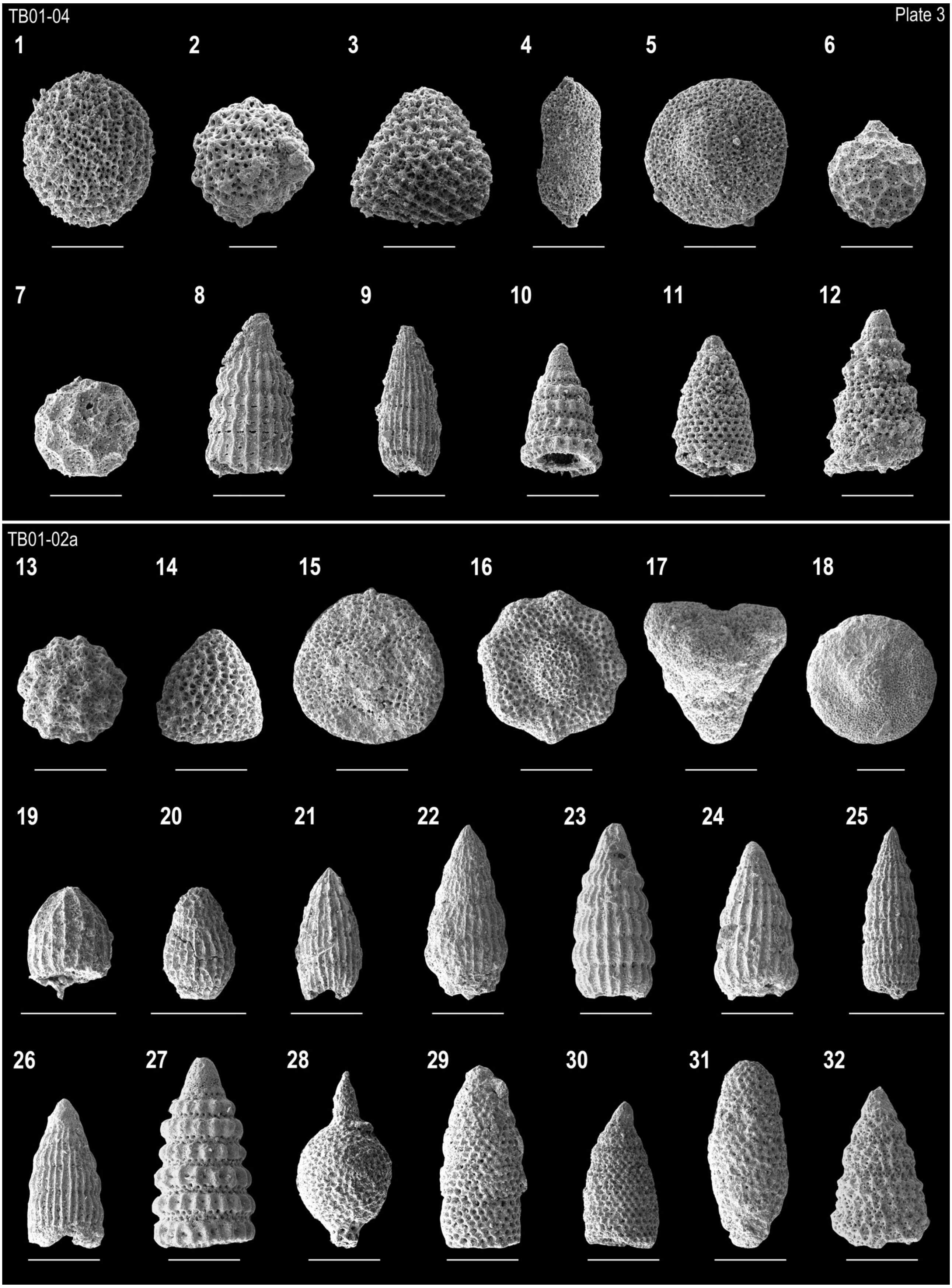
TB01-04
Plate 3
1
2
3
4
5
6
7
8
9
10
11
12
TB01-02a
13
14
15
16
17
18
19
20
21
22
23
24
25
26
27
28
29
30
31
32

三重県鳥羽地域における上部白亜系的矢層群（四万十帯）の放散虫年代：予察報告

中江　訓・栗原敏之

要　旨

紀伊半島東部に位置する鳥羽地域における野外地質調査と放散虫化石に基づく時代決定により，的矢層群の泥岩がコニアシアン期–カンパニアン期を示すことが明らかにされた．この層群は四万十帯（北帯）に属し，古アジア大陸下にクラプレートが沈み込むプレート境界に沿って形成されたものである．放散虫化石を産する51地点のうち7地点の露頭から比較的保存の良い放散虫化石群集が得られ，これらは３つの地質時代（前期コニアシアン期，前期カンパニアン期ないし中期サントニアン期–中期カンパニアン期，中期–後期カンパニアン期）に分類される．このことは，的矢層群がさらに細分できる可能性があることを示している．

難読･重要地名

Anori：安乗，Hiyama：桧山，Ijika：石鏡，Isobe：磯部，Kii：紀伊，Kuzaki：国崎，Matoya：的矢，Matsuo：松尾，Osatsu：相差，Shima：志摩，Shimanto：四万十，Toba：鳥羽，Tsuiji：築地，Ugata：鵜方．

地質調査総合センター研究資料集

地質調査総合センターの最新出版物

5 万分の 1 地質図幅	茂原・母島列島・新潟及び内野・播州赤穂	
20 万分の 1 地質図幅	横須賀（第 2 版）・大分（第 2 版）・松山（第 2 版）	
200 万分の 1 地質編集図	No. 4	日本地質図（第 5 版）
	No. 11	日本の火山（第 3 版）
特殊地質図	No. 12	富士火山地質図（第 2 版）
海洋地質図	No. 87	金華山沖表層堆積図（1:20 万）
	No. 88	見島沖海底地質図（1:20 万）
鉱物資源図	No. 7	南西諸島（1:50 万）
構造図	No. 14	全国主要活断層活動確率地図
火山地質図	No. 18	蔵王火山地質図（1:2.5 万）
	No. 19	九重火山地質図（1:2.5 万）
水文環境図	No. 9	富士山
空中磁気図	No. 46	養老断層地域高分解能空中磁気異常図
	No. 47	富士火山地域高分解能空中磁気異常図
重力図	No. 30	徳島地域重力図（ブーゲー異常）
	No. 31	京都地域重力図（ブーゲー異常）
	S3	甲府地域重力構造図（ブーゲー異常）
海外地球科学図	アジア鉱物資源図（1:500 万）	
	東アジア地域地震火山災害情報図（1:1000 万）	
海陸シームレス地質図	S-5	海陸シームレス地質情報集「駿河湾北部沿岸域」
燃料資源図	FR-3	燃料資源地質図「関東地方」
土壌評価図	E-6	表層土壌評価基本図 「茨城県地域」
数値地質図	G-16	20 万分の 1 日本シームレス地質図　DVD 版
	G-17	九州地質ガイド
	GT-4	全国地熱ポテンシャルマップ
	S-2	海陸シームレス地質情報集「新潟沿岸域」
	S-3	海陸シームレス地質情報集「福岡沿岸域」
	V-3	口永良部島火山地質データベース
	P-2	日本重力データベース　DVD 版
	G20-1	20 万分の 1 数値地質図幅集「北海道北部」第 2 版
	G20-2	20 万分の 1 数値地質図幅集「北海道南部」第 2 版
その他	日本の熱水系アトラス	
	海と陸の地球化学図	
	関東の地球化学図	

事務局
国立研究開発法人 産業技術総合研究所
地質調査総合センター
地質情報基盤センター　出版室
https://www.gsj.jp/inquiries.html

Secretariat Office
National Institute of Advanced Industrial Science and Technology
Geological Survey of Japan
Geoinformation Service Center Publication Office
https://www.gsj.jp/en/

地質調査研究報告 第68巻 第2号
平成29年4月5日　発行

国立研究開発法人 産業技術総合研究所
地質調査総合センター

〒305-8567
茨城県つくば市東1-1-1 中央第7

Bulletin of the Geological Survey of Japan
Vol.68 No.2 Issue April 5, 2017

Geological Survey of Japan, AIST

AIST Tsukuba Central 7, 1-1-1, Higashi,
Tsukuba, Ibaraki 305-8567 Japan

AIST16-G68699-68-2

Online ISSN：2186-490X
Print ISSN：1346-4272

地質調査研究報告

BULLETIN
OF THE
GEOLOGICAL SURVEY OF JAPAN

Vol. 68 No. 2 2017

CONTENTS

Special Issue:
New data on depositional ages of the Mesozoic, Shima Peninsula—the Toba District—

Bulletin of the Geological Survey of Japan Vol. 68, No. 2, P. 23–86 2017

地 調 研 報
Bull. Geol. Surv. Japan
Vol. 68, No. 2, 2017

Geological Survey of Japan, AIST